PB94-142007

Gravity-Load-Designed Reinforced Concrete Buildings: Seismic Evaluation of Existing Construction and Detailing Strategies for Improved Seismic Resistance

by

G.W. Hoffmann[1], S.K. Kunnath[2], A.M. Reinhorn[3] and J.B. Mander[4]

July 15, 1992

Technical Report NCEER-92-0016

NCEER Project Number 91-3111B

NSF Master Contract Number BCS 90-25010
and
NYSSTF Grant Number NEC-91029

1 Structural Engineer, TVGA Engineering, Orchard Park, New York; formerly Graduate Research Assistant, Department of Civil Engineering, State University of New York at Buffalo
2 Assistant Professor, Department of Civil Engineering, University of Central Florida
3 Professor, Department of Civil Engineering, State University of New York at Buffalo
4 Assistant Professor, Department of Civil Engineering, State University of New York at Buffalo

NATIONAL CENTER FOR EARTHQUAKE ENGINEERING RESEARCH
State University of New York at Buffalo
Red Jacket Quadrangle, Buffalo, NY 14261

REPRODUCED BY:
U.S. Department of Commerce
National Technical Information Service
Springfield, Virginia 22161

50272-101

REPORT DOCUMENTATION PAGE	1. REPORT NO. NCEER-92-0016	2.	3. PB94-142007

4. Title and Subtitle
Gravity-Load-Designed Reinforced Concrete Buildings: Seismic Evaluation of Existing Construction and Detailing Strategies for Improved Seismic Resistance

5. Report Date
July 15, 1992

6.

7. Author(s)
G.W. Hoffmann, S.K. Kunnath, A.M. Reinhorn, J.B. Mander

8. Performing Organization Rept. No.

9. Performing Organization Name and Address
State University of New York at Buffalo
Department of Civil Engineering
Buffalo, New York 14260

10. Project/Task/Work Unit No.

11. Contract(C) or Grant(G) No.
(C) BCS 90-25010
(G) NEC-91029

12. Sponsoring Organization Name and Address
National Center for Earthquake Engineering Research
State University of New York at Buffalo
Red Jacket Quadrangle
Buffalo, New York 14261

13. Type of Report & Period Covered
Technical report

14.

15. Supplementary Notes
This research was conducted at the State University of New York at Buffalo and was partially supported by the National Science Foundation under Grant No. BCS 90-25010 and the New York State Science and Technology Foundation under Grant No. NEC-91029.

16. Abstract (Limit: 200 words)
An analytical investigation of the performance of reinforced concrete buildings designed primarily for gravity loads is presented. In first part, the seismic performance of non-ductile reinforced concrete frame bjildings in regions of low to moderate seismicity is evaluated. Several significant aspects of non-ductile detailing are modeled using rational simplifications of expected member behavior at critical sections. The detailing configurations included in the analysis are: 1) discontinuous positive flexural reinforcement; 2) lack of joint shear reinforcement; and 3) inadequate transverse reinforcement for core confinement. Inelastic time history analyses are carried out under moderate to severe earthquake excitations. The first phase of the investigation established that most of the structural damage could be attributed to non-seismic details at beam-column joints or interfaces. Consequently, the second part of the study was concerned with examining the effects of improving these details in a marginal way so that the seismic performance could be enhanced without resorting to a full seismic design. An extensive parametric study of the same buildings with refined detailing characteristics is carried out to establish simple techniques to improve the seismic resistance of gravity-load-designed buildings. The important feature of the study is that the buildings are not-redesigned for lateral forces, but only that the detailing in critical regions is altered to achieve improved performance.

17. Document Analysis a. Descriptors

b. Identifiers/Open-Ended Terms
Gravity load design. Reinforced concrete buildings. Inelastic response analysis. Existing buildings. Detailing. Retrofitting. Beam column joints. Column confinement. Jacketing. Bottom beam bars. Development length. Joint shear capacity. Experimental evaluation. Inelastic time history analysis. Beam confinement. Positive reinforcement. Earthquake engineering.

c. COSATI Field/Group

18. Availability Statement	19. Security Class (This Report)	21. No. of Pages
Release unlimited	Unclassified	162
	20. Security Class (This Page) Unclassified	22. Price

PREFACE

The National Center for Earthquake Engineering Research (NCEER) was established to expand and disseminate knowledge about earthquakes, improve earthquake-resistant design, and implement seismic hazard mitigation procedures to minimize loss of lives and property. The emphasis is on structures in the eastern and central United States and lifelines throughout the country that are found in zones of low, moderate, and high seismicity.

NCEER's research and implementation plan in years six through ten (1991-1996) comprises four interlocked elements, as shown in the figure below. Element I, Basic Research, is carried out to support projects in the Applied Research area. Element II, Applied Research, is the major focus of work for years six through ten. Element III, Demonstration Projects, have been planned to support Applied Research projects, and will be either case studies or regional studies. Element IV, Implementation, will result from activity in the four Applied Research projects, and from Demonstration Projects.

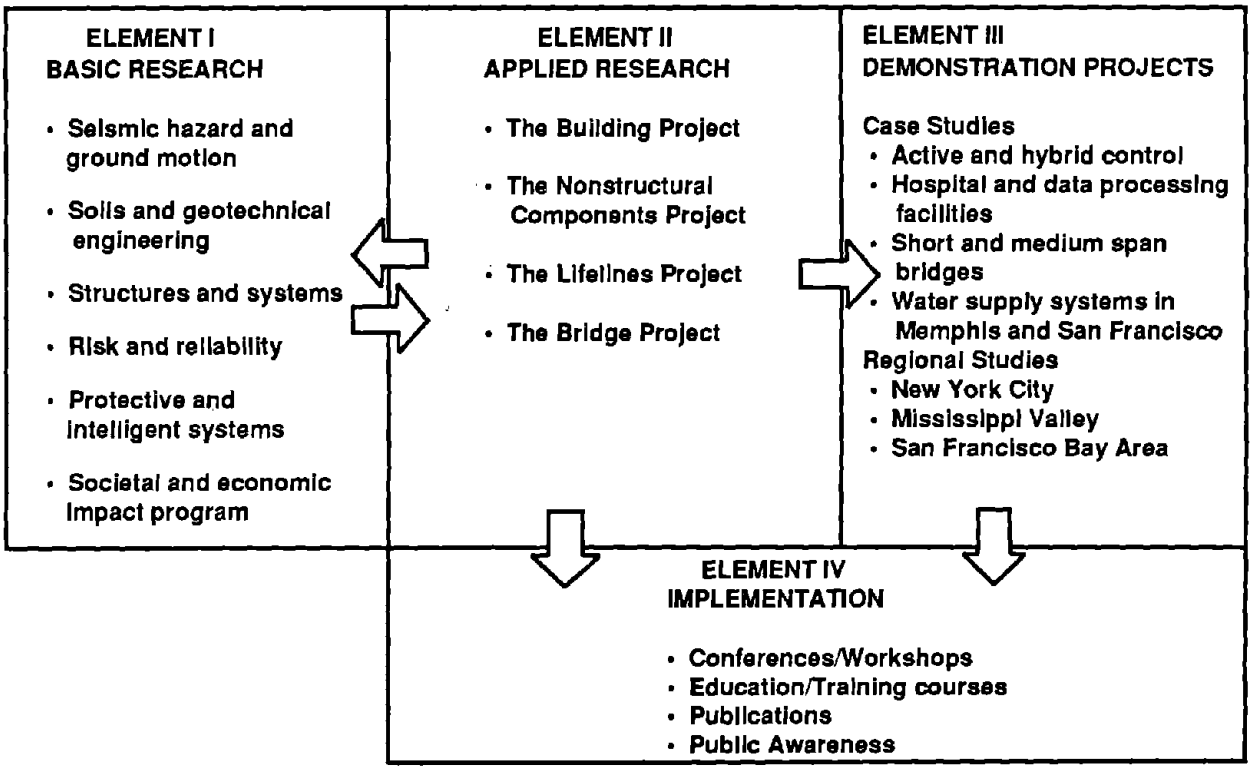

Research in the **Building Project** focuses on the evaluation and retrofit of buildings in regions of moderate seismicity. Emphasis is on lightly reinforced concrete buildings, steel semi-rigid frames, and masonry walls or infills. The research involves small- and medium-scale shake table tests and full-scale component tests at several institutions. In a parallel effort, analytical models and computer programs are being developed to aid in the prediction of the response of these buildings to various types of ground motion.

Two of the short-term products of the **Building Project** will be a monograph on the evaluation of lightly reinforced concrete buildings and a state-of-the-art report on unreinforced masonry.

The **structures and systems program** constitutes one of the important areas of research in the **Building Project**. Current tasks include the following:

1. Continued testing of lightly reinforced concrete external joints.
2. Continued development of analytical tools, such as system identification, idealization, and computer programs.
3. Perform parametric studies of building response.
4. Retrofit of lightly reinforced concrete frames, flat plates and unreinforced masonry.
5. Enhancement of the IDARC (inelastic damage analysis of reinforced concrete) computer program.
6. Research infilled frames, including the development of an experimental program, development of analytical models and response simulation.
7. Investigate the torsional response of symmetrical buildings.

One of the major thrusts of the research at NCEER has been the evaluation of the performance of concrete frame structures that had been designed only for gravity loads. A variety of design details, common in most parts of the country, have been studied experimentally and analytically at several institutions. The main goal of these investigations has been the development of analytical tools for the prediction of the response of lightly reinforced concrete structures. This report summarizes an analytical study of the expected performance of 3, 6, and 9 story frames to a set of typical ground motions. The analytical model has been based on the results of the experimental research. The response of structures with various design details is compared in terms of maximum response, damage levels, and expected failure types for several levels of ground motion.

ABSTRACT

Recent awareness of a potential seismic event in regions of low to moderate seismicity have led to concerns of safety and vulnerability of reinforced concrete buildings in which ductile detailing has not been provided explicitly in the design process.

An analytical investigation of the performance of reinforced concrete buildings designed primarily for gravity loads is presented in a two-part evaluation. In the first part, the seismic performance of non-ductile reinforced concrete frame buildings in regions of low to moderate seismicity is evaluated. Several significant aspects of non-ductile detailing are modeled using rational simplifications of expected member behavior at critical sections. The detailing configurations included in the analysis are: (1) discontinuous positive flexural reinforcement; (2) lack of joint shear reinforcement; and (3) inadequate transverse reinforcement for core confinement. Inelastic time history analyses of three, six, and nine story buildings are carried out under moderate to severe earthquake excitations. The essential parameters of the response are examined with a view to identifying vulnerability of such buildings to a potential seismic design event.

The first phase of the investigation established that most of the structural damage could be attributed to non-seismic details at beam-column joints or interfaces. Consequently, the second part of the study was concerned with examining the effects of improving these details in a marginal way so that the seismic performance could be enhanced without resorting to a full seismic design. An extensive parametric study of the same buildings with refined detailing characterstics is carried out to establish simple techniques to improve the seismic resistance of gravity-load-designed buildings. The important feature of the study is that the buildings are not re-designed for lateral forces, but only that the detailing in critical regions is altered to achieve improved performance.

For structural engineers in the eastern and mid-western United States who are concerned with seismic performance and possible retrofit of existing buildings, and in the design of new structures, the results of this investigative study provide a number of useful insights. A discussion of estimated additional costs associated with the implementation of these detailing strategies is provided to assess the economic feasibility of such enhancements. Indirectly, the study provides information on the effects of retrofit strategies involving the confinement of beam-column joints through jacketing, wherein the purpose is to improve column confinement, ensure adequate development length in bottom beam bars, and provide full joint shear capacity. The study also provides a methodology to evaluate structural retrofit through inelastic analysis and damage indicators.

ACKNOWLEDGEMENTS

Financial support for this work was provided through the National Center for Earthquake Engineering Research (NCEER) under Grant Number NCEER 91-3111B. The funding is gratefully acknowledged.

The authors wish to thank Professor Richard N. White, Professor Peter Gergely and Attila Beres for their suggestions and comments on the content of this report.

A note of thanks is also extended to Joseph Bracci, Michael Riley, Roy Lobo and Rodolfo Valles for their assistance in the inelastic evaluations of the structures presented in the report.

Preceding page blank

TABLE OF CONTENTS

Preceding page blank

LIST OF FIGURES

LIST OF TABLES

SECTION 1

INTRODUCTION TO THE EVALUATION OF EXISTING STRUCTURES

Due to the enormous loss of life and property resulting from recent earthquakes in Mexico City and San Francisco, considerable public interest in this country has been directed towards the damaging effects of earthquakes. And more recently, earthquakes of a moderate level which occurred in Quebec in the north-eastern region of the North American continent, have increased general awareness of the threat of seismic events outside zones of high seismicity. These concerns of seismic vulnerability are compounded by the fact that seismologists predict a moderate to major earthquake along the New Madrid fault in the not too distant future.

This study deals with a two-part investigation into the seismic performance of buildings in low to moderate seismic zones where buildings are designed primarily for gravity loads. In the first part, the seismic performance of non-ductile reinforced concrete frame buildings is evaluated. Included in the evaluation are aspects of modeling certain detailing configurations which are inherent in nonductile design, such as: discontinuous positive flexural reinforcement; lack of joint shear reinforcement; and inadequate transverse reinforcement for core confinement. Inelastic time history analyses of three, six, and nine story buildings are carried out under low to moderate earthquake excitations. The essential parameters of the response are examined with a view to identifying vulnerability of such buildings to a potential seismic event.

The second part of the study is concerned with examining the effects of improving the non-seismic detailing in a marginal way so that the seismic performance is enhanced without resorting to a full seismic design. An extensive parametric study of the same buildings with refined detailing characteristics is carried out to explore simple techniques to improve the seismic resistance of gravity-load-designed buildings.

1.1 Motivation

Given the potential risk of damage to concrete buildings from a moderate earthquake in regions of low to moderate seismicity, the need for simple yet reliable evaluation of existing construction is

becoming a matter of growing concern to the practicing community. While analytical tools for nonlinear seismic analysis exist, the real issue is whether the modeling of certain nonductile detailing is properly accounted for in the evaluations.

The purpose of this study is to provide a simple rational procedure to analyze existing concrete buildings that were designed primarily for gravity loads. The procedure permits modeling of non-ductile detailing in an implicit manner so that existing analytical tools can be used to carry out the required seismic evaluations. The analyses presented in this report attempt to provide engineers with some preliminary data on the potential performance of typical gravity-load designed RC buildings subjected to moderate earthquake motion. The results presented here can also be used as a guideline for setting up damage-limiting criteria and for consideration of seismic upgrading, if needed.

For structural engineers in the eastern and mid-western United States who are concerned with seismic performance and possible retrofit of existing buildings, and in the design of new structures, the results of this investigative study provide a number of useful insights. Indirectly, the study provides information on the effects of retrofit strategies involving the confinement of beam-column joints through jacketing, wherein the purpose is to improve column confinement, ensure adequate development length in bottom beam bars, and provide full joint shear capacity. The study also provides a methodology to evaluate structural retrofit through inelastic analysis and damage indicators.

1.2 Background and Previous Research

The subject of evaluating the seismic risk or vulnerability of existing or proposed structures is not new, though the application of the same techniques to nonductile or gravity-load designed construction is both recent and undeveloped.

Four separate but related areas of research have contributed greatly in the development of this investigation. The first of these deals with the general subject of inelastic behavior of reinforced concrete frames. In the earliest building models, the entire structure was idealized as a shear beam with internal nodes representing floor masses. The development of DRAIN-2D (Kaanan and Powell, 1971) was significant in making possible the analysis of RC frames in the inelastic range. Numerous enhancements to DRAIN have also been reported in the literature wherein newer member and

hysteretic models were incorporated into the DRAIN program. More recently, IDARC (Park et al., 1987; Kunnath et al., 1992) was developed at the State University of New York at Buffalo with several significant features for reliable modeling of RC structures. Among others, IDARC included a shear wall model, a distributed flexibility element model, and a versatile hysteretic model. All evaluations presented in this report are based on analyses carried out using IDARC.

A second area of research that contributed towards this study is the behavior of RC beam-column joints. This area of study has been studied extensively, both experimentally and analytically, primarily for well-detailed connections. Still, not much is clearly understood nor well explained about the behavior of beam-column joints, especially the post-cracking shear behavior and the concrete contribution to the shear strength, both before and after cracking. This uncertainty causes difficulty when modelling beam-column joints, forcing approximate methods and mechanical idealizations to be used. Nonetheless, the work of Park and Paulay (1974), Paulay (1989), as well as the report released by ACI Committee 352 (1976), provided major input into the modeling schemes used in this study. Experimental work that has been of significant benefit in understanding the behavior of beam-column joints and in subsequent modeling includes work of Otani et al. (1984; 1985) and Pessiki et al. (1990).

The third general subject area utilized in this research is that of damage evaluation of reinforced concrete members and structures. Common within all work in the field of damage evaluation is the quantification of damage based on the physical serviceable state of the component or system, based on empirical correlations using ductility ratio and/or energy absorption. This approach of quantifying damage is very useful for comparative studies such as those presented in this report. A review of damage models is reported in DiPasquale and Cakmak (1987) and Bracci et al. (1989). The model used in this study is based on the formulation of Park et al. (1984).

The last area of study that impacts the scope of this report is the broad area of seismic risk assessment of lightly reinforced concrete buildings. Since the Eastern United States is not the exclusive location of lightly reinforced concrete structures or the gravity load design philosophy, it seems inappropriate to infer that this subject has limited breadth based on geography. Documents of importance that were reviewed prior to this study included the guidelines set forth by the Applied Technology Council (1989) and the work of Reinhorn et al.(1988).

1.3 Discussion of Seismic Design Philosophies

Several structural considerations have long been recognized as being of paramount importance for the safe transmission of seismically induced inertia forces and the building remaining in a serviceable state thereafter. A short synopsis of general criterion that are considered when designing for seismic resistance is presented as follows.

1) Moment-resisting frames should fail in a slow ductile flexural yielding manner as opposed to a brittle fracture type of failure such as joint shear, concrete crushing or column buckling.
2) It is equally important that the failure mechanism be such that all gravity loads are still safely transmitted to the ground after the seismic event has passed. To help accomplish this, current seismic design recommendations propose the use of a strong column-weak beam design be employed to assure column capacity remains after a full mechanism has formed.
3) Ductility capacity of potential plastic hinge regions should be adequate to withstand large rotations without the brittle crushing of the concrete compression zone. Similarly, detailing configurations should be such to insure that longitudinal reinforcement does not buckle should cover concrete be rendered ineffective.
4) An attempt to restrict the level of inter-story drift should be made to assure the protection of interior utilities and the comfort of occupants.

More specific to beam-column joints, Park and Paulay (1974) suggest the following criteria should be considered in order to achieve satisfactory seismic performance of joint regions within R/C frames.

1) The strength of the joint should be equal or greater than that of the members framing into it. More specifically, the joint shear capacity of a beam-column joint should be such to assure that flexural yielding of the beams and columns framing into it would precede joint shear failure.
2) Detailing in the joint region should assure that adjoining members may develop their full capacity.

3) Lap type splices of reinforcement should be located as far from the joint as practical. Longitudinal bars should not be terminated within a joint without suitable anchorage. Detailing should be such to insure that longitudinal bars continuing through the joint do not buckle.

4) The joint should be detailed with consideration given to the ease of reinforcement assembly and concrete placement.

The preceding issues are introduced at this point to outline current accepted seismic design practice for reinforced concrete frames. Subsequent chapters will delve into these considerations in greater detail and show the importance of adhering to a seismic design approach as well as illustrate the consequences of different detailing strategies.

SECTION 2

DESCRIPTION OF TYPICAL STRUCTURE

The building configuration selected was a typical office building or similar frame structure that may be found in many cities in the Eastern United States. A symmetric floor plan and floor levels of equal height were used to avoid any irregular behavior that might lead to complexities in the interpretation of the dynamic response. Since this research was an investigation into the adequacy of reinforcement detailing, it was necessary to assure that the model was free from any peculiar features that could obscure the results obtained from the modeling of separate reinforcing details. Fig. 2.1 shows the typical floor plan.

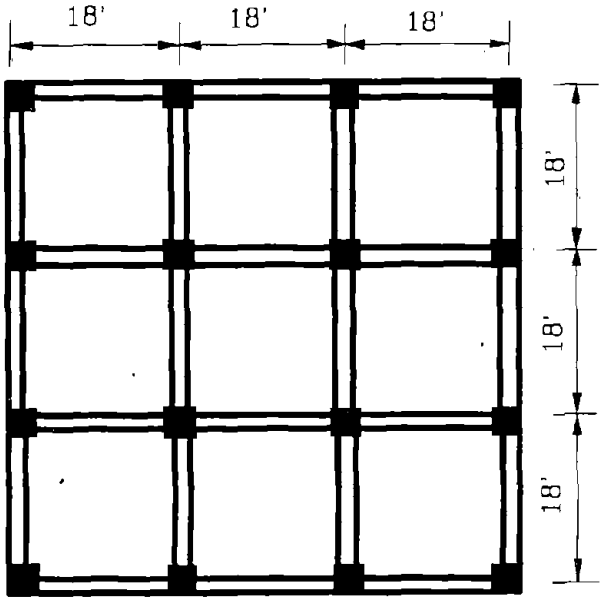

Figure 2.1 Typical Floor Plan

Three structures of identical floor plan and story height, but of different overall height, were evaluated to ensure that the examination of joint detailing covered a broad range of applicable building heights. Buildings of 3, 6 and 9 stories were modelled as shown in Figure 2.2.

2.1 General Aspects of the Gravity-Load Designed Building

The buildings were designed without consideration for seismic loads, in accordance with code requirements prescribed in ACI 318-89. Structural elements were designed for a factored load of 1.4D + 1.7L, where a uniformly distributed live load of 50 psf was used in accordance to ANSI code (1982) provisions for minimum loads for office buildings.

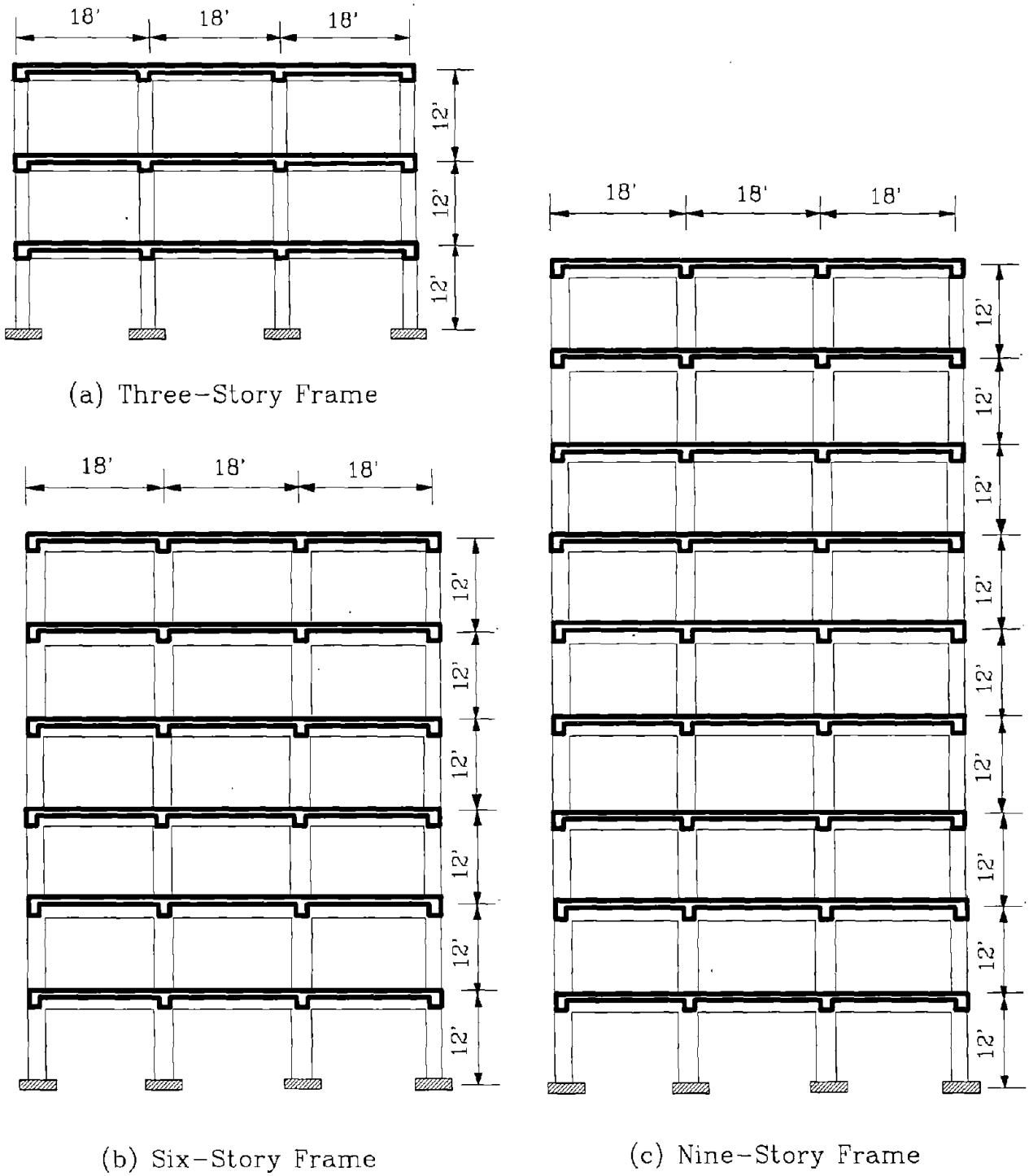

Figure 2.2 Elevations of Analyzed Frames

Beams were treated as continuous T-beams required to resist factored shears and moments at critical sections only. Since gravity load forces governed over those from wind loads for beams, the reinforcing profiles of the beams were identical regardless of story level. See Fig. 2.3 for the beam reinforcing profile along with the corresponding beam cross-sections at the critical locations. For the top story, it was assumed, for simplicity, that factored snow loads and roof dead loads were of the same order as the floor loads.

Columns were also designed to resist the worst case combination of moment and axial load that occurred from the governing combination of factored wind and gravity loads. Column cross-sections were redesigned every three story levels. That is, the cross-section was the same for all levels of the 3-story building, two different sections were used for the 6 story building and three different sections were used for the 9-story design. Fig. 2.4 shows the general profile of the columns along with the specific detailing of each cross-section corresponding to the three sets of story levels.

Concrete was assumed to have an unconfined compressive strength of 4000 psi while steel reinforcement was assumed to have a yield strength of 40000 psi.

2.2 Characteristic Behavior of Gravity-Load-Designed Structures

Some common aspects of reinforcement detailing in gravity-load design are summarized below. These features contribute significantly to the vulnerability of moment-resisting frames under seismic loads.

One such feature is the practice of discontinuing bottom flexural reinforcement at the interior joints and the simple termination of these bottom bars at the exterior joints. ACI code provisions stipulate that one quarter of the positive flexural reinforcement be extended at least 6 inches into the support. This practice is more than adequate in cases where gravity load governs due to the support region of beams being in negative flexure. Also, it is generally adequate when considering wind loads because for low-rise structures, the combination of unfactored dead load and factored wind load still may not produce positive moments in the beams at the supports. It must be pointed out, however, that the code requires adequate anchorage when the member in question is part of a primary lateral load resisting system (moment resisting frame). However, this provision would not apply or might be ignored if gravity loads governed or lateral loads were small or ignored completely.

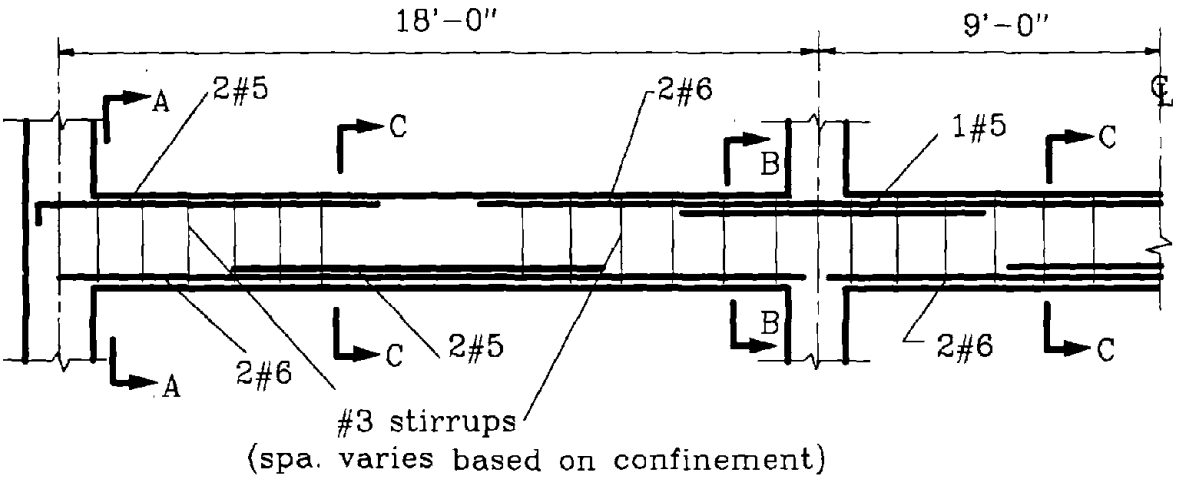

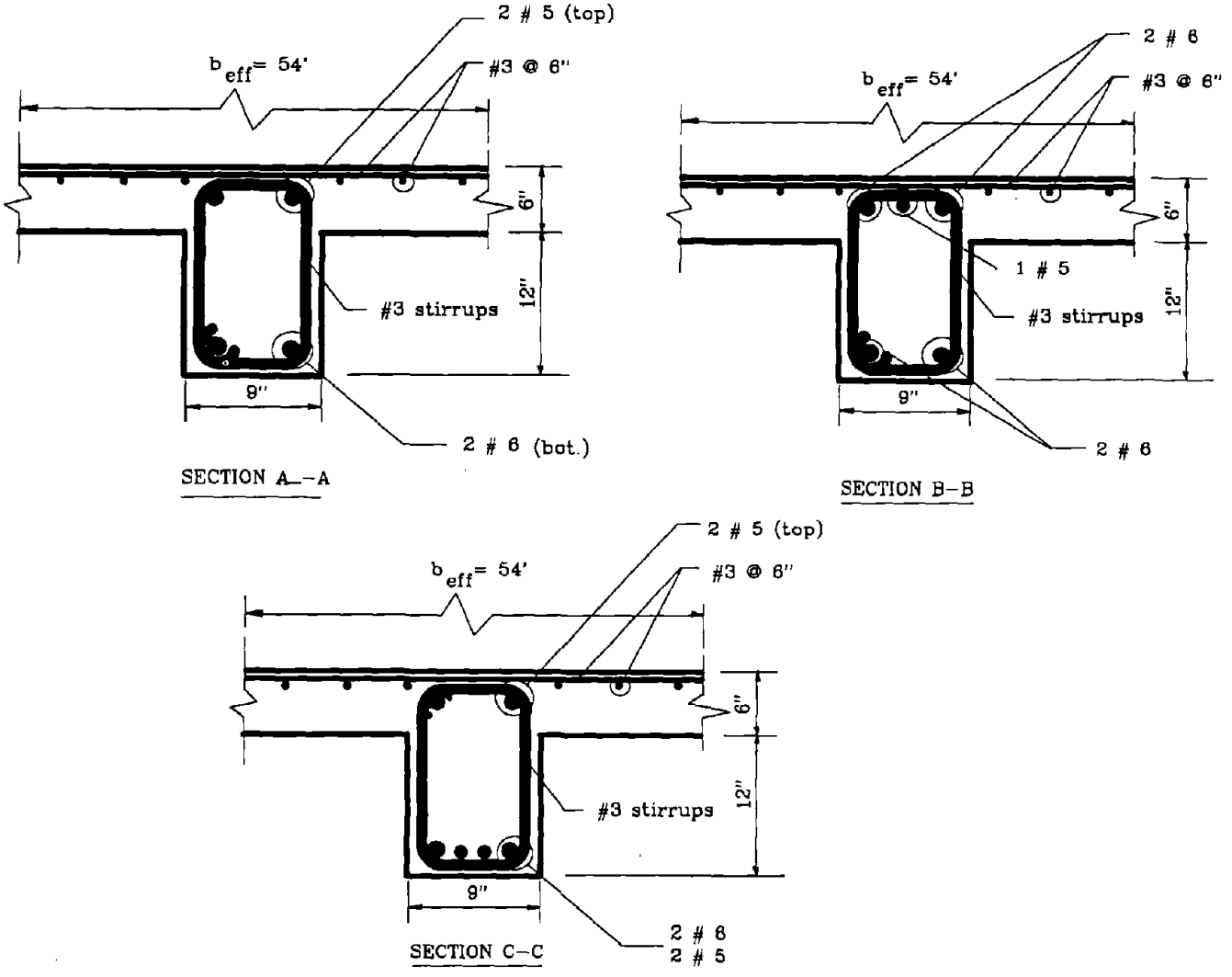

Figure 2.3 Beam Reinforcement Details

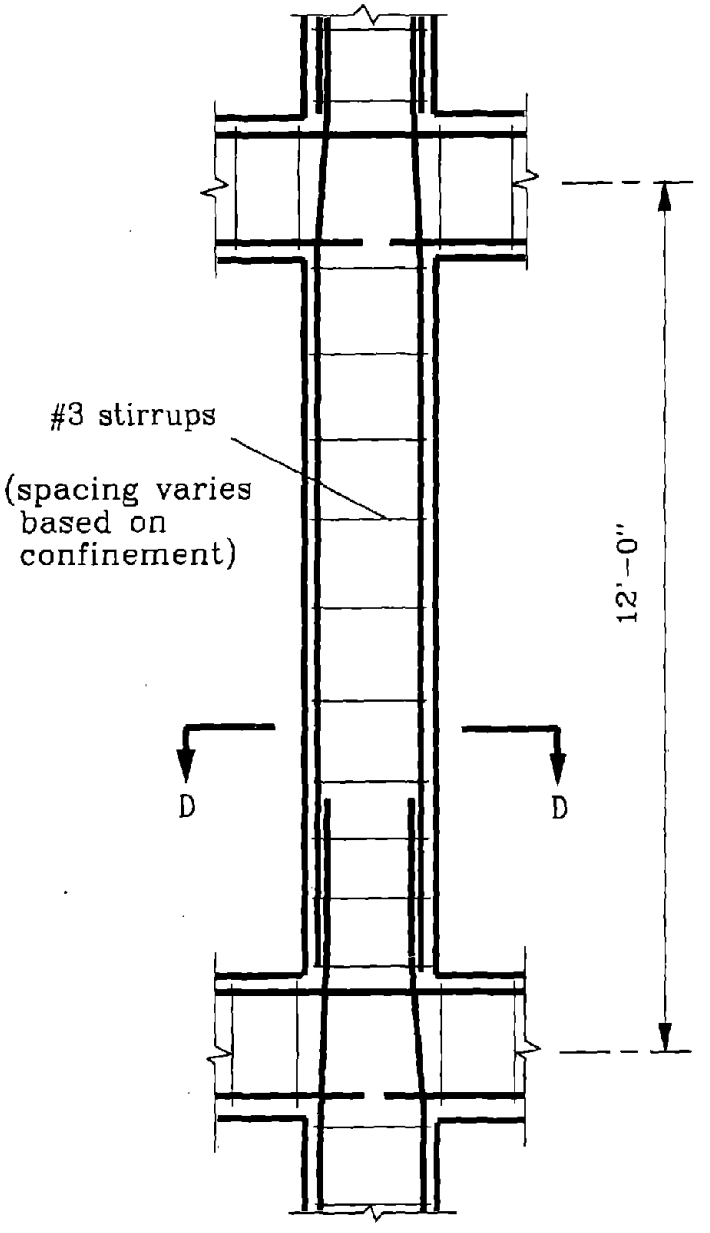

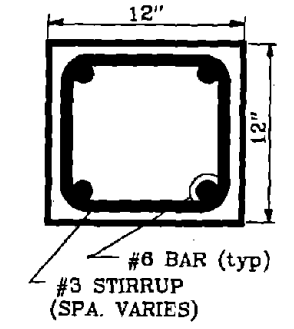

a) Columns Supporting Less than 4 Floors

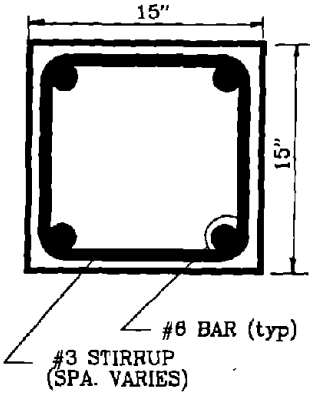

b) Columns Supporting 4 to 6 Floors

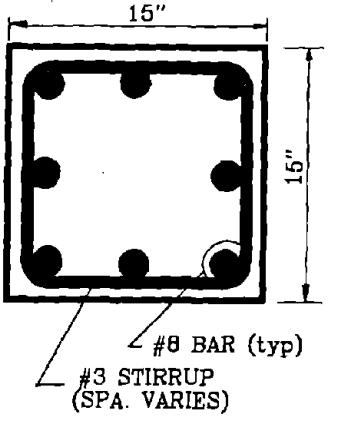

c) Columns Supporting Over 6 Floors

SECTION D–D

Figure 2.4 Column Reinforcement Details

A second practice is the assumption that beam-column joints behave rigidly and are sufficient in strength to transfer moments through the joints. The ACI code makes no provision for assuring joint shear strength in routine designs and also overlooks the problem of minimum joint shear strength in its provisions for seismic design. Again, the code does include a provision for using a *minimum* area of shear reinforcement within the joint for connections that are part of a primary seismic load resisting system. However, as discussed earlier, this provision would not apply or may be ignored if gravity loads are of primary concern. A detailed discussion of joint shear strength is presented later. It will be noted here that the omission of transverse hoops within the joint, or any other type of joint shear steel for that matter, is the common practice in gravity-load designed structures.

The third issue of concern is the distribution of transverse reinforcement within the members for the resistance of shear forces. Code provisions require that stirrups be spaced at no more than one half the effective depth of the member. However, this is not required when the factored shear is less than one half the shear capacity of the concrete as is often the case in columns where shear forces, even including wind effects, are small. The code reserves any discussion of minimum confinement to the section on special provisions for seismic design. In defense of the code, gravity load failure mechanisms are generally such that due to the redundancy within the frame, plastic hinge rotations near the supports are generally quite small, and confinement of the compression block is not likely to be a problem.

An interesting feature of the construction practice is the location of the longitudinal bar splices for the columns. It was very common, for the ease of construction, to locate these splices just above the beam near the joint. Under lateral loads, this is the location of the highest moment. Also, the two bars in the splice are generally in contact with each other, adversely effecting the effectiveness of the bond between the bar and the surrounding concrete. Further, if the placement of the column bars is not closely checked, the bend in the overlapping bar could be inward towards the center of the column, reducing the effective internal moment arm of the cross-section. Nonetheless, albeit an interesting detailing feature, so long as the splice is fairly confined and the overlap is of sufficient length, it is not generally a significant problem and is not a feature examined in this study.

Another characteristic of the gravity-load-design philosophy, not specific to detailing, is the intended failure mechanism associated with this practice. The failure mechanism resulting from a gravity-overload is generally a series of isolated beam mechanisms, with hinges first forming at the beam supports and then additional load is distributed to the beam as if it was simply supported until a midspan hinge occurs forming a complete mechanism. This mechanism is interesting due to the failure being localized to the overloaded region and does not initiate total structure collapse. However, when subjected to lateral overloads, the failure mechanism that develops in gravity-load-designed structures is often a column sidesway mechanism (soft-story) or combination of mechanisms. These mechanisms are highly undesirable because they do not transmit gravity loads after the seismic event has passed. For laterally loaded structures, the mechanism most desirable and often associated with good seismic detailing is the beam-sidesway mechanism.

SECTION 3

MODELING OF BUILDING FOR INELASTIC ANALYSIS

3.1 Computational Tool: IDARC

The computer program IDARC, Version 2.2, developed by Park et al. (1987) and enhanced by Kunnath et al. (1991), was used for all the dynamic analyses. IDARC is an inelastic dynamic analysis program for RC frame-wall structures which attempts to quantify the damage to major structural elements on a scale from zero to one. Several important capabilities unique to IDARC are described in brief below.

IDARC Version 2.2 allows direct input of moment-curvature properties which are characteristic of structural elements in the building. This is in addition to the option of inputting section dimensions and reinforcement details from which the program generates the moment-curvature properties. This feature is useful when modeling structures which have been previously damaged or when modeling existing structures with unknown reinforcing details and moment-curvature properties can only be estimated. It is also possible to model various failure modes which can not be described by typical flexural yielding behavior. Two such failure phenomenon which have been modelled in this study are flexural bar pullout and joint shear failure.

IDARC uses a trilinear moment-curvature backbone envelope to estimate the stiffness, moment and deformation at any given time step during the analysis. Another important feature of the program is the ability to specify a avriety of hysteretic behavior patterns using certain control parameters, α, β & γ, where α models the stiffness deterioration, β models the strength degradation and γ models the pinching, slip or crack-closing behavior. Also, since the hysteretic parameters can be specified separately for different members, the effect of the level of axial load on hysteretic behavior as well as the simulation of specific behavior such as flexural bar slip can be modelled indirectly. Fig. 3.1 shows the moment-curvature backbone curve and Fig. 3.2 illustrates the effect of each of the hysteretic parameters used in IDARC.

In addition to the above mentioned modeling capabilities, another feature of IDARC is its damage indexing feature. The use of a damage indicator is extremely useful when comparing the results of numerous analyses wherein essential parameters such as dissipated energy and ductility demand are somehow incorporated into the index. The damage model used in this study is the modified Park model (Kunnath et al., 1990) in which damage is expressed as a combination of deformation damage and damage resulting from dissipated energy. Additional discussion of the damage model may be found in Section 4.3.

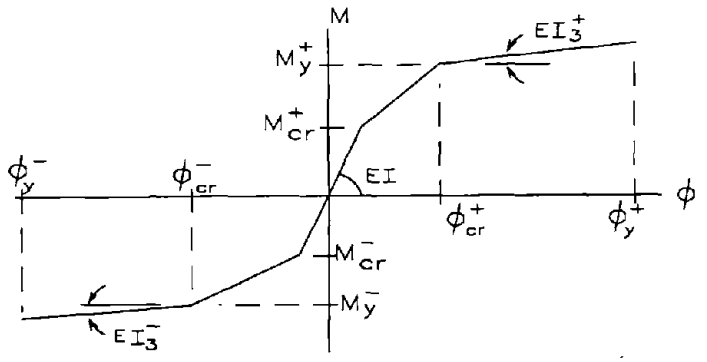

Figure 3.1 Trilinear Moment-Curvature Skeleton Curve

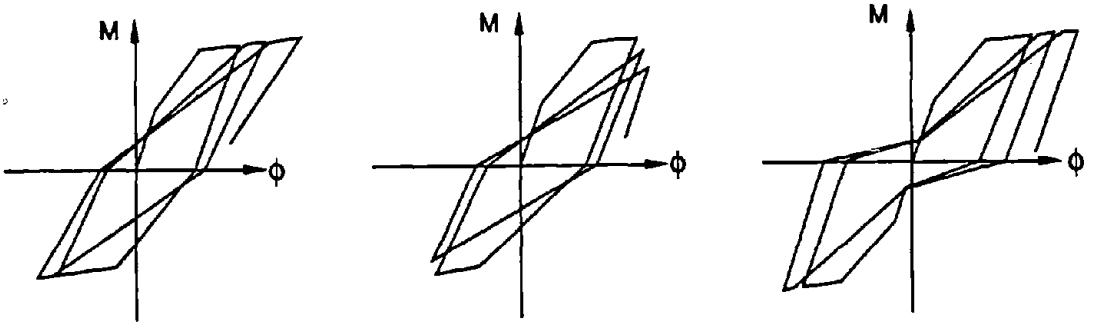

(a) Stiffness Degradation, α (b) Strength Degradation, β (c) Pinching Behavior γ

Figure 3.2 Effects of Hysteretic Parameters

The IDARC program is, therfore, utilized in evaluating overall structural performance owing to changes in the following characteristics of detailing: (1) the effect of continuous positive reinforcement, (2) the presence of sufficient joint shear steel, and (3) variations in the level of confinement within beams, columns and both.

3.2 Modeling of Discontinuous Positive Reinforcement

A typical practice associated with gravity-load-designed RC structures is the termination of the bottom steel in beams (positive reinforcement) within the beam-column joint. Upon large lateral loading, these beams have a tendency of not being able to reach their yield moment because the bond between the positive reinforcement and the joint concrete is insufficient to develop the yield force in the steel. This allows the steel to gradually slip through the joint upon further seismically induced deformation (displacement loading) until ultimately a "pullout" condition is reached. Fig. 3.3 is an illustration of an interior beam-column joint subjected to discontinuous bar pullout.

It should be noted that this bar "slip" is very small and usually is difficult to visually detect during testing of indeterminate frames. Also, it must be remembered that most of the tensile force in the bar undergoing slip is maintained and that the strength degradation associated with bar slip occurs during reversed cycling and is due to the bar deformations grinding the concrete that is in contact with the deformations. The increase in moment after "slip" initiates is provided by the upward migration of the neutral axis causing a smaller compressive block to resist an essentially constant tension force, significantly increasing the compressive stresses and strains in this region until crushing of the extreme fibers occurs. Migration of the neutral axis leads to an increase of the internal moment arm between the centroid of the compression block and slightly diminished tension force, thus *theoretically* allowing additional moment to be resisted despite actual bar force being slightly reduced. It has been seen that the behavior of a beam experiencing bar pullout is initially very similar to a beam experiencing flexural yielding, with a significant difference, in that it weakens rapidly over many loading cycles. The stiffness deterioration, strength degradation and the level of slip are greatly magnified in discontinuously reinforced beams as a result of the bar deformations grinding the concrete and substantially reducing the steel-concrete interlock. Eventually, after many cycles, the capacity of the section reduces to near zero since most of the concrete in contact with the bar is eroded into powder.

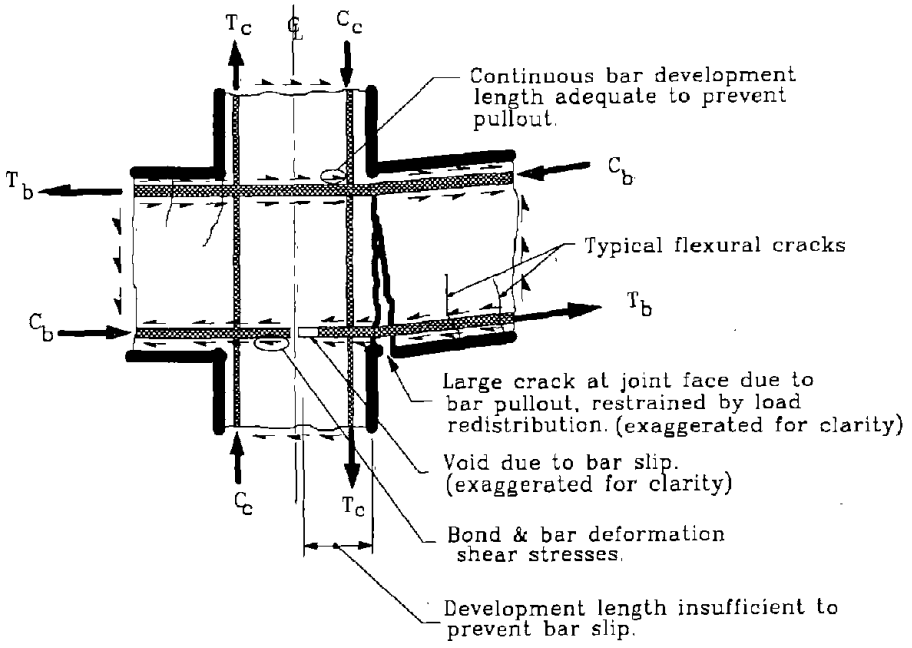

Figure 3.3 Discontinuous Bar Pullout

The required development length for flexural reinforcement can be estimated by the larger value obtained from the following ACI-318 equations (Ch. 12.2.2):

$$l_{db} = 0.04 A_b \frac{f_y}{\sqrt{f'_c}} \quad \text{or} \tag{3.1}$$

$$l_{db} = 0.0004 d_b f_y \tag{3.2}$$

It is proposed to calculate the equivalent moment capacity of a member prone to bar slip based on the yield force of the effective area of the tension steel. We can assume that the effective area of tension steel is equal to the ratio of embedment length to development length multiplied by the actual steel area. That is:

$$A_{eff} = \frac{l_{embedment}}{l_{db}} A_s \tag{3.3}$$

Subsequently, the "pullout" moment capacity can be calculated using this effective area in the usual manner. It can be shown that for typical T-beams prone to bar slip in positive bending, the moment at the initiation of slip is approximately equal to the ratio of the embedment length to the development length multiplied by the yield moment. That is:

$$M_{pullout} \approx \frac{l_{embedment}}{l_{db}} M_y \tag{3.4}$$

So, in essence, the yield strength of the steel in positive bending is all that needs to be adjusted.

For example, the beam cross-section B-B shown in Fig. 2.3 has a calculated positive moment capacity of 540 k-in assuming full anchorage of the bottom reinforcement. Actually the discontinuous bottom reinforcement (2-#6 bars) has an embedment length of 7.5". The necessary embedment length for full development of yield strength for a #6 bar is taken as the greater of the lengths calculated from equations 3.1 and 3.2:

$$l_{db} = 0.04 \frac{\pi (0.75")^2}{4} \frac{40000}{\sqrt{4000}} = 11.2" \quad \text{or}$$

$$l_{db} = 0.0004\ (0.75")\ (40000) = 12.0" \qquad (\textit{governs})$$

The corresponding "pullout" capacity is then:

$$M_{pullout} = \frac{7.5"}{12.0"}(540\ k-\text{in}) = 338\ k-\text{in}$$

3.3 Modelling of Joint Shear Capacity

Characteristic of gravity-load-designed RC structures is the lack of transverse reinforcement within the joint region. It is widely accepted that the longitudinal steel running through the joint is not efficient at resisting shear and is commonly neglected when computing shear capacity. This lack of a shear resistance mechanism can lead to non-ductile failures once the concrete's shear capacity has been exceeded. Even structures designed in accordance with the ACI318-89 seismic provisions are often insufficient in joint shear capacity. The code provision for continuation of transverse hoops through the joint is based on minimum joint confinement while the issue of minimum joint shear capacity is not addressed. Fig. 3.4 illustrates the joint shear failure that occurs when transverse hoops are insufficient to resist the large shears induced by the transmission of axial forces induced by the steel and concrete internal couple. Tests on beam-column joint specimens carried out at the State University of New York at Buffalo (Winters et al., 1991) support the contention that the ACI seismic provisions for transverse steel through the joint are inadequate. A scale model beam-column joint designed in accordance to ACI seismic provisions was tested under lateral load and joint shear failure occurred before a flexural mechanism developed. This premature failure indicates that joints designed solely in accordance to code requirements may be insufficient in shear strength for the transmission of axial forces into shear forces, thus not permitting framing members to reach their yield capacity. So, as is often the case in structural failures, the joint fails in shear, which in essence, hinges all the members framing into it, forcing lateral load to be redistributed to other portions of the structure.

As long as some level of joint continuity is maintained, either from continuous flexural reinforcement or transverse hoops, the joint will maintain a high percentage of its strength. Through aggregate interlock, the concrete should still be able to transfer longitudinal axial forces into the shear forces through the joint to some degree even without the presence of transverse reinforcement. However, upon cyclic loading, the joint strength and stiffness will deteriorate at a very rapid rate. Transverse reinforcement, however, even if inadequate to prevent formation of a joint hinge, will certainly restrain the size of the shear cracks, better maintaining the original joint shear strength and preventing such rapid degradation of stiffness.

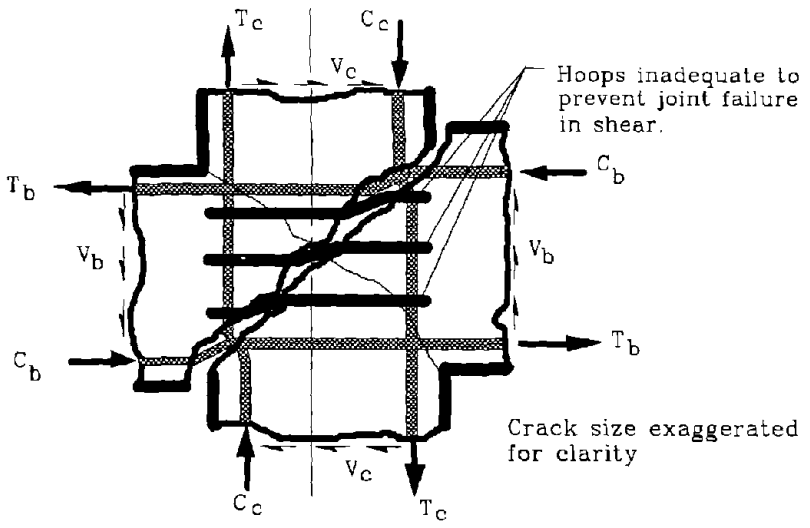

Figure 3.4 Joint Shear Failure

To avoid difficult computer modeling of the behavior of a reinforced concrete joint, especially when inelastic and deteriorating,[1] flexural properties of the members framing into the joint can be adjusted to reflect the capacity of the joint. This is to say that we can reduce the capacity of the flexural members to reflect the moment in said member that would induce a joint shear equal to the calculated joint shear capacity. Figure 3.5a shows a free body diagram of an interior beam-column assemblage (reproduced from Paulay, 1989) between it's points of contraflexure and Figure 3.5b shows the equilibrium of an interior column between it's points of contraflexure with the beam moments resolved into axial components. Simple equilibrium of Fig. 3.5b in the horizontal direction yields:

$$V_{jh} = C_b + T_b - V_c \tag{3.5}$$

where:

$$C_b = T_b = \frac{M_b}{Z_b} \tag{3.6}$$

where: Z_b = Internal moment arm of beam

Z_c = Internal moment arm of column

---

1 Work is currently underway at the University of Buffalo to include a joint element in the global stiffness matrix within the program IDARC.

Summing moments of Fig. 3.5a and expressing beam shear in terms of an equivalent beam moment yields:

$$V_c = V_b \frac{l_b}{l_c} = \frac{M_b}{\frac{(l_b - h_c)}{2}} \frac{l_b}{l_c} = \frac{2M_b}{l_c\left(1 - \frac{h_c}{l_b}\right)} \tag{3.7}$$

Substituting back into Eq. (3.5):

$$V_{jh} = \frac{2M_b}{Z_b} - \frac{2M_b}{l_c\left(1 - \frac{h_c}{l_b}\right)} \tag{3.8}$$

Defining $(V_{jh})_u$ as the horizontal joint shear capacity and solving for the limiting beam moment to prohibit joint failure:

$$M_b \leq \frac{(V_{jh})_u}{2\left(\frac{1}{Z_b} - \frac{1}{l_c\left(1 - \frac{h_c}{l_b}\right)}\right)} \tag{3.9}$$

Similarly, Fig. 3.5d shows a free body diagram of a beam between points of contraflexure with column moments resolved into axial components. Equilibrium of Fig. 3.5d in the vertical direction yields:

$$V_{jv} = C_c + T_c - V_b \tag{3.10}$$

Again, summing moments of Fig. 3.5d about point O and expressing column shear in terms of an equivalent column moment yields:

$$V_b = V_c \frac{l_c}{l_b} = \frac{M_c}{\frac{(l_c - h_b)}{2}} \frac{l_c}{l_b} = \frac{2M_c}{l_b\left(1 - \frac{h_b}{l_c}\right)} \tag{3.11}$$

and back substituting as before we obtain:

$$V_{jv} = \frac{2M_c}{Z_c} - \frac{2M_c}{l_b\left(1 - \frac{h_b}{l_c}\right)} \tag{3.12}$$

Then, defining $(V_{jv})_u$ as vertical joint shear capacity and solving for the limiting column moment to prohibit joint failure:

$$M_c \leq \frac{(V_{jv})_u}{2\left(\frac{1}{Z_c} - \frac{1}{l_b\left(1 - \frac{h_b}{l_c}\right)}\right)} \tag{3.13}$$

Using this procedure of calculating moments to induce joint shear failure of an interior beam-column subassemblage, formulations for the equivalent moment to induce joint shear failure can be made for exterior, interior top floor and exterior top floor (corner) beam-column joints. Figures 3.6, 3.7 and 3.8 show, in respective order, the subassemblage equilibrium and one corresponding shear diagram of an exterior, interior top floor and exterior top floor beam-column joints. Values for horizontal and vertical joint shear, as well as the equivalent member end moments required to induce joint shear failure (in terms of joint shear capacity) are presented in Table 3.1.

The current ACI Code has no provisions for estimating the effect of axial load and transverse reinforcement on the shear capacity of beam-column joints. The code merely suggests a limiting capacity of $20\sqrt{f'_c}A_j$ for the joint, independent of axial load and transverse reinforcement ratio. For the purpose of this study, it was imperative to have an estimate of the shear capacity of an unreinforced beam-column that included the effect of axial load and level of confinement.

The equation below, developed by ACI Committee 352 (1976), was used to better illustrate the variation in joint shear strength induced by axial load and level of confinement. A slight modification of the γ term was used to increase the joint strength obtained from transverse joint confinement linearly from 1.0 to 1.4 as the ratio of transverse beam area to joint face area increased from 0 to 1. It should be noted that no adjustment would be made to the β term for joints where sufficient joint steel was present to resist seismically induced shears, (as ACI Committee 352 suggests) because the purpose of using this equation is to estimate the concrete contribution to the joint shear strength.

$$V_j = 3.5\beta\gamma\sqrt{f'_c\left(1+0.002\frac{N_u}{A_g}\right)}A_{eff} \tag{3.14}$$

where:

β = 1.0 (Type II joints)
γ = 1.0 - 1.4 (based on transverse confinement)
f'_c = unconfined compressive strength
N_u = Axial load transmitted through joint
A_g = Gross area of joint resisting gravity load
A_{eff} = effective area of joint corresponding to the direction of the shear force, i.e.
$A_{eff} = A_{cv} = b'_{eff}d_{eff}$ for vertical joint shear; and $A_{eff} = A_{ch} = b'_{eff}d_{eff}$ for horizontal joint shear, where b'_{eff} = effective joint width perpendicular to direction of the shear force and d_{eff} = effective joint depth parallel to the direction of the shear force

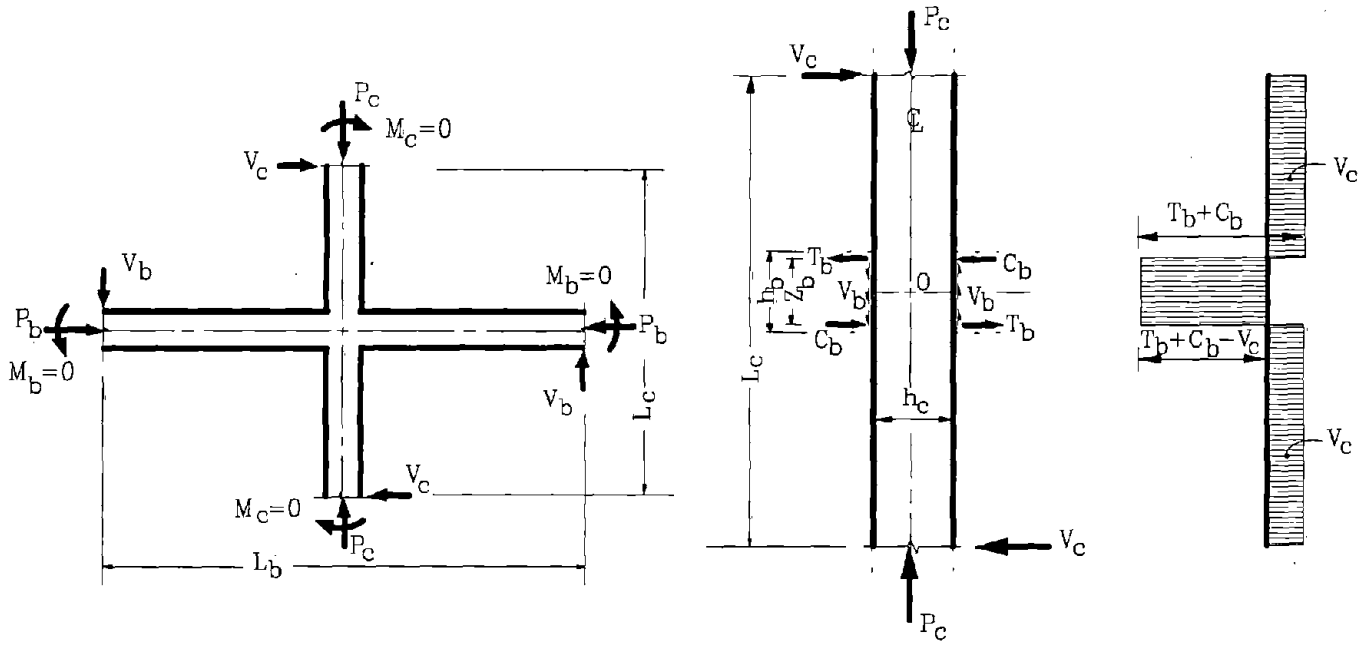

(a) Beam–Column (b) Column Equilibrium (c) Shear Diagram

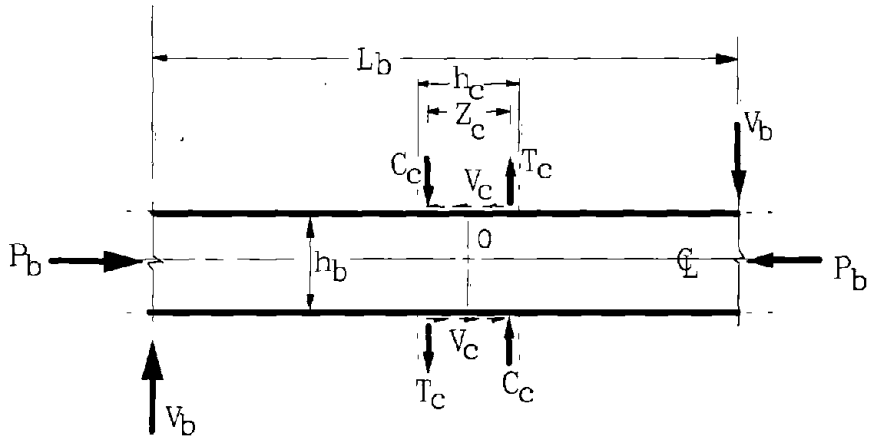

(d) Beam Equilibrium Between Contraflexure Points

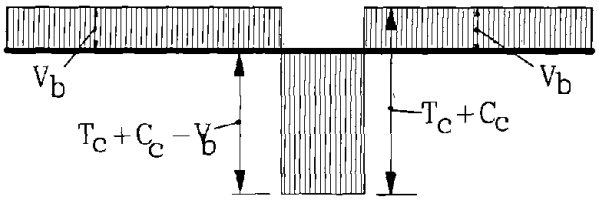

(e) Beam Shear Diagram

Figure 3.5 Equilibrium of Interior Beam-Column Subassemblage (Paulay, 1989)

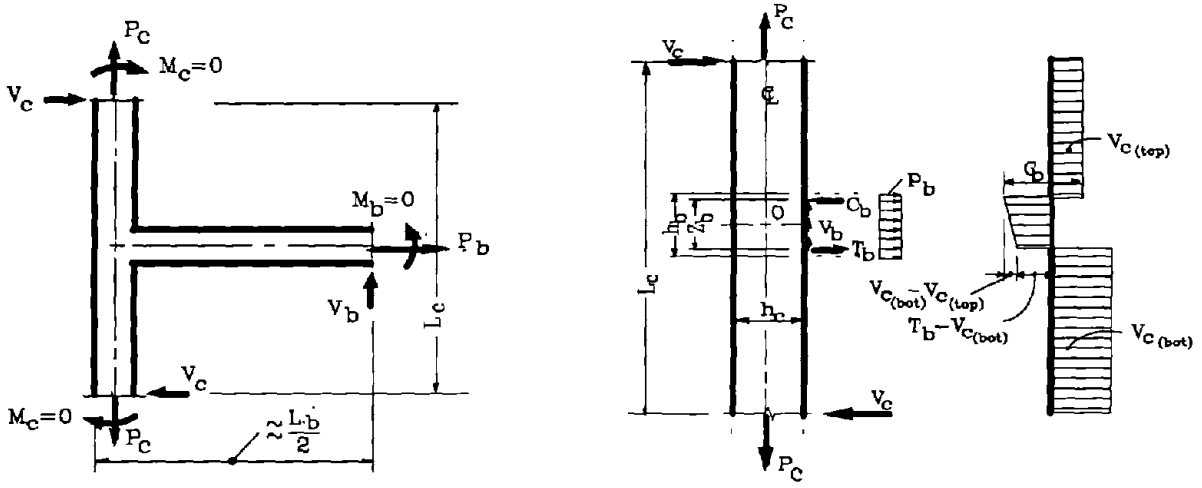

Figure 3.6 Equilibrium of Exterior Beam-Column Subassemblage

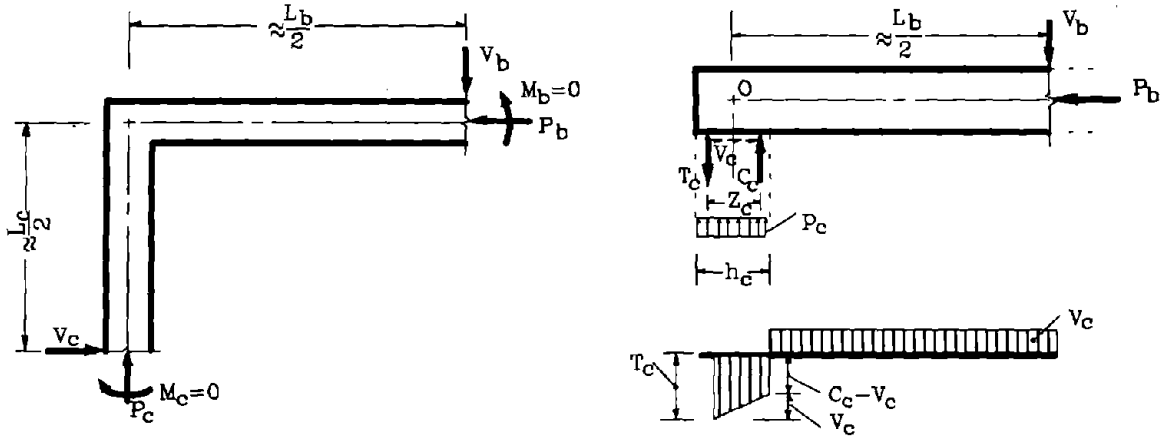

Figure 3.7 Equilibrium of Interior Top Floor Beam-Column Subassemblage

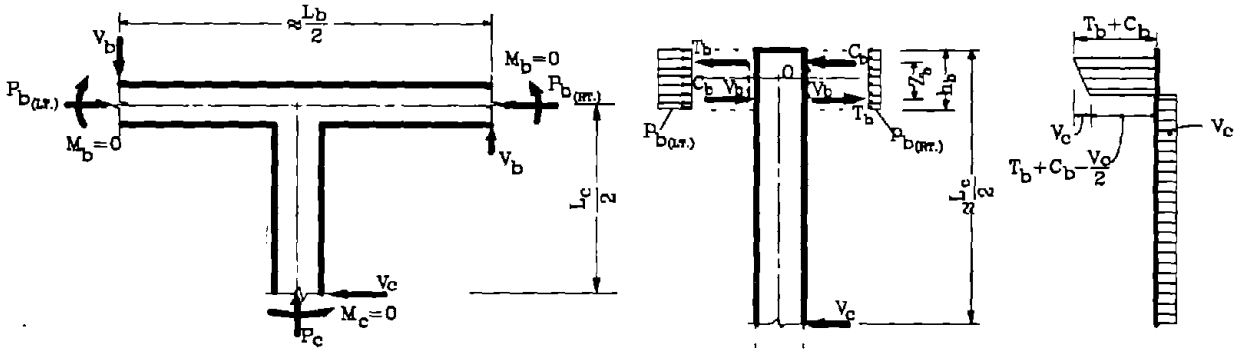

Figure 3.8 Equilibrium of Exterior Top Floor Beam-Column Subassemblage

Table 3.1 Summary of Induced Joint Shear

Location of joint	Joint Shear	Moment to Induce Joint Shear Failure* 12" Columns ($Z_c \approx 9$")	15" columns ($Z_c \approx 12$")
Interior Joint	$V_{jh} = \frac{2M_b}{Z_b} - \frac{2M_b}{l_c\left(1 - \frac{h_c}{l_b}\right)}$	$M_b \leq 9.0(V_{jh})_u$	$M_b \leq 9.1(V_{jh})_u$
	$V_{jv} = \frac{2M_c}{Z_c} - \frac{2M_c}{l_b\left(1 - \frac{h_b}{l_c}\right)}$	$M_c \leq 4.7(V_{jv})_u$	$M_c \leq 6.4(V_{jv})_u$
Exterior Joint	$V_{jh} = \frac{M_b}{Z_b} - \frac{M_b}{l_c\left(1 - \frac{h_c}{l_b}\right)}$	$M_b \leq 18.0(V_{jh})_u$	$M_b \leq 18.1(V_{jh})_u$
	$V_{jv} = \frac{2M_c}{Z_c} - \frac{M_c}{l_b\left(1 - \frac{h_b}{l_c}\right)}$	$M_c \leq 4.6(V_{jv})_u$	$M_c \leq 6.2(V_{jv})_u$
Interior Top Floor Joint	$V_{jh} = \frac{2M_b}{Z_b} - \frac{M_b}{l_c\left(1 - \frac{h_c}{l_b}\right)}$	$M_b \leq 8.5(V_{jh})_u$	$M_b \leq 8.5(V_{jh})_u$
	$V_{jv} = \frac{M_c}{Z_c} - \frac{M_c}{l_b\left(1 - \frac{h_b}{l_c}\right)}$	$M_c \leq 9.5(V_{jv})_u$	$M_c \leq 12.8(V_{jv})_u$
Exterior Top Floor Joint	$V_{jh} = \frac{M_b}{Z_b} - \frac{M_b}{2l_c\left(1 - \frac{h_c}{l_b}\right)}$	$M_b \leq 18.0(V_{jh})_u$	$M_b \leq 17.0(V_{jh})_u$
	$V_{jv} = \frac{M_c}{Z_c} - \frac{M_c}{2l_b\left(1 - \frac{h_b}{l_c}\right)}$	$M_c \leq 9.2(V_{jv})_u$	$M_c \leq 12.4(V_{jv})_u$

*Note: $l_b = 216$", $l_c = 144$", $Z_b \approx 16$", $h_b = 18$", $h_c = 12$" & 15"

Figure 3.9 illustrates the effective joint dimensions for both vertical and horizontal shear.

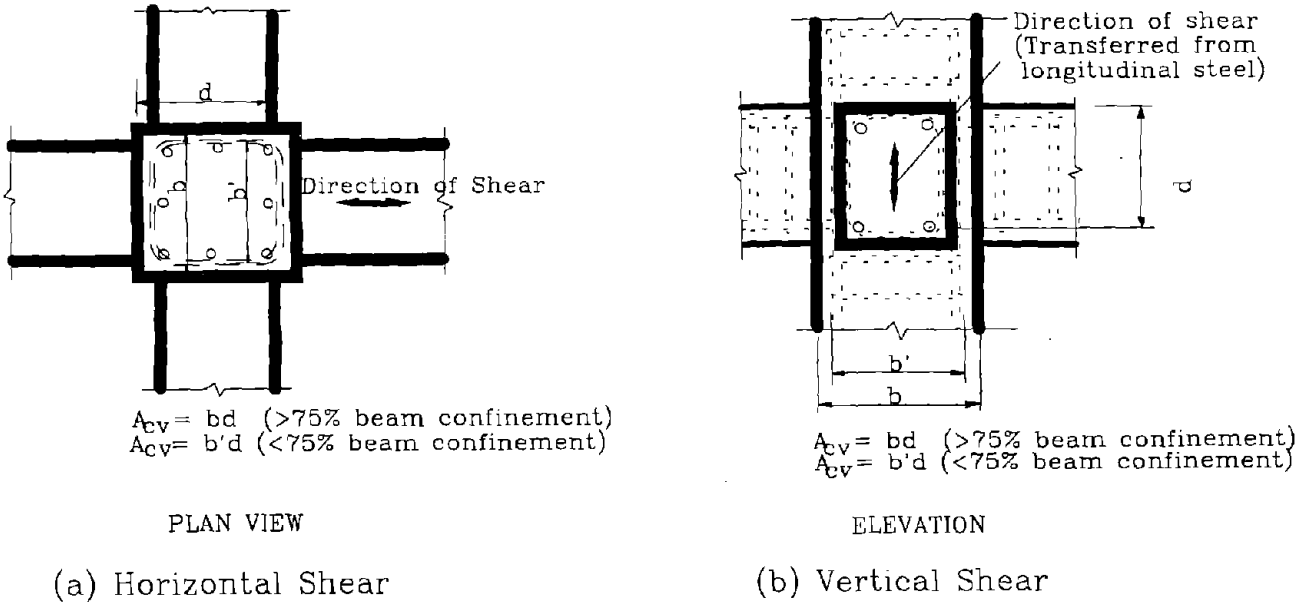

Figure 3.9 Determination of Effective Shear Area

An equation for the contribution of transverse steel is presented below though, for the purpose of this study, a comparison of unreinforced joints versus "fully" reinforced joints is all that was desired. That is, the effect in the overall structural behavior from assuring that flexural members reach their capacity (fully reinforced) as compared to the case in which joint hinging occurs and load redistribution takes place (unreinforced) was attempted to be modelled. This means that the influence of the steel need not be quantified because it is assumed, for the purpose of computer modelling, that the steel provided is such to assure flexural hinging of framing members prior to joint shear failure. Nonetheless, for the purpose of showing illustrative examples of details with adequate transverse reinforcement within the joint, the steel contribution must be quantified.

The contribution of steel can be estimated from ACI-318 equations as:

$$V_s = \frac{A_s F_y (\sin\alpha + \cos\alpha)\, d}{s} \tag{3.15}$$

for transverse hoops. Or simply:

$$V_s = \Sigma A_s F_y (\sin\alpha + \cos\alpha) \tag{3.16}$$

for longitudinal bars bent diagonally through the joint for shear resistance, where:

A_s = Area of steel provided for shear resistance

F_y = Yield strength of steel

α = angle of inclination of shear steel

s = spacing of transverse reinforcement through the joint

d = effective depth of section in direction of shear (see Fig. 3.9)

Two examples of beam-column joints with additional steel provided through the joint to which is intended to insure "full capacity" are presented in Fig. 3.10 and 3.11 and are subsequently analyzed for joint capacity.

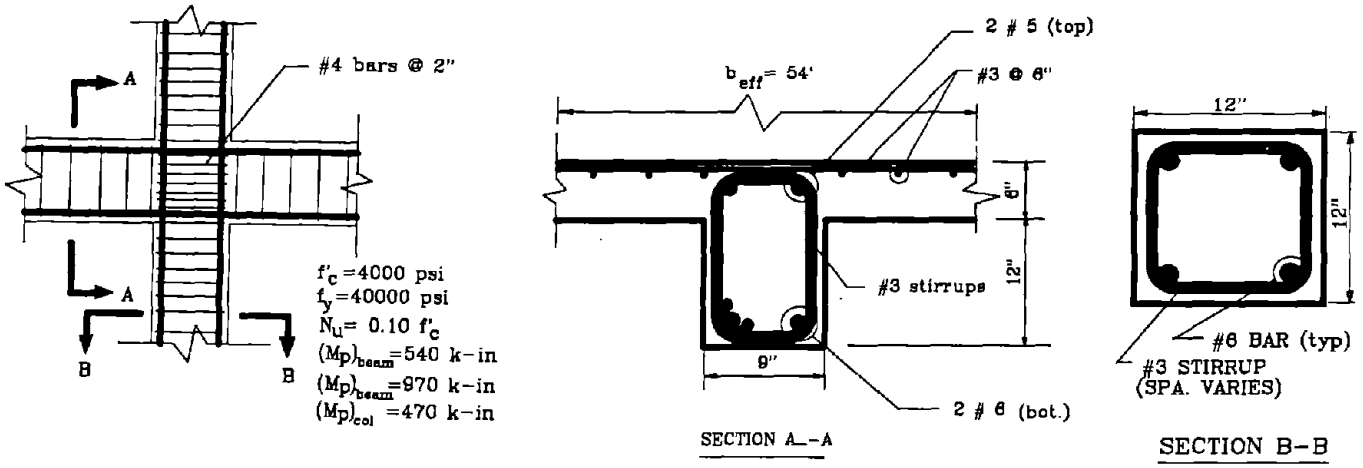

Figure 3.10 Fully Reinforced Joint Using Transverse Hoops

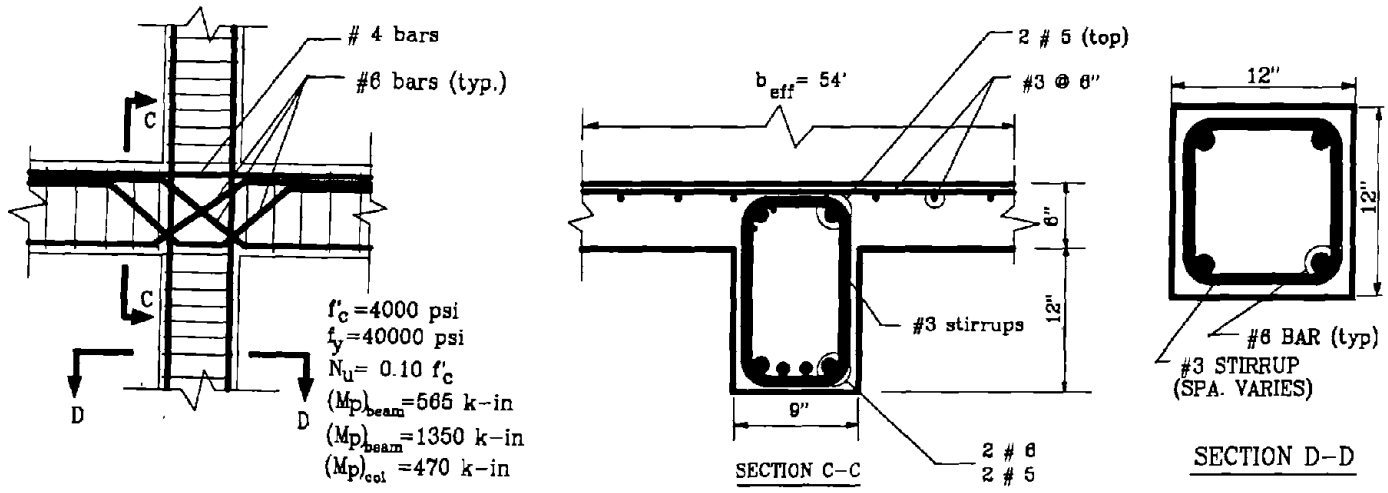

Figure 3.11 Fully Reinforced Joint Using Diagonal Longitudinal Bars

The maximum induced vertical shear that may occur in a joint occurs during the formation of a column sidesway mechanism (see Fig. 3.12) and can be calculated by Eq.(3.8). Using dimensions and moment capacities shown in Figures 3.10 and 3.11, we obtain:

$$(V_{jv})_{\max} = \frac{2(470k \cdot \text{in})}{9"} - \frac{2(470k \cdot \text{in})}{216"\left(1 - \frac{18"}{144"}\right)} = 99.5\ kips$$

The maximum induced horizontal shear that may occur in a joint occurs during the formation of a beam sidesway mechanism (see Fig. 3.13) and can be calculated by Eq.(3.12). Using dimensions and moment capacities shown in Fig. 3.10, we obtain:

$$(V_{jh})_{\max} = \frac{(540k \cdot \text{in} + 970k \cdot \text{in})}{16"} - \frac{(540k \cdot \text{in} + 970k \cdot \text{in})}{144"\left(1 - \frac{12"}{216"}\right)} = 83.3\ kips$$

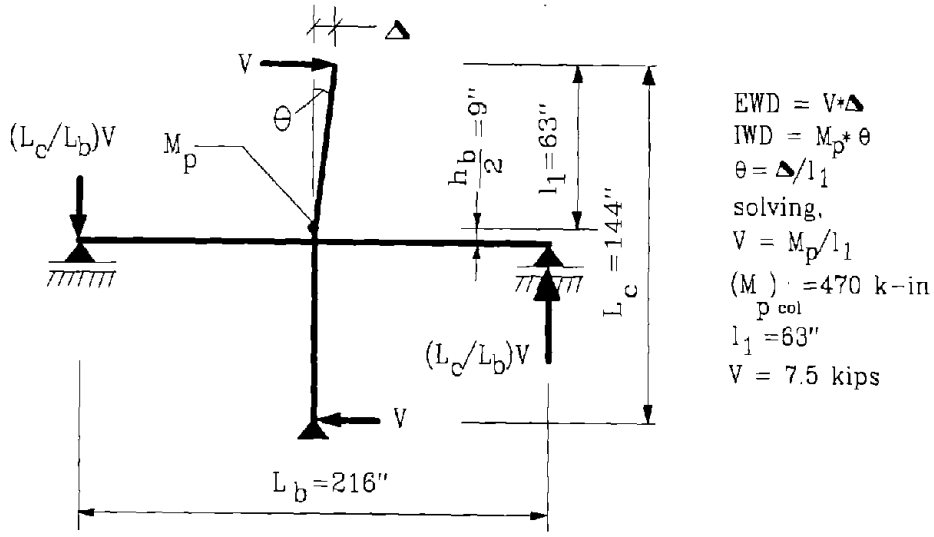

Figure 3.12 Column Sidesway Mechanism

Similarly, using dimensions and moment capacities shown in Fig. 3.11, we obtain:

$$(V_{jh})_{\max} = \frac{(565k \cdot \text{in} + 1350k \cdot \text{in})}{16"} - \frac{(565k \cdot \text{in} + 1350k \cdot \text{in})}{144"\left(1 - \frac{12"}{216"}\right)} = 105.6\ kips$$

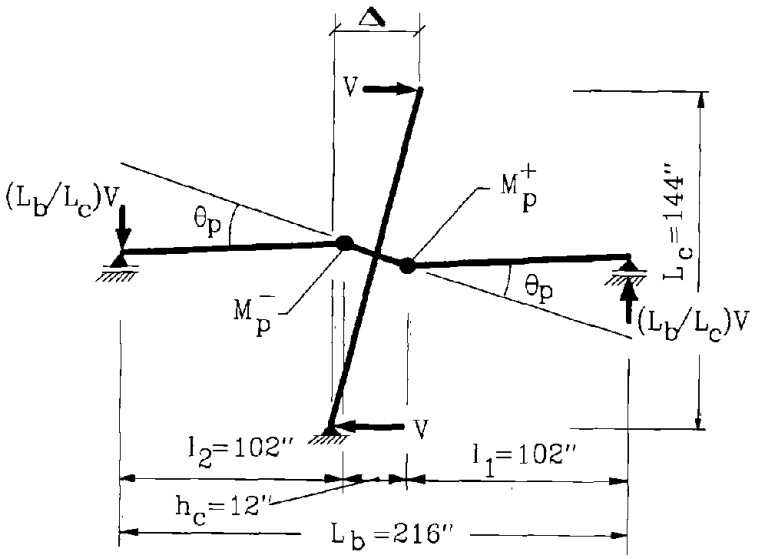

EWD = V*Δ

IWD = $(M_p^+ + M_p^-)*\theta$

$\theta = \Delta / l_1$

solving,

$$V = \frac{(M_p^+ + M_p^-)L_b}{2*L_c l_1}$$

Fig. 3.10:

M_p^+=540 k-in

M_p^-=970 k-in

V = 11.1 kips

Fig. 3.11:

M_p^+=565 k-in

M_p^-=1350 k-in

V = 13.9 kips

Figure 3.13 Beam Sidesway Mechanism

For these maximum induced shears to be transmitted through the joint, sufficient shear strength must be present. Joint shear strength can be estimated by adding the contribution of shear strength provided by the concrete to that provided by the steel.

$(V_{jh})_n = (V_c)_h + (V_s)_h$ for horizontal shear.

$(V_{jv})_n = (V_c)_v + (V_s)_v$ for vertical shear.

The concrete contribution can be estimated using Eq. 3.14, and conservatively assuming the column axial stress, $N_u/A_g = 0.1(f'_c) = 0.4$ ksi and no transverse beams ($\gamma = 1.0$):

$$(V_c)_h = \frac{3.5(1.4)(1.0)\sqrt{4000(1+0.002(400))}}{1000}(9")(10.5") = 39.3 \ kips$$

$$(V_c)_v = \frac{3.5(1.4)(1.0)\sqrt{4000(1+0.002(400))}}{1000}(9")(16.5") = 61.7 \ kips$$

The steel contribution can be estimated using Eq. 3.14 and 3.15.

For Fig. 3.10 with transverse hoops through the joint:

$$(V_s)_v = (V_s)_h = \frac{(2 \times 0.196\ in^2)(40\ ksi)(\sin 0° + \cos 0°)}{2"} \cdot 9" = 70.6\ kips$$

For Fig. 3.11 with diagonal longitudinal bars through the joint:

$$(V_s)_v = (V_s)_h = (2)\ (0.441\ in^2)(40\ ksi)(\sin 45° + \cos 45°)$$
$$+ (2)\ (0.441\ in^2)(40\ ksi)(\sin(-45°) + \cos(-45°)) = 50.0\ kips$$

Table 3.2 summarizes the joint shear capacities and joint shear forces acting on the two details and indicates whether the details are adequate to insure that a flexural mechanism will form prior to a joint failure mechanism. As indicated in the right hand column of Table 3.2, the joint detail with transverse hoops (Fig. 3.10) had a calculated shear capacity sufficient to insure the full capacity of the framing members. Conversely, the joint detail with the diagonal bar arrangement (Fig. 3.11) had sufficient capacity to allow a column sidesway mechanism to form, but was insufficient in horizontal joint shear strength to insure that the beams reach their full capacity. This deficiency could lead to the formation of an unfavorable joint shear failure mechanism. However, it should be pointed out that due to the strong-beam weak-column nature of both details, an undesirable column-sidesway mechanism would most likely preclude a beam-sidesway mechanism, relieving the joint of additional shear forces, thus under this simplified model, joint failure probably would not have taken place.

Table 3.2 Summary of Joint Forces and Capacities of Sample Details

	Induced Joint Shear (kips)		Concrete Shear Strength Contribution (kips)		Steel Shear Strength Contribution (kips)		Joint Shear Capacity (kips)		Joint Adequacy	
	V_{jh}	V_{jv}	$(V_c)_h$	$(V_c)_v$	$(V_s)_h$	$(V_s)_v$	$(V_{jh})_n$	$(V_{jv})_n$	Hor.	Vert.
Trans. Hoops Through Joint (Fig.3.10)	83.3	99.5	39.3	61.7	70.6	70.6	111.0	132.3	OK	OK
Diagonal Flexural Bars (Fig.3.11)	105.6	99.5	39.3	61.7	50.0	50.0	89.3	111.7	N.G.	OK

It should be noted that the shear capacity formulas presented are semi-empirical, pertain to idealized models, and are subject to a limited degree of experimental reproducibility. However for the purpose of this research, in which overall effects of structures with totally unreinforced joints are to be compared to those with "fully" reinforced joints, the ACI Committee 352 equation for concrete shear strength (Eq. 3.13) proves to be a useful estimation.

3.4 Modelling of Confinement

Yet another feature characteristic of gravity-load-designed structures is the omission of transverse steel in flexural members for the purpose of core concrete confinement. Transverse steel in gravity-load details is generally designed to resist shear forces. The need for additional hoops for confinement and ductility is generally not considered, since the philosophy behind gravity-load-design is to prevent a mechanism from forming and maintain the ability to safely transmit gravity loads to the ground. Thus under vertical loading, even if beam hinging occurs near the joint face, hinge rotations will be small due to the flexural stiffness provided from the now simply supported mid-span region. However, under strong lateral loading, once beam hinging occurs, beam end rotations of the same direction may be very large since the beam provides no additional stiffness in the lateral direction. Subsequently, the concrete in the hinge region is subjected to large strains, and without proper confinement, this concrete may not be able to develop it's full confined strength without crushing. This crushing of the core concrete is a brittle fracture failure and is much less tolerable than the slow ductile failure associated with flexural yielding. Hence, additional steel must be provided for confinement, and subsequently, the need to estimate the effect of confinement on ductility have become evident.

The effect of transverse steel on ultimate curvatures has generally been estimated using empirical correlations to volumetric reinforcing ratio, or charts developed from a handful of tests. This would still prove to be a good representation of the effect of hoop steel, however, more theoretically exact methods were determined to be preferable for the purpose of this study. For this research, a computer program (Mander, 1983), employing a fiber model analysis, was used, to capture the effects of varying the transverse reinforcing ratio on the ultimate curvature. The program divides a specified cross section into numerous layers of finite depth distinguishing between cover and core concrete (using unconfined vs. confined properties) and employing equilibrium and strain compatibility considerations to calculate the moment-curvature relation in an iterative process.

A comparison of the ultimate curvature obtained from the computer program to that obtained from accepted hand calculated methods was made, not only to verify the results of the program, but to serve as a guide to choosing ultimate curvatures for input in the program IDARC. Example 6.2 in Park and Paulay (1974) was used to serve as a comparison for the ultimate curvatures obtained from the above-mentioned program and those obtained from an accepted hand calculation method. The hand calculation method was developed by Park and Paulay and utilizes the familiar α, γ and Z parameters for obtaining the compressive force in the confined concrete and the internal moment arm.

Fiber Model Analysis (Mander, 1983): $\phi_u = 0.00175\ rad/in$

Park & Paulay (1974): $\phi_u = 0.00133\ rad/in$

Therefore, $\phi_u / \phi_{fiber} = 0.76$

Numerous levels of confinement were modelled, and it was determined that, for the clarity of this research, the terms poor, fair and well would be used to indicate the level of confinement. A condensed summary of the hoop spacing that corresponds with the terms poor, fair and well confined is as follows:

Poorly confined:

3 bars @ 12" (12" columns)
3 bars @ 15" (15" columns)
3 bars @ 12" (18" T-beams)

Fairly confined:

3 bars @ 8" (12" columns)
3 bars @ 8" (15" columns)
3 bars @ 8" (18" T-beams)

Well confined:

3 bars @ 3" (12" columns)
3 bars @ 4" (15" columns)
3 bars @ 4" (18" T-beams)

3.5 Calibration of Hysteretic Parameters

The hysteretic parameters, α, β & γ incorporated in the IDARC program to respectively model stiffness degradation, strength degradation and pinching behavior have been calibrated with experimental test results. The hysteretic behavior of selected critical members as well as the overall dynamic response of scaled models of a typical structural system have been used in an attempt to realistically model these parameters.

3.5.1 Calibration of Hysteretic Parameters for Overall Structural Response

A three-story one-third scale reinforced concrete model was built and dynamically tested at the University of Buffalo (Bracci et al., 1992). The 1952 (N 21 E) Taft earthquake scaled to a peak ground acceleration of 0.20 g was used as the input acceleration for one of the tests. Displacement time histories were recorded for each story level. The displacement time history of the three story model was later simulated using the IDARC computer program. All moment-curvature properties of the one-third scale building were calculated and modelled in the same manner as outlined in the previous discussions. The hysteretic parameters were adjusted in an attempt to match the displacement response obtained from the computer simulation to that observed in the experimental test. As can be seen from Fig. 3.14, the computer simulation proved to be reasonably accurate and thus the set of hysteretic parameters used was essentially calibrated to yield an accurate dynamic response.

3.5.2 Calibration of Hysteretic Parameters for Individual Members

The same three story scale model (Bracci et al., 1992) mentioned earlier was subjected to the 1952 Taft earthquake record at a scaled peak ground acceleration of 0.20 g in one of the earlier tests. The building was constructed with load cells located in the columns at midheight so axial forces, shears and moments could be recorded at these locations. Potentiometers were placed in strategic locations prior to testing to allow the deformations of specific locations (or cross sections) to be recorded at intervals of 0.01 seconds. Subsequent to the test, moments and curvatures of various members at specific cross sections were calculated from the data recorded from the load cells and potentiometers at the recording interval.

Again, the program IDARC was used to model and simulate the observed experimental behavior. As can be seen in Fig. 3.15, the moment-curvature histories obtained from the computer program reasonably simulate those obtained from the actual test. The identified parameters were used in the analysis of existing nonductile RC buildings. These parameters had to be modified subsequently for cases where the detailing configurations were enhanced. A discussion of the changes will be presented in Section 6.

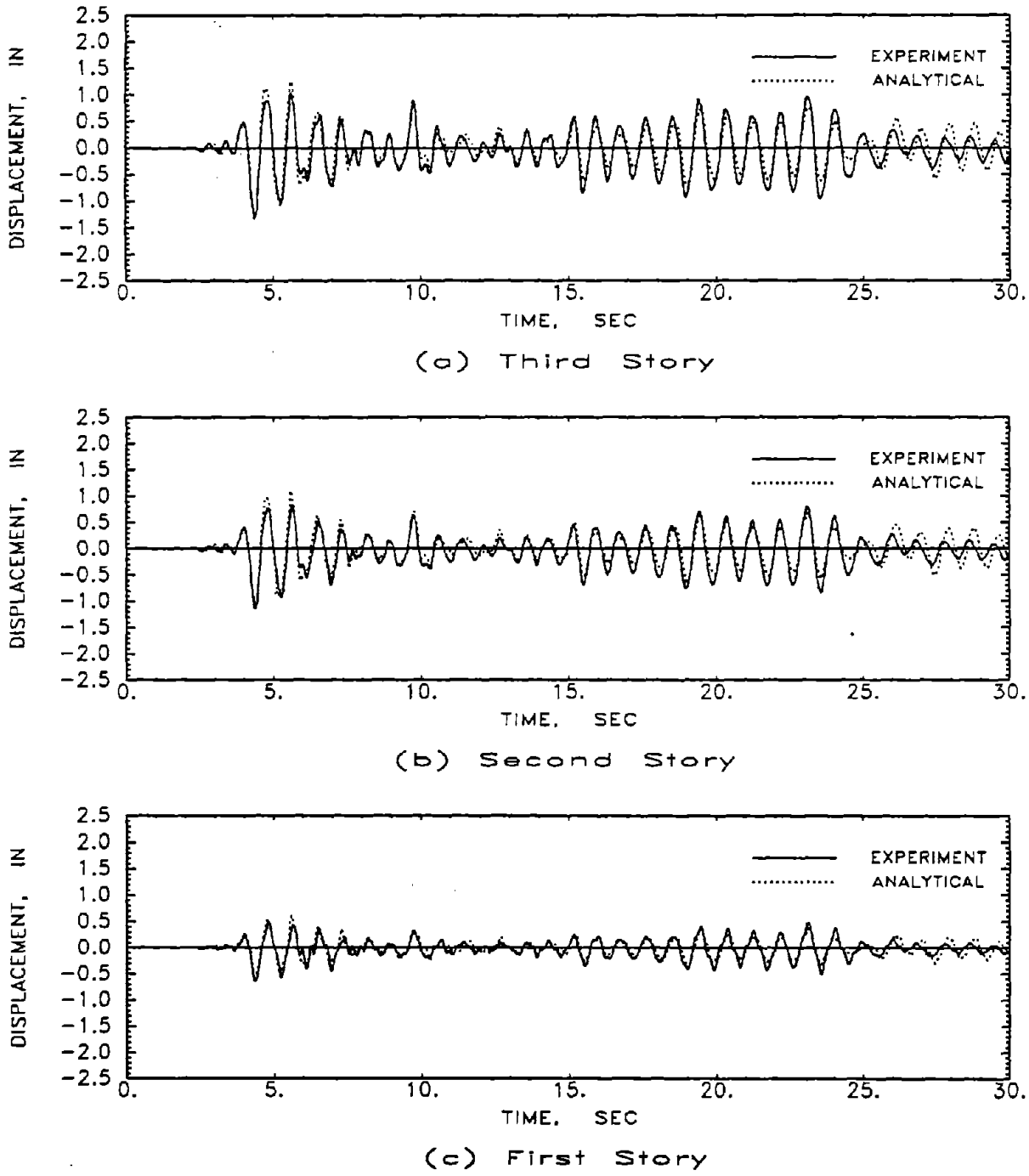

Figure 3.14 Time History Comparison of Three-Story Model

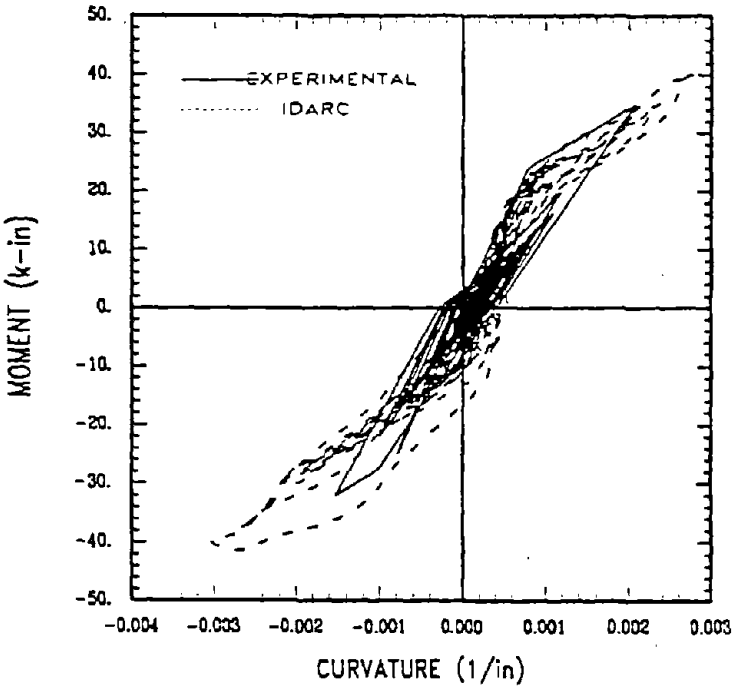

(a) Typical Interior Column

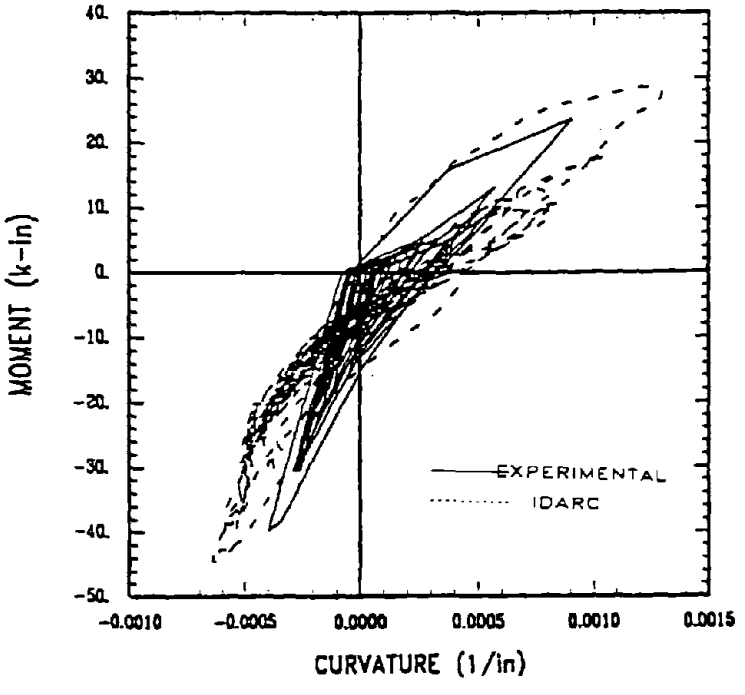

(b) Typical Exterior Beam

Figure 3.15 Moment-Curvature Comparison of Three Story Model

SECTION 4

EVALUATION METHODOLOGY

4.1 Selection of Ground Motions

Seismic activity in eastern and central United States is not well defined given the relatively smaller magnitudes and considerably fewer occurrences. However, it should be noted that while the ratio of peak ground acceleration of maximum credible to maximum expected earthquake is about 5:4 in the western United States (Whitman[1]), the same ratio could be as high as 6:1 in the east coast (for critical facilities). This amounts to saying that the degree of damage from a maximum credible earthquake in a region of low seismicity can be much higher than the induced damage of a maximum credible earthquake in a region of high seismicity.

Several East Coast records were considered (Saguenay, Painsville, Goodnow, etc.), however, these earthquakes generally have predominant periods between 0.3 and 0.7 seconds. This band of predominant periods was too narrow for this study, in which buildings with periods ranging from 0.7 to 1.8 seconds were being studied. In an attempt to attain meaningful results from the analysis of each building using the same input ground motion, accelerograms were selected which had a broad range of fundamental periods within the amplified region of the response spectra. Four separate earthquake records were chosen for the evaluation.

It has been suggested that the 1985 Nahanni earthquake, which actually occurred in the Northwest territories of Canada, may be considered as a typical earthquake in the northeast region of the United States (Papageorgiou, 1987). Inclusion of a typical Eastern North American earthquake within this research was necessary to verify the assumption that existing non-seismically detailed RC structures are under a significant risk of suffering severe damage from even "typical" earthquakes. This should not be misinterpreted to say that existing Eastern structures are only in risk from seismic events of a moderate magnitude, such as the Nahanni earthquake. On the contrary, some seismologists do contend that earthquakes of significantly higher energy content cannot be ruled out. Hence, it was decided to include in the evaluations a more significant earthquake with higher energy content.

For this study, the Nahanni earthquake record was scaled to a peak ground acceleration (PGA) of 0.20 g to correspond with the stipulation that this is the level of the maximum "credible" earthquake in many regions of interest in the East. Figure 4.1 shows the Nahanni accelerogram and the response spectrum corresponding to PGA of 0.20 g.

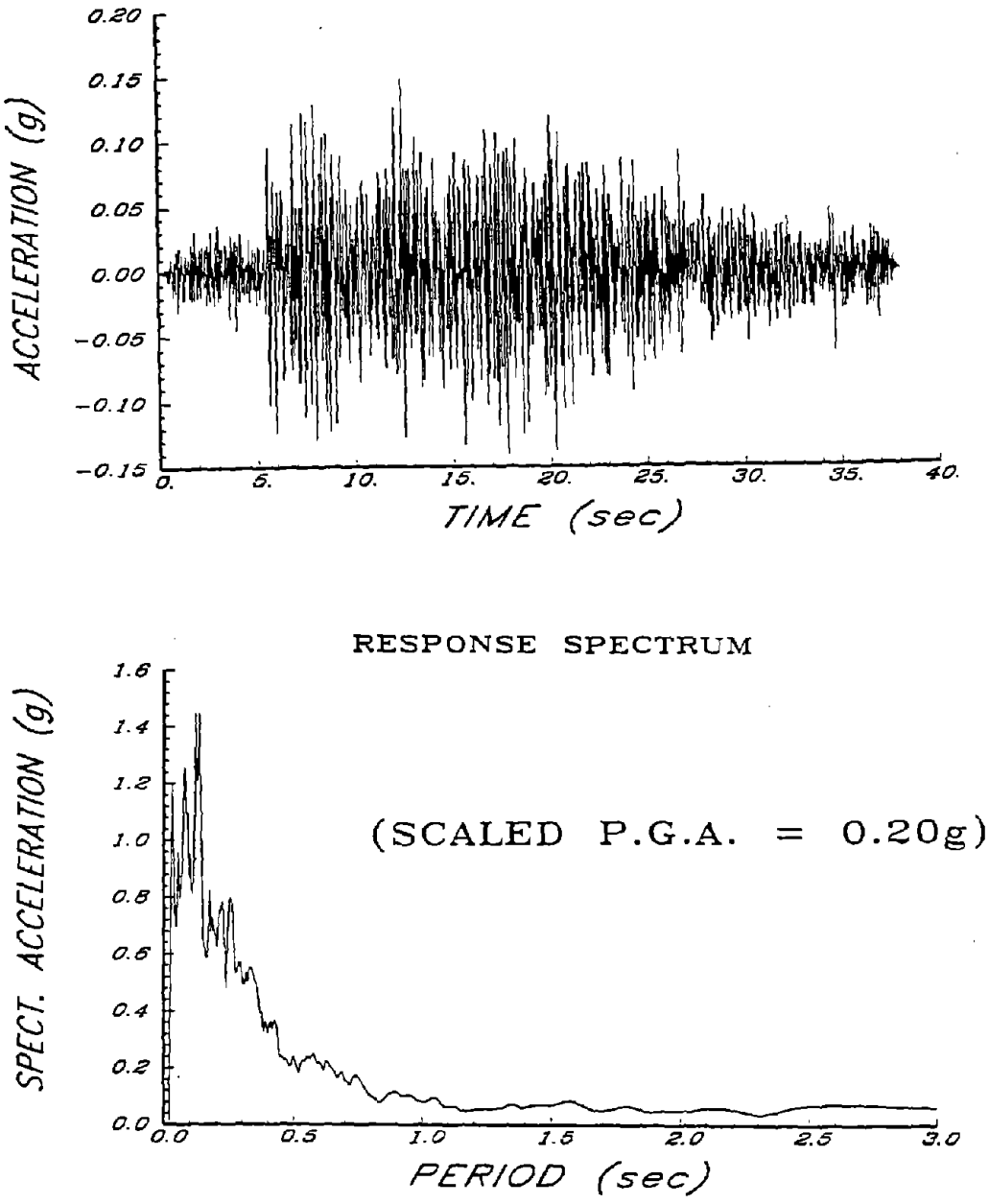

Figure 4.1 Time History and Response Spectrum of the 1985 Nahanni Earthquake

The second seismic record considered for evalaution was an artificial earthquake generated to fit the specifications of the UBC (1988) design spectrum. Since routine seismic design in many regions is performed with the assistance of the UBC design spectrum or equivalent, it is of interest to examine levels of story shear and drift obtained with a spectrum-compatible accelerogram. The artificial earthquake was constructed using the computer program SIMQKE (Gasparini and Vanmarke, 1976) which utilizes input of spectral velocity for various periods to construct a ground motion time history that would produce such a response spectrum. In contrast to analyses performed

using the actual earthquake records scaled to 0.20 g, the artificial earthquake was scaled to a PGA of 0.15 g which would correspond to a maximum spectral acceleration of 0.30 g. Figure 4.2 shows the artificial earthquake and its spectrum.

The first set of two records would correspond to a "moderate" earthquake, which may very well be in the order of magnitude of the maximum "probable" earthquake in many regions of low to moderate seismicity.

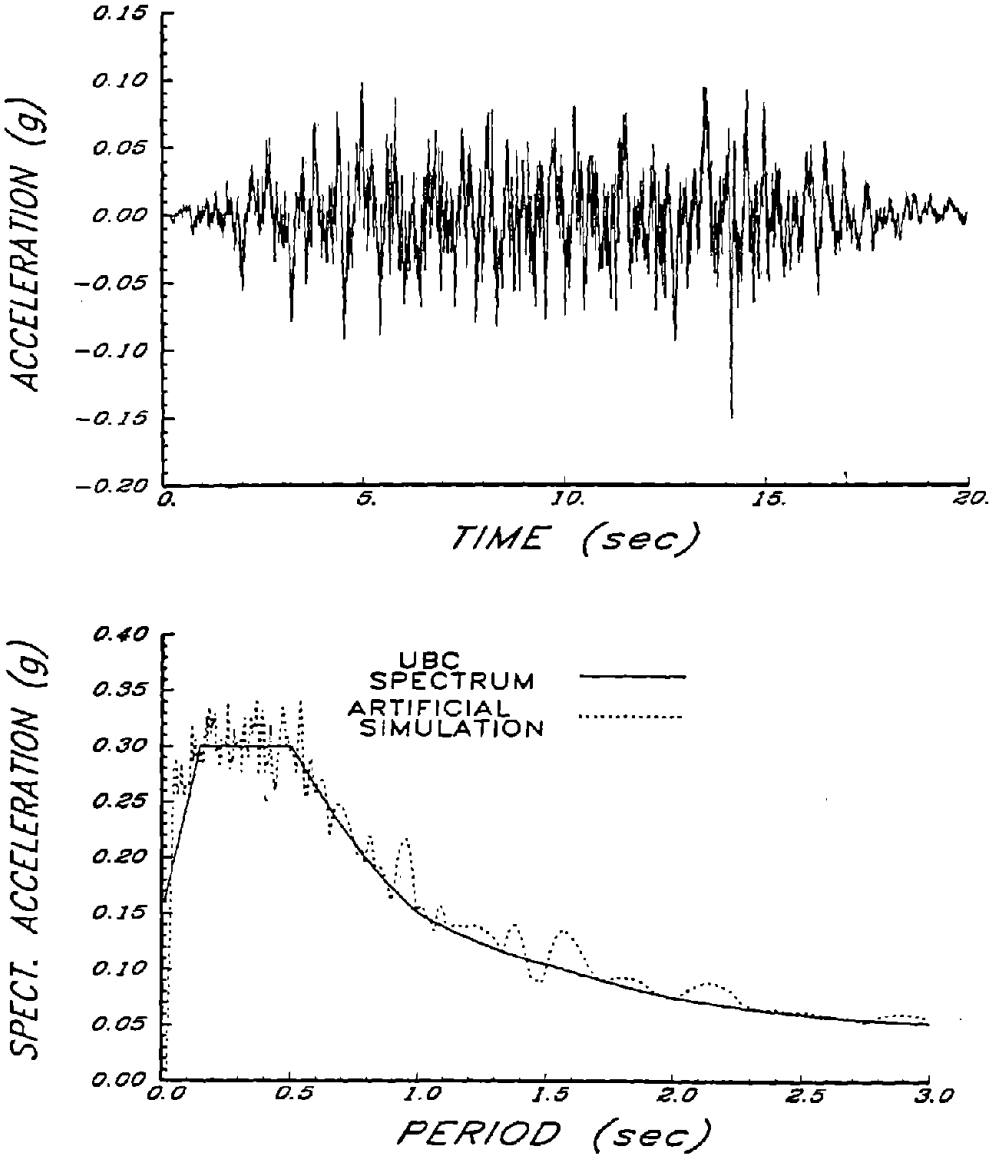

Figure 4.2 Time History and Response Spectra for Artificial Earthquake

As pointed out earlier, it was also the intent of this study to evaluate gravity-load designed buildings under potentially "severe" earthquakes. Results from this latter set of evaluations would also be useful in zones of moderate to high seismicity, where there still exist a stock of older buildings without proper seismic detailing. For this purpose, the 1940 El Centro (S 00 E) and the 1952 Taft (N 21 E) earthquake records were used as typical "severe" earthquakes. Time histories and spectra of the two records are shown in Figures 4.3 and 4.4 respectively.

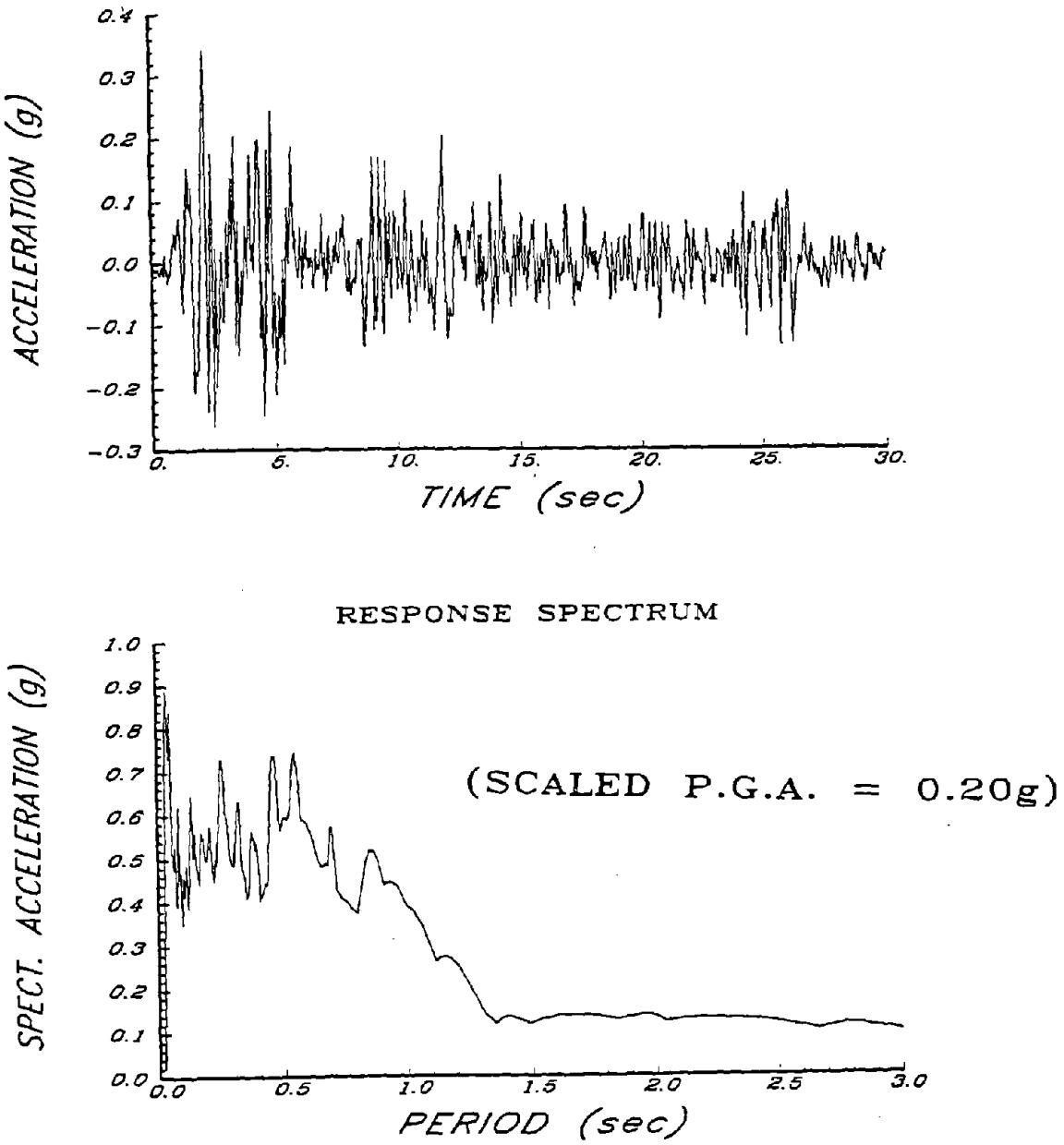

Figure 4.3 Time History and Response Spectrum of the 1940 El Centro Earthquake

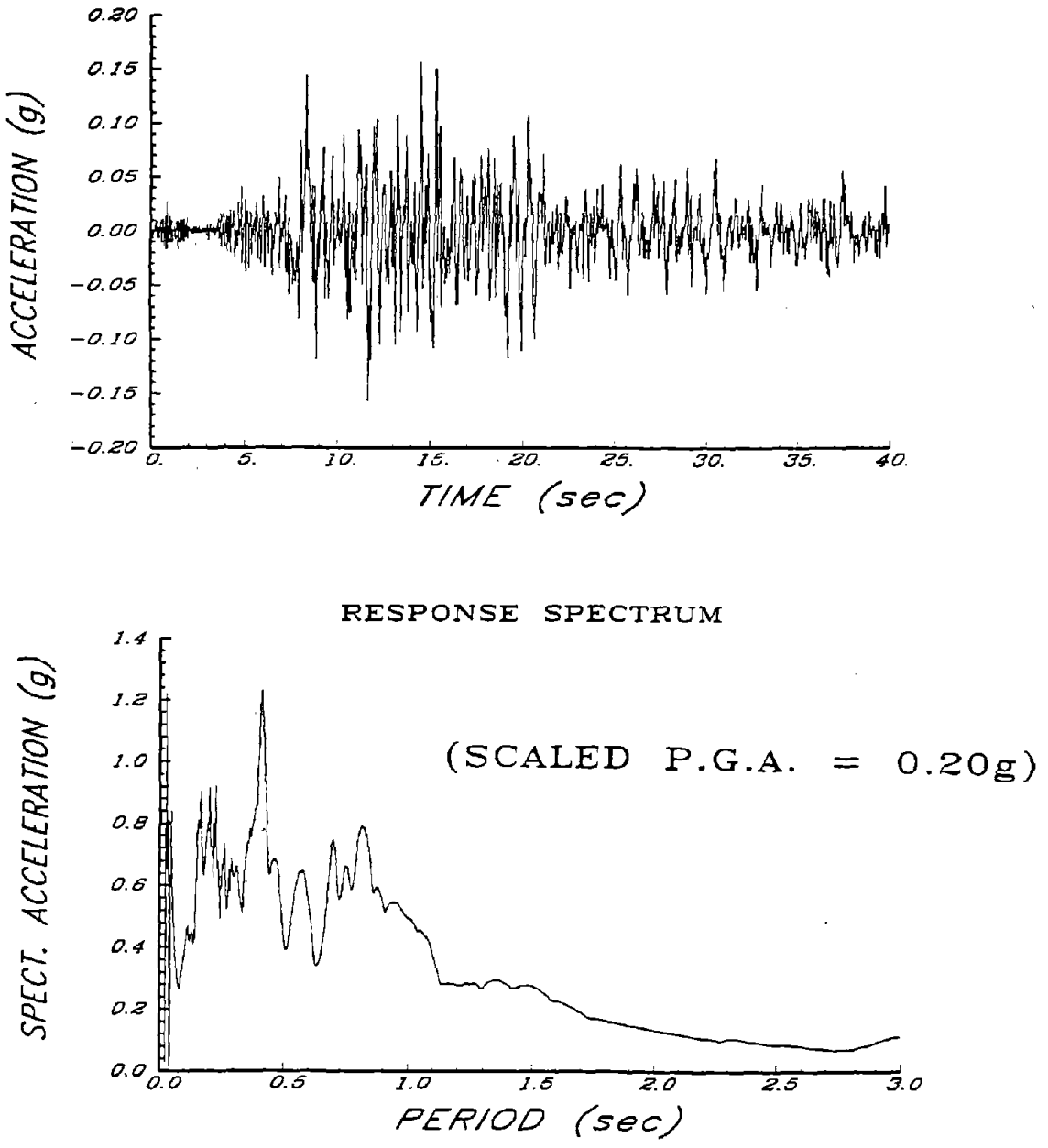

Figure 4.4 Time History and Response Spectrum of the 1952 Taft Earthquake

4.2 Inelastic Time History Analyses

All analyses were performed using the computational tool, IDARC, described earlier in Section 3.1. The duration of the inelastic analysis was selected to be 30 seconds for the analyses performed using the Nahanni, El Centro and Taft records, while a duration of 20 seconds was used with the spectrum-compatible earthquake.

The time step of analysis used for the computer simulations was 0.002 seconds. Since IDARC does not perform an iterative nonlinear analysis, it was necessary to use a small time step to avoid any accumulation of unbalanced forces during the response analysis. Comparisons of analyses performed under much smaller time steps showed nearly no difference in response, thus it was determined that a time step of 0.002 was sufficient for the purposes of this research.

4.3 Damage Modelling

The damage model developed by Park and Ang (1985) has been incorporated into the computer program IDARC which also using a weighting scheme to compute global damage at story levels and for the entire structure. The damage index is calibrated between 0.0 and 1.0, with 0.0 meaning no damage and 1.0 representing total collapse (or failure). The damage index can be separated into two terms, D_1 and D_2. The first term, D_1, represents the deformation damage which is the ratio of maximum deformation to ultimate deformation. The second term, D_2 represents the damage due to dissipated hysteretic energy. Total damage is expressed as the linear combination of these damage components as follows:

$$D = \frac{\delta_m}{\delta_u} + \frac{\beta}{\delta_u P_y} \int dE \tag{4.1}$$

where:

D = Damage index scaling the structural damage from zero to one
δ_m = Maximum deformation of structural element of interest
δ_u = Ultimate deformation of element of interest under monotonic loading
P_y = Yield strength of member of interest
$\int dE$ = dissipated hysteretic energy
β = rate of strength degradation

Story level damage indices and the damage index for the total structure are determined using a weighted average of the individual component damage indices, D_i as follows:

$$D = \Sigma \lambda_i D_i \quad ; \quad \lambda_i = \frac{E_i}{\Sigma E_i} \tag{4.2}$$

where:

λ_i = Energy weighting factor
E_i = Total energy absorbed by each component

The damage index used within the program IDARC has been calibrated based on the correlations made by Anagnostopolous et al. (1989), Park et al.(1985) and Bracci et al.(1989). Based on these descriptions of degrees of damage of various concrete members, their visual appearance and usability, a scale of damage indices has been defined and is presented in Table 3.1 for reinforced concrete beams and columns subjected to cyclic loading.

Table 4.1 Correlation of Damage Indices and Damage States

USABILITY[1]	DEGREE OF DAMAGE[2]	DAMAGE (SERVICE) STATE	LIMIT STATE DAMAGE INDEX	APPEARANCE[3]
(1)	(2)	(3)	(4)	(5)
		Undamaged	0.00	Undeformed/Uncracked
Usable	Slight	Serviceable	0.20-0.30	Moderate cracking
	Minor to Moderate	Repairable	0.50-0.60	Spalling of concrete cover Severe cracking
Temporarily Unusable	Moderate to Severe	Irrepairable		Buckled bars, exposed core
		Collapse	> 1.00	
Unusable	Collapse			Loss of shear/axial capacity

[1] Acc. to Anagnostopoulous et al. (1989)
[2] Acc. to Park et al. (1985)
[3] Acc. to Bracci (1989)

SECTION 5

EVALUATION OF NON-SEISMIC DETAILED STRUCTURE

5.1 Interpretation of Results

Each of the 3, 6 and 9 story structures (Section 2) were analyzed using the four separate earthquake records (Section 4) as input ground motions. The fundamental period and maximum base shear coefficient, expressed as a fraction of building weight, obtained from the inelastic static analysis are presented in Table 5.1. Note the relatively high fundamental periods of these buildings which indicate the high flexibility of these moment resisting frame systems.

Table 5.1 Fundamental Periods and Base Shear Coefficients

Building Type	Fundamental Period	Maximum Base Shear Coefficient
3 Story	0.79 s	0.056
6 Story	1.15 s	0.037
9 Story	1.48 s	0.028

From the results of the analysis, the final state of the all three frames are obtained and shown in Figures 5.1 - 5.2. Only the results of the response to the Taft earthquake and the spectrum-compatible record are shown since they represent the typical "moderate" and "severe" seismic events.

It is interesting to note that no uniform mechanism forms in these frames. Damage to the columns is fairly light for the artificial earthquake and significant damage is primarily found in the beams, particularly in lower regions of the structure where many of the columns remained elastic or cracked without yielding. Almost all beams had yielded despite the input ground motion being of a "moderate" intensity (PGA = 0.15 g). This is a result of the low effective capacity of the beams caused by insufficient bar anchorage and inadequate joint capacity.

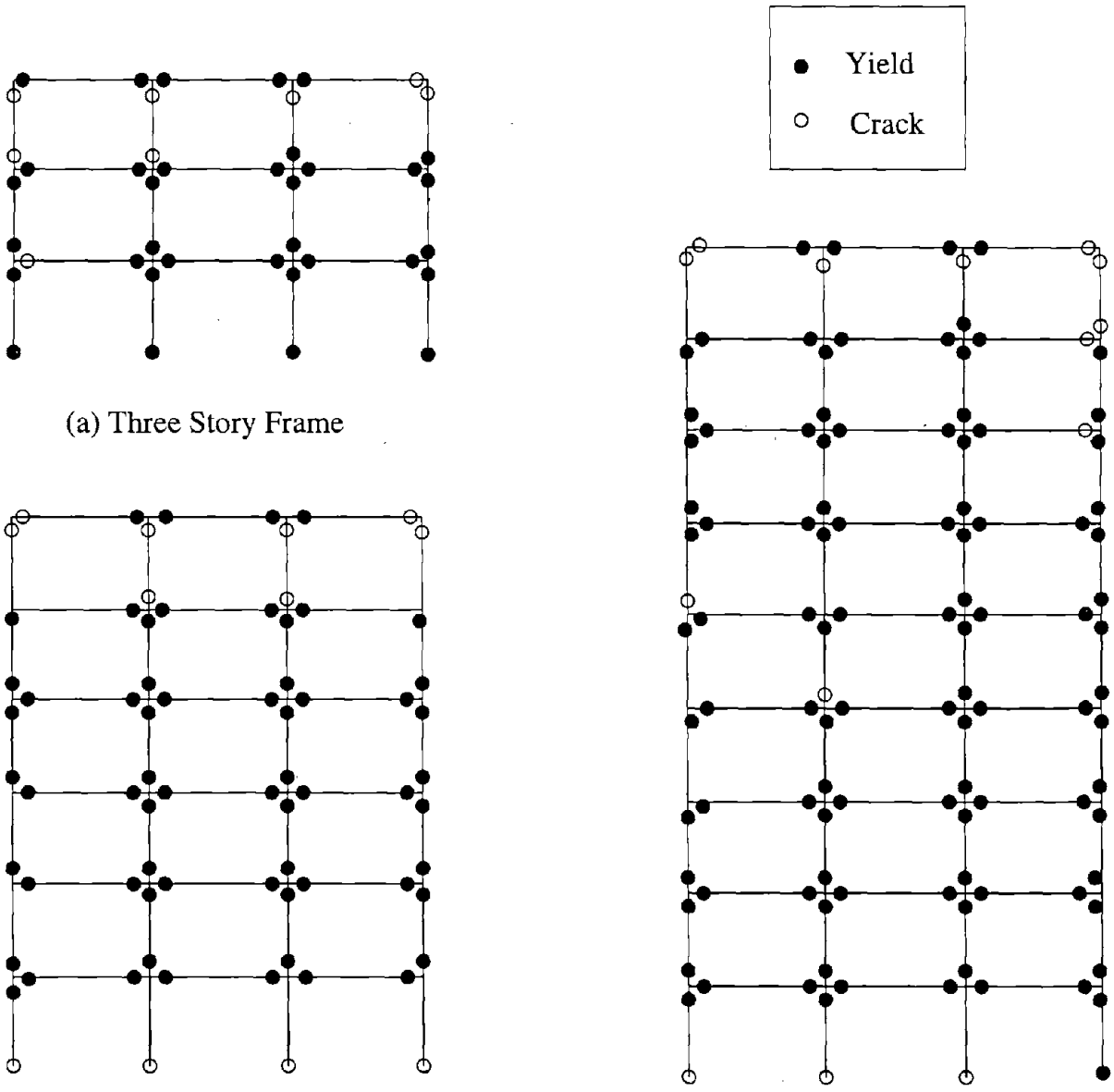

(a) Three Story Frame

(b) Six Story Frame

(c) Nine Story Frame

Figure 5.1 Final State of Frames for Gravity-Load-Designed Frame Subjected To Taft Earthquake (PGA = 0.20 g)

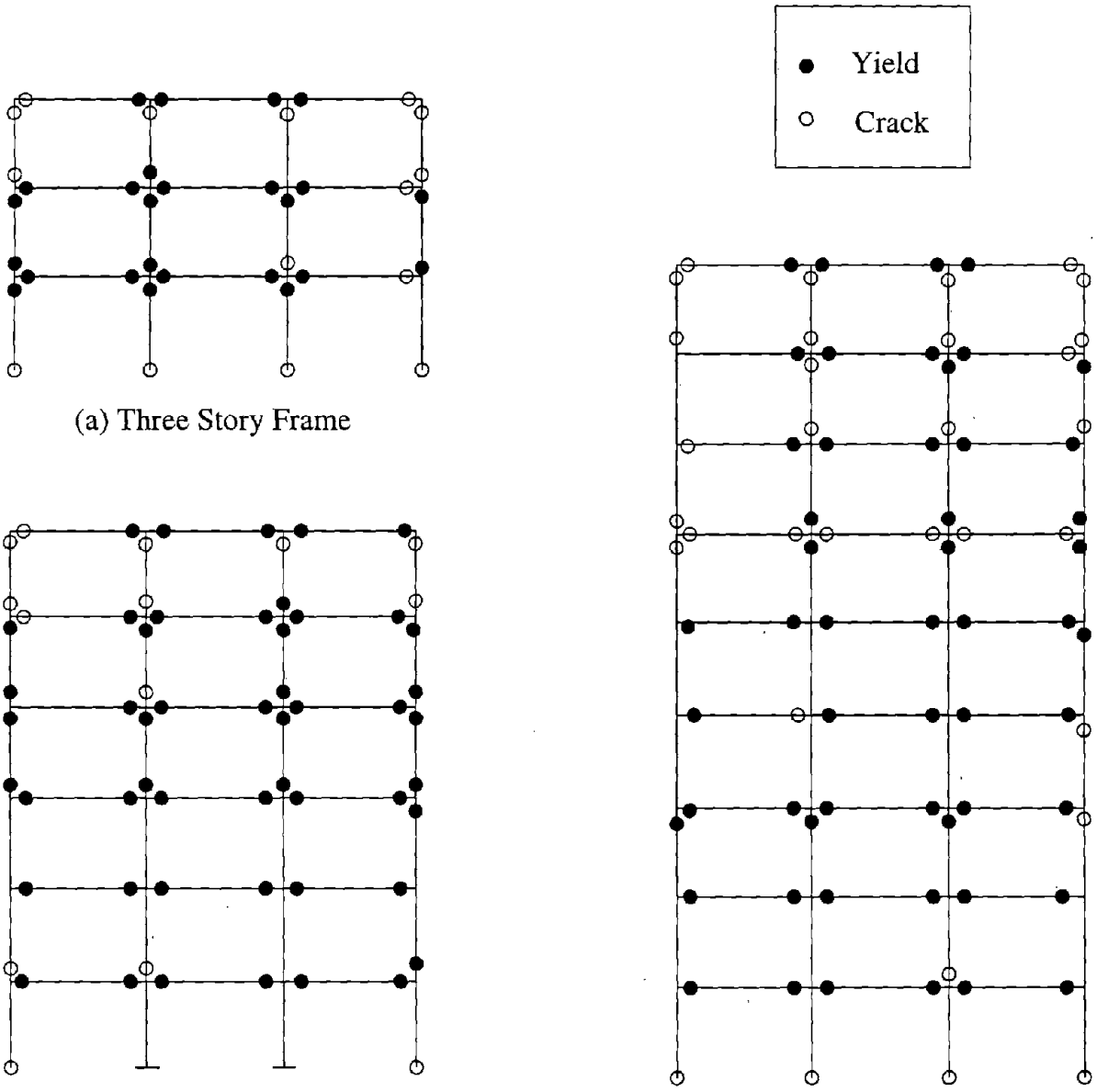

(a) Three Story Frame

(b) Six Story Frame

(c) Nine Story Frame

Figure 5.2 Final State of Frames for Gravity-Load-Designed Frame Subjected To Artificial Earthquake (PGA = 0.15 g)

Inspection of the frames subjected to the Taft earthquake reveals that widespread yielding, which translates into heavy damage, occurred in both columns and beams, with failure or impending collapse for all three structures. During the Taft ground motion, the 6 story structure formed a column sidesway mechanism (soft-story) with the columns hinging just above the third floor level where the transition in column size occurs. The 9 story structure experienced the formation of several column mechanisms, also during the Taft motion. The same detrimental soft-story effect occurred in the same location during the analysis of the 6 story frame using the artificial ground motion, however, the computed drifts and damage do not indicate severe damage.

It was determined that these soft-story effects were attributable to inadequate joint shear strength. Joint shear failure prevents the columns from resisting any additional moment and in essence forms a hinge. Results from the analysis have also indicated that much of the damage incurred by the beams can be attributed to large deformations resulting from the premature hinging of the beams under positive bending. This loss of beam stiffness helped contribute to the large inter-story drifts observed in the frame.

The maximum story drifts obtained, expressed as a percent of story height, are presented in Table 5.2.

Table 5.2 Maximum Inter-Story Drifts

Building Type	Artificial Earthquake PGA = 0.15 g	Nahanni PGA = 0.20 g	El Centro PGA = 0.20 g	Taft PGA = 0.20 g
3 Story:	0.53%	0.31%	1.16%	3.06%
6 Story:	0.95%	0.51%	2.67%	4.47%
9 Story:	0.63%	0.61%	1.17%	1.83%

As indicated by Table 5.2, the maximum story drift occurs during the Taft earthquake in the six story building with a magnitude of 4.47%. This drift took place between the third and fourth story level as did the 2.67% maximum drift from the analysis performed using the El Centro ground motion. This region, just above the third story level, is the location of a column size transition and is where complete column hinging led to a soft story effect resulting in these high story drifts.

The maximum drift observed from analyses performed using the two *moderate* ground motions was 0.95% also occurring in the six story structure in this apparent weak zone between the third and fourth story levels. Observations made from complete story drift profiles (Tables C-2 and C-3 in the Appendix) indicate that maximum story drifts were consistently greater than 0.4% during the artificial earthquake and greater than 0.3% during the Nahanni earthquake.

A complete summary of all story drifts and story shears for analyses of the gravity-load-designed structures performed using all four earthquakes, can be found in Appendix C under the headings 3REAL, 6REAL and 9REAL.

Figures 5.3 and 5.4 display the computed damage in the beams and columns respectively at each story level for all four earthquakes used in the study. A weighted average is used to translate individual member damage to story level damage. These plots easily identify the location and severity of the damaged members as well as giving a comparative indication of the difference in damage intensity between a moderate (say Nahanni) and a severe (say Taft) earthquake. A complete listing of story level damage indices for columns and beams for the gravity-load-designed structures for all four earthquakes can be found in Appendix B under the headings 3REAL, 6REAL and 9REAL.

As can be seen from Fig. 5.3 and 5.4, high levels of damage were present in both the beams and columns after the analysis using the severe earthquakes, Taft and El Centro. For both of these ground motions, it was seen that the damage observed in virtually every element was in the order of 0.5 or greater, especially in the lower story levels. The damage observed in all structures as a result of the severe ground motions corresponds with the damage states of *irreparable* to *collapse* based on the damage correlations previously outlined.

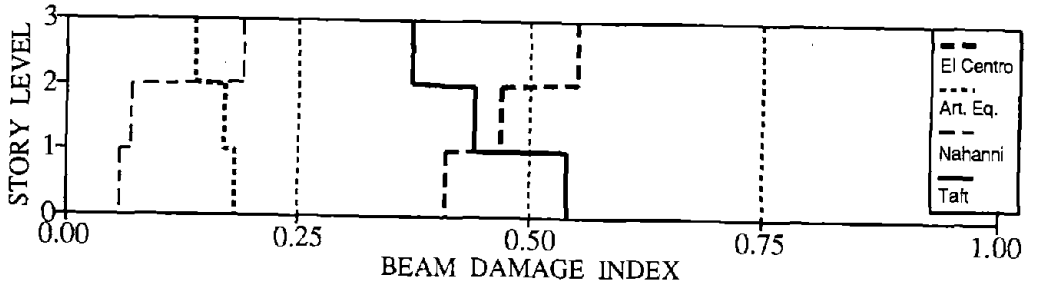

a) 3 STORY FRAME

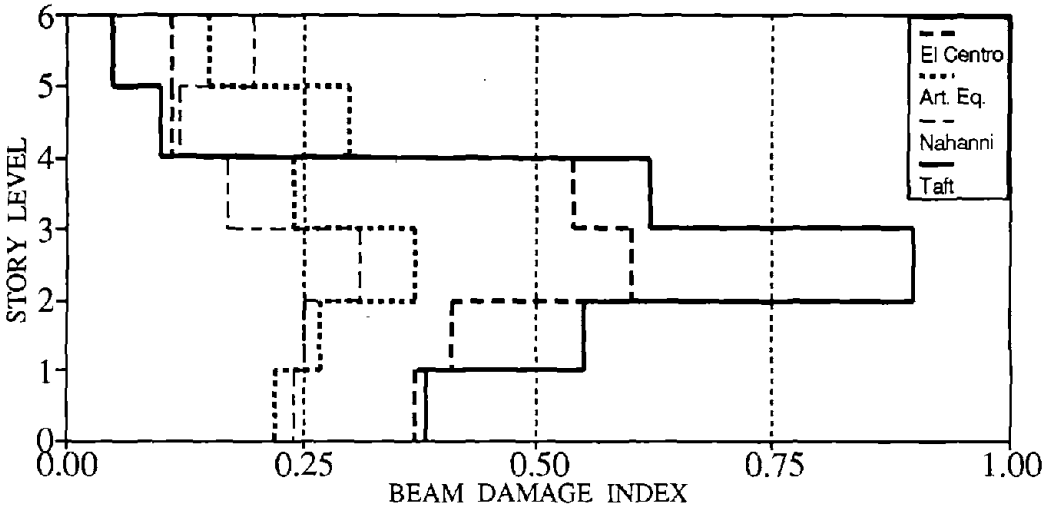

b) 6 STORY FRAME

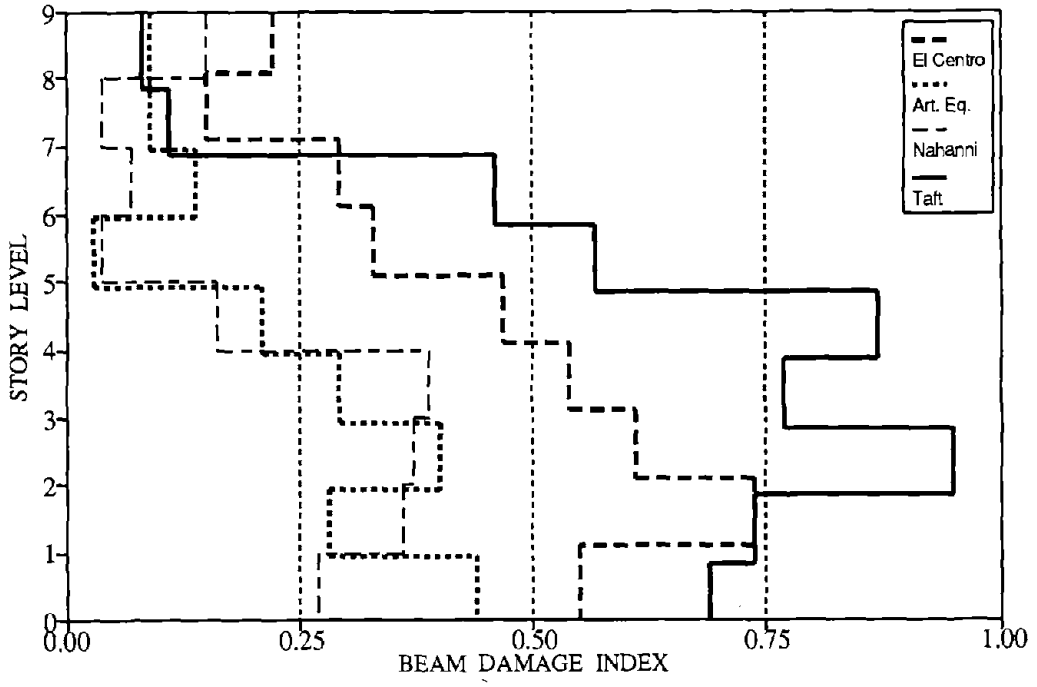

c) 9 STORY FRAME

Figure 5.3 Damage Distribution in Beams of Gravity-Load-Designed Frames

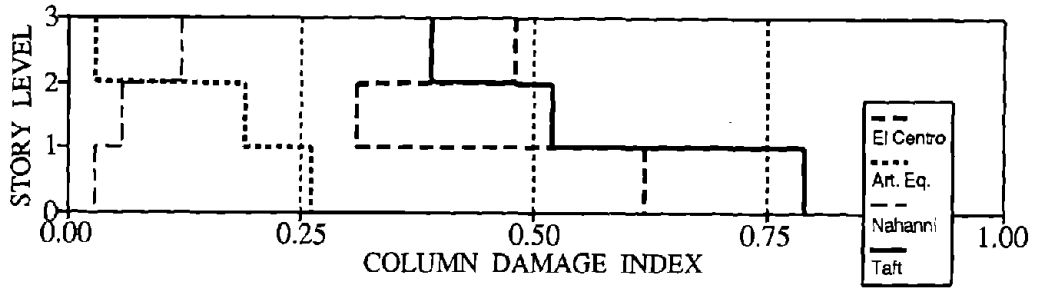

a) 3 STORY FRAME

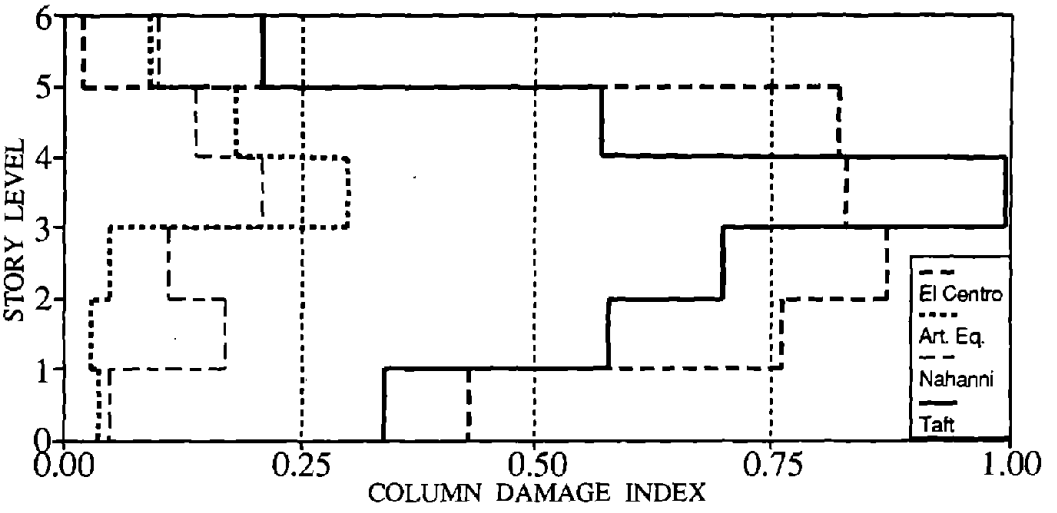

b) 6 STORY FRAME

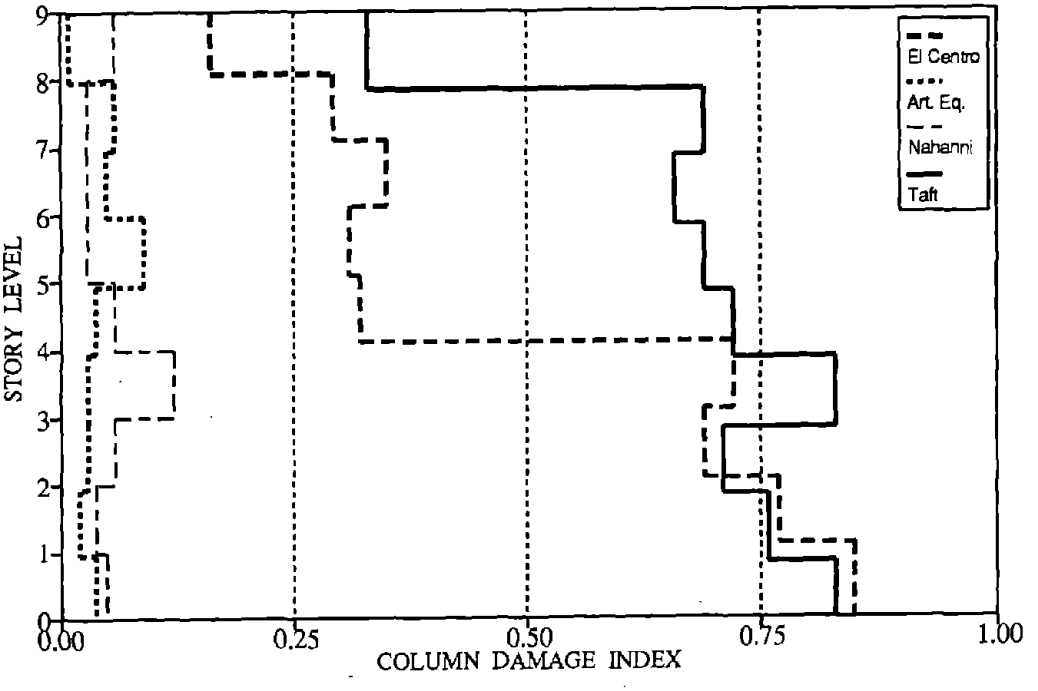

c) 9 STORY FRAME

Figure 5.4 Damage Distribution in Columns of Gravity-Load-Designed Frames

It is further seen that when the building was subjected to a moderate level earthquake, such as Nahanni or the artificial earthquake, the buildings suffered significant but not severe damage. Damage indices in the order of 0.10 - 0.30 were observed in all three structures corresponding to a damage state of *"repairable"*. Of interest to note is that the beams were slightly more damaged than the columns, except in the lower story levels of the nine story structure where beam damage was much greater than column damage. The small column damage in the lower levels of the nine story structure is a clear result of the high column to beam strength ratio in this region. This tends to indicate that inadequate positive moment strength and beam ductility is of greater concern than joint shear strength or column confinement. However, in the upper story levels, where beam and column strengths are much closer, the similar damage values indicate that the damage contribution between beam bar pullout, joint shear failure and poor beam or column confinement is not clearly discernible.

5.2 General Performance of Non-Seismically Detailed Structure

From an overview of the damage plots and the maximum drift for each of the buildings, it is clear that the non-seismically detailed structure, intended to model typical buildings constructed in regions of low seismicity is inadequate to withstand earthquakes of a large magnitude.

However, the adequacy of existing non-seismically detailed structures subjected to moderate ground motions, is less discernable. As can be seen from the damage statistics, these buildings performed reasonably well when subjected to the ground motions of moderate energy content. The maximum inter-story drifts observed from analyses performed using these *moderate* ground motions are within the maximum allowable drift recommendations of both the UBC and ATC-22 guidelines. Even though these structures would most likely remain standing if subjected to low to moderate ground motions, there remains much uncertainty as to the serviceability and repairability of these structures. Several key points introduced in Section 1 regarding the desirable seismic behavior of multistory frames must be reiterated at this time. These considerations include:

- That the failure mechanism be such to maintain service load capacity
- That members fail in a ductile manner and avoid a brittle fracture type of failure
- That ductility capacity in plastic hinge zones be such to withstand large rotations without the crushing of concrete in the compression zone.

In view of these considerations, gravity-load-designed structures are vulnerable to damage from two distinct possibilities: potential joint shear failures; and likely strong-beam weak column effects leading to soft story collapses. While the effects are obvious in severe earthquakes, it is possible that earthquakes of moderate intensity can also cause significant damage. The magnitude of damage will depend largely on the energy content of the earthquake. The evaluations presented here cover two types of earthquakes: (a) mild to moderate events with minimal energy input, and (b) severe ground shaking with substantial energy input such as those occurring in active seismic zones. Any likelihood of a seismic event within this spectrum of records should be a matter of concern for gravity load designed buildings.

Subsequent sections will introduce detailing strategies for improving the seismic resistance without resorting to a full seismic design.

SECTION 6

INTRODUCTION TO SEISMIC DETAILING STRATEGIES

6.1 Alternatives for Enhanced Seismic Resistance

An obvious solution to enhance the performance of structures for seismic resistance is to increase the size of the members within the structure. The idea is to stiffen the beams and columns to decrease the deformation of the structure, thus reducing story drifts and ultimately decreasing damage. It might first be assumed that the added strength associated with the larger members should also reduce the amount of yielding that members experience. However, this approach has several drawbacks. By stiffening the structure, the fundamental period is decreased. For structures with periods in excess of 0.5 seconds, the period shift is most often towards the amplified portion of response spectra of typical earthquakes. This leads to the structure experiencing larger relative accelerations. Higher relative accelerations along with the substantial increase in building mass, inherently obtained when member sizes were increased, will attract more seismic forces and possibly lead to increased damage potential.

Another approach to enhance seismic performance of RC frames is to provide more strength in members by increasing the level of reinforcement to that which is necessary to keep the structure virtually elastic during the expected ground motion. This is difficult to accomplish without increasing member size. A significant increase in reinforcement ratio, keeping member sizes constant, will greatly increase member strength while just slightly increasing stiffness. Special attention must be given to assure that a state of over-reinforcement does not exist which could lead to a non-ductile crushing of the concrete within a member or at the joint face. It is also obvious that when members inevitably yield, these highly reinforced members, due to decreased ductility would have poor rotational capacity. Further, providing additional longitudinal reinforcement would tend to provide high strength in regions of the structure that do not necessarily require a strength increase, such as the column midheight region. This approach would lead to a substantial increase in the building cost.

It is clear that both the above approaches, stiffening the structure or strengthening the members by added reinforcement, would in general improve seismic performance of most RC frame structures. It is also clear that both of these approaches do this at a significant added construction expense.

Since the probability of a severe seismic event is low, the need to resort to a full seismic design is not justified. Hence, the proposed alternative in this study is to enhance certain detailing configurations at critical regions which provide the necessary strength and ductility to avoid failure due to a moderate earthquake.

Two primary objectives are addressed in the second phase of this study:

1) Show how certain detailing arrangements within members and joints influence the overall structural behavior of multistory RC frames.
2) Verify certain specific detailing arrangements and quantify how much improvement can be obtained from the utilization of these detailing enhancements.
3) Estimate how much additional cost would be added and then justify this additional cost in terms of improved performance and reliability.

Although it appears the improved strategies evaluated herein and their costs apply to new construction, the mechanical principles that govern the behavior of these details can also be appplied toward the development of retrofit techniques.

6.2 Illustration of Detailing Strategies

There are three specific detailing features that were chosen to be examined. These features, introduced in Section 3, are:

1) Effect of providing continuity or sufficient end anchorage of positive flexural reinforcement in beams.
2) Effect of providing transverse reinforcement or diagonal flexural reinforcement within beam-column joints to ensure joint shear strength.
3) Effect of providing additional transverse reinforcement in plastic hinge zones for enhanced confinement and rotational capacity.

The background and discussion of code provisions regarding these features is discussed in Section 1. Methods of modeling and discussion of the mechanics pertaining to each of these features is described in Section 3.

Fig. 6.1 presents a set of illustrations showing numerous combinations of the detailing features. These figures represent typical interior beam-column joints containing various arrangements of reinforcement to represent the features being examined. Figures of exterior and top floor beam-columns are not provided, however structures were modelled with these joints accordingly to the mechanics governing the behavior of these details. Since the provision of additional confinement can be implemented at varying degrees (eg. poor, fair and well confined) and can be specific to beams only or columns only or both beams and columns, it is important to examine numerous combinations so to obtain results that clearly depict the effect of each. Fig. 6.2 shows the typical cross-sections that are consistent for all the details.

Table 6.1 includes the acronyms representing the sixteen detailing combinations studied, denoting the specific details that were modelled in each analysis. It should be made clear that analyses performed on the three, six and nine story structures had beam-column joints that contained only one of the sixteen detailing combinations. The last number in each acronym refers to the level of confinement provided (4=well confined, 8=fairly confined, no number=poorly confined). See Section 3.4 for further interpretation of confinement levels. Table 6.1 further provides a brief comment regarding each detail, describing either the purpose behind the detailing arrangement or what the detail is intended to represent. The relative *effects* of the different strategies are compared to the original gravity-load-designed detail (REAL).

The first four details listed in Table 6.1 are of particular interest. These are the details which influence member and joint strength and have a significant effect on the dynamic behavior of the structure. The remaining details are similar versions of the first four details but with varying levels of confinement. Although confinement is a very important feature in this detailing study, it has little effect on member strength and stiffness. The effect of confinement is reflected more in the ductility capacity which in turn is reflected in the final damage indices. The last four details are included to examine the effect of providing additional confinement in either the beams or the columns. Again this effect is with respect to the *poorly* detailed structure only. Examining the effect of confining beams and columns separately will allow for determining the order of importance of confining these members and also help in determining what confinement level is adequate for both members.

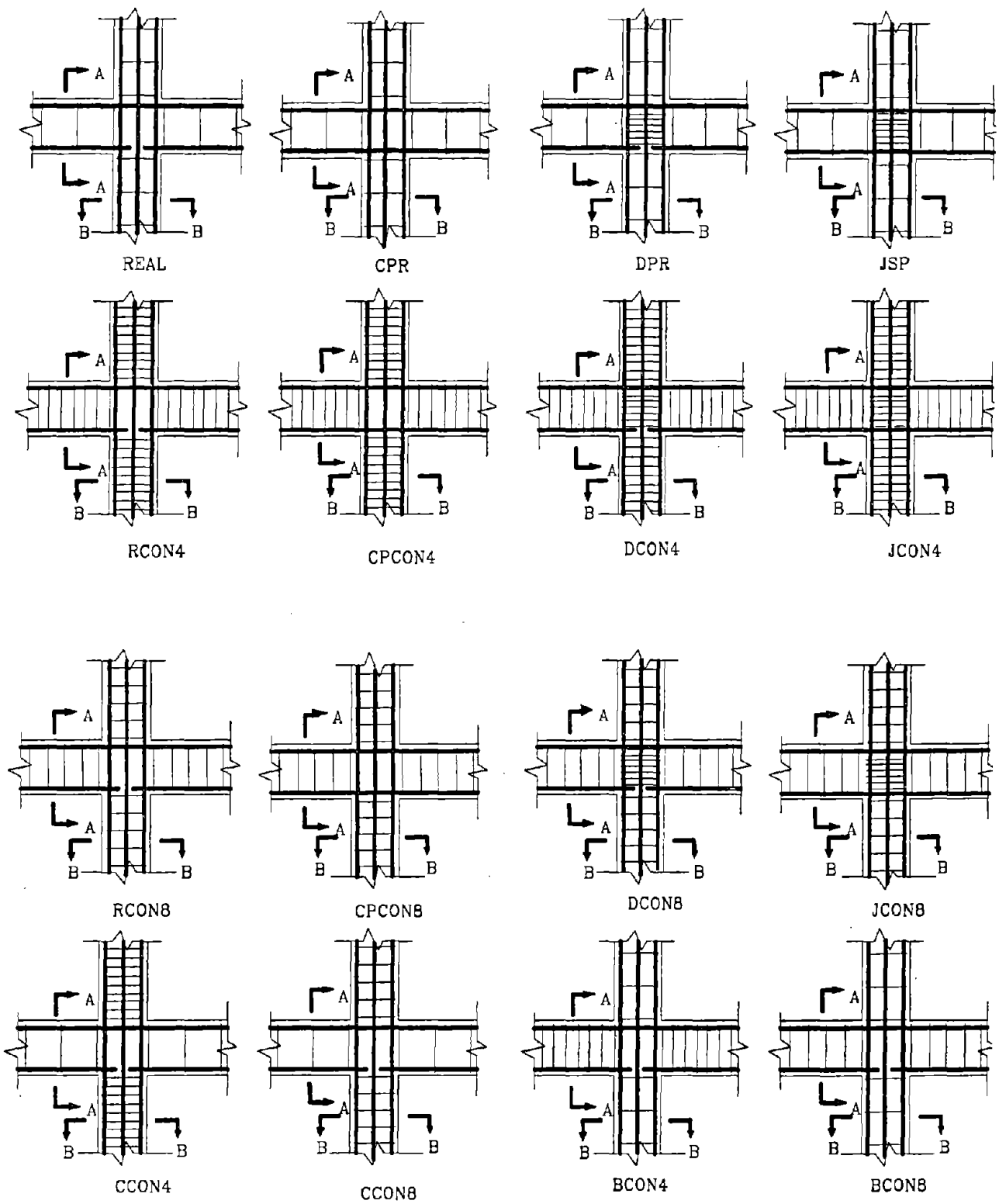

Figure 6.1 Representative Detailing Configurations Analyzed

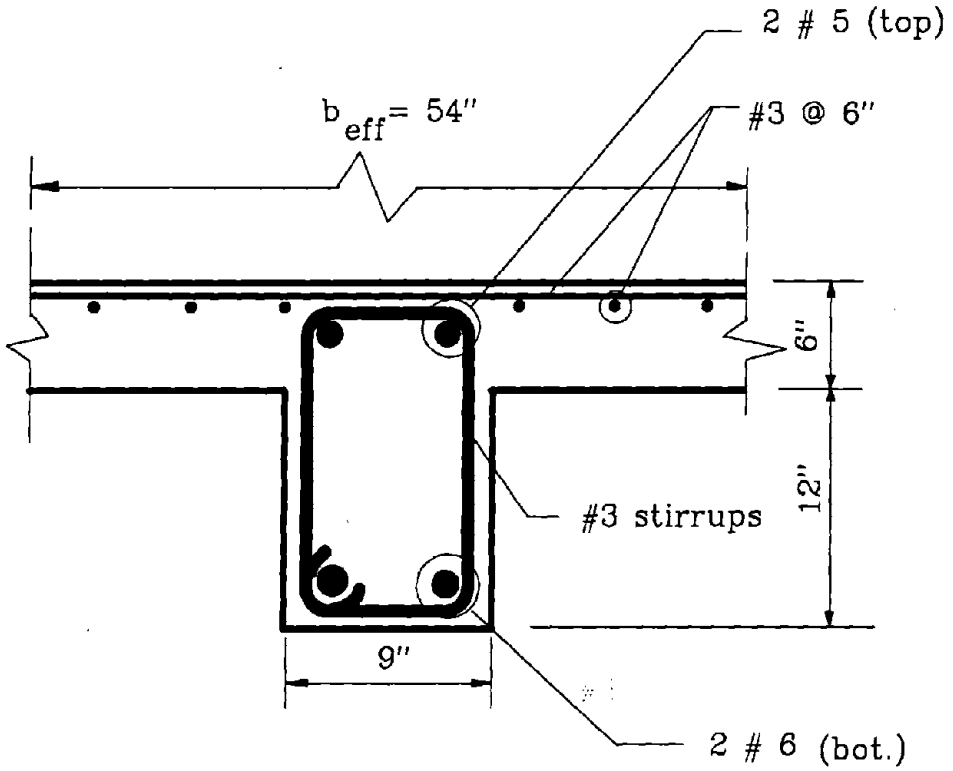

SECTION A–A

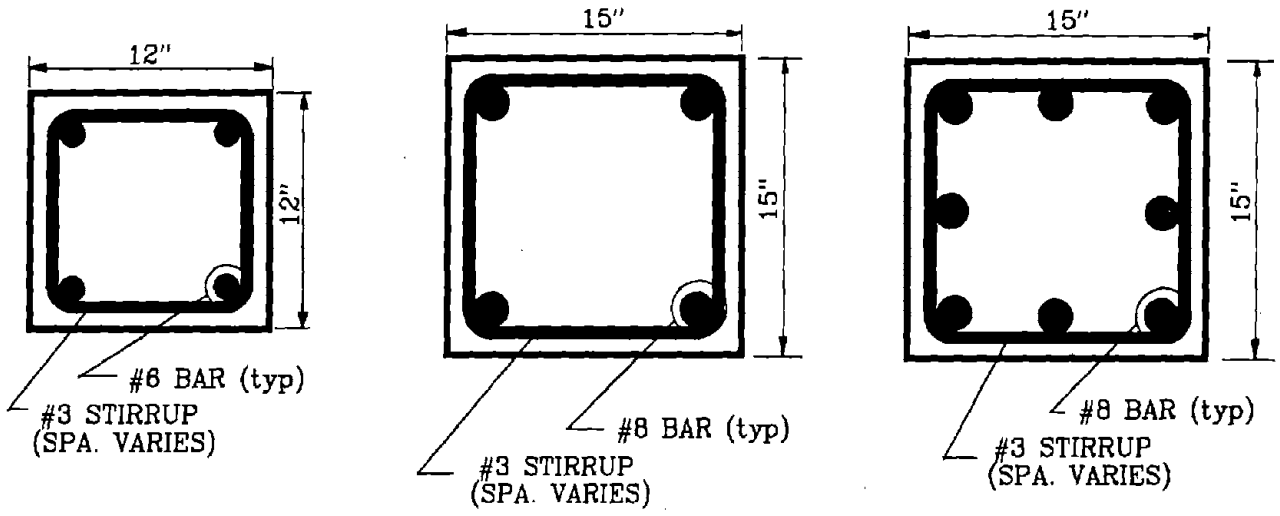

a) Columns Supporting Less than 4 Floors

b) Columns Supporting 4 to 6 Floors

c) Columns Supporting Over 6 Floors

SECTION B–B

Figure 6.2 Typical Member Cross-Sections For All Details

Table 6.1 Description of Detailing Combinations

Detailing Acronym	Continuous or Anchored Positive Flex. Reinforcement	Sufficient Joint Steel Provided	Level of Confinement Provided	Comments
REAL	NO	NO	POOR	Typical Gravity-Load-Designed Detail
CPR	YES	NO	POOR	Effect of Continuing Positive Flexural Reinforcement
DPR	NO	YES	POOR	Effect of Providing Sufficient Joint Shear Strength
JSP	YES	YES	POOR	Both Joint Steel and Continuous Positive Flexural Reinforcement Provided
RCON4	NO	NO	WELL	Effect of Providing Full Confinement
RCON8	NO	NO	FAIR	Effect of Providing Fair Confinement
CPCON4	YES	NO	WELL	Detail CPR with Full Confinement
CPCON8	YES	NO	FAIR	Detail CPR with Fair Confinement
DCON4	NO	YES	WELL	Detail DPR with Full Confinement
DCON8	NO	YES	FAIR	Detail DPR with Fair Confinement
JCON4	YES	YES	WELL	Detail JSP with Full Confinement
JCON8	YES	YES	FAIR	Detail JSP with Fair Confinement
CCON4	NO	NO	Columns: Well Beams: Poor	Effect of Full Column Confinement
CCON8	NO	NO	Columns: Fair Beams: Poor	Effect of Moderate Column Confinement
BCON4	NO	NO	Columns: Poor Beams: Well	Effect of Full Beam Confinement Only
BCON8	NO	NO	Columns: Poor Beams: Fair	Effect of Moderate Beam Confinement

It should be noted that although the detail JCON4 appears to be the full seismic design from the point of view of the ACI code, it is included here only to show the effect of providing full joint shear strength which is required to ensure that the full flexural strength of adjoining members can be achieved prior to joint failure. As mentioned in Section 3.3, this issue is not appropriately addressed in current code provisions.

SECTION 7

EVALUATION OF DETAILING STRATEGIES

7.1 Description of Comparative Study

The presentation of analytical results from this research study is separated in two parts. Section 7.2 will examine results obtained from the evaluation of detailing strategies affecting the strength of the joint or adjoining members. This includes the provision of sufficient development length for positive flexural reinforcement and the provision of sufficient joint steel. The effects of these enhancements will be evaluated primarily on the basis of inter-story drift and overall story damage. In all cases, the performance of gravity-load designed buildings presented in Section 5 will be used as a frame of reference with which to compare the different strategies.

Section 7.3 will evaluate the effect of providing additional transverse reinforcement for the purpose of enhanced confinement. The effect of confinement is limited to providing additional ductility or rotational capacity to members which in turn helps to reduce relative damage in beams and columns. The effects of confinement are thus treated separately to make the task of comparative evaluation more intelligible.

Typical plots of inter-story drifts, story shears, and damage distribution are included for selected earthquakes only. The results presented are intended to provide information on the following:

1) To ascertain whether overall building height has significant influence on structural behavior or whether the change in response between different analyses is governed primarily by the varying detailing arrangements.

2) To check if specific behavioral characteristics observed in one analysis are consistent with those obtained in other analyses. This also includes the effect of loading history on the overall response.

An overall summary of the average damage index statistics is presented in Section 7.4. Damage indices for members are averaged and then compared to the benchmark structure (REAL) to give a quick assessment of the change in overall damage and the level of benefits, if any, derived from the detailing strategy.

Finally, Section 7.5 will be devoted to the discussion of the merits and drawbacks of each of the detailing strategies studied. Overall evaluation will be based on both computed damage statistics and inter-story drift reductions.

7.2 Effect of Detailing Strategies in Joint Region

The primary four detailing schemes used in the joint area have been previously discussed in Section 6 and presented in Table 6.1. These detailing strategies affect primarily the joint and member strength. The acronyms used for these schemes are:

1) REAL
2) CPR
3) DPR
4) JSP

Of the four earthquakes used in the simulations, the one that produced the severest damage in most cases was the Taft accelerogram. Both the Nahanni and the artificially generated record produced similar results since they both represented minor earthquakes. Given the large database of results that were generated, only a few typical behavior patterns are selected for final review and study. All the results to be presented in this Section consist of a typical minor earthquake (Nahanni) and a typical severe earthquake (Taft).

Figure 7.1 shows the final damaged state of all frames analyzed using the Taft earthquake. The distribution of component cracking and yielding give a good qualitative view of the effects of the different detailing configurations on the overall inelastic structural response.

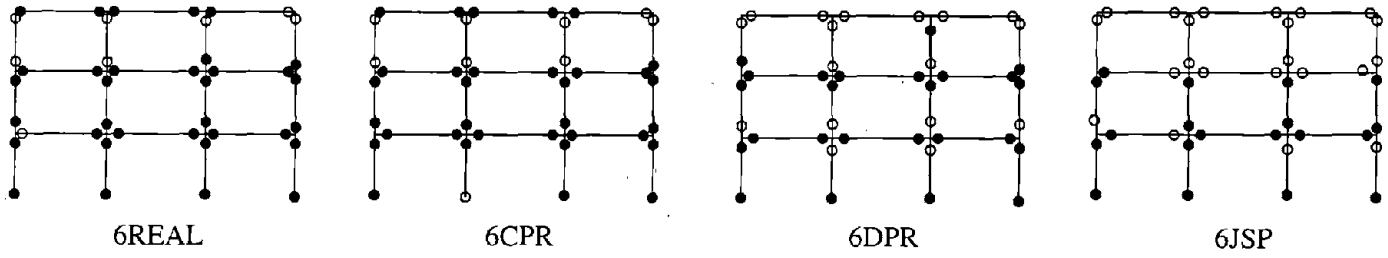

6REAL 6CPR 6DPR 6JSP

(a) 3 Story Frames

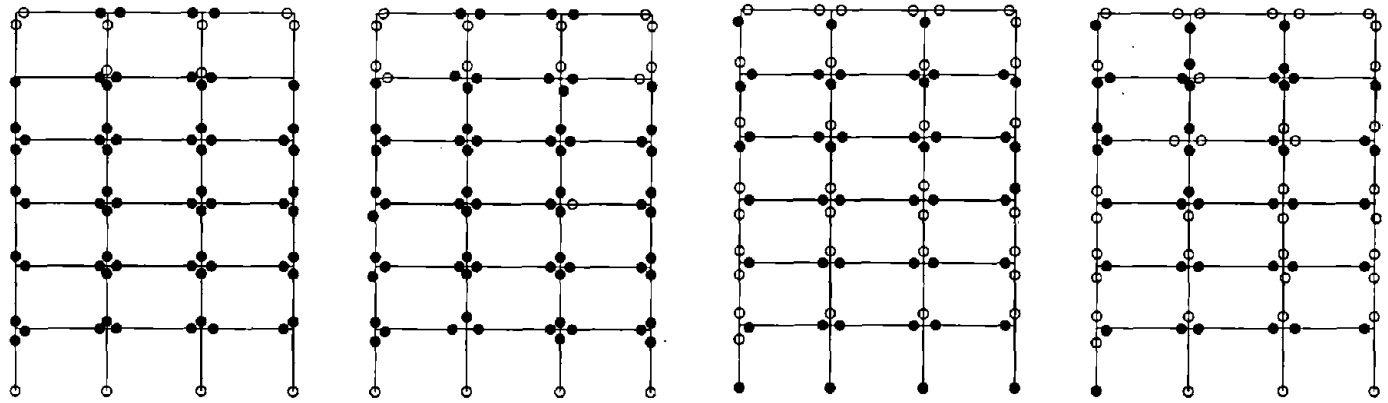

6REAL 6CPR 6DPR 6JSP

(b) 6 Story Frames

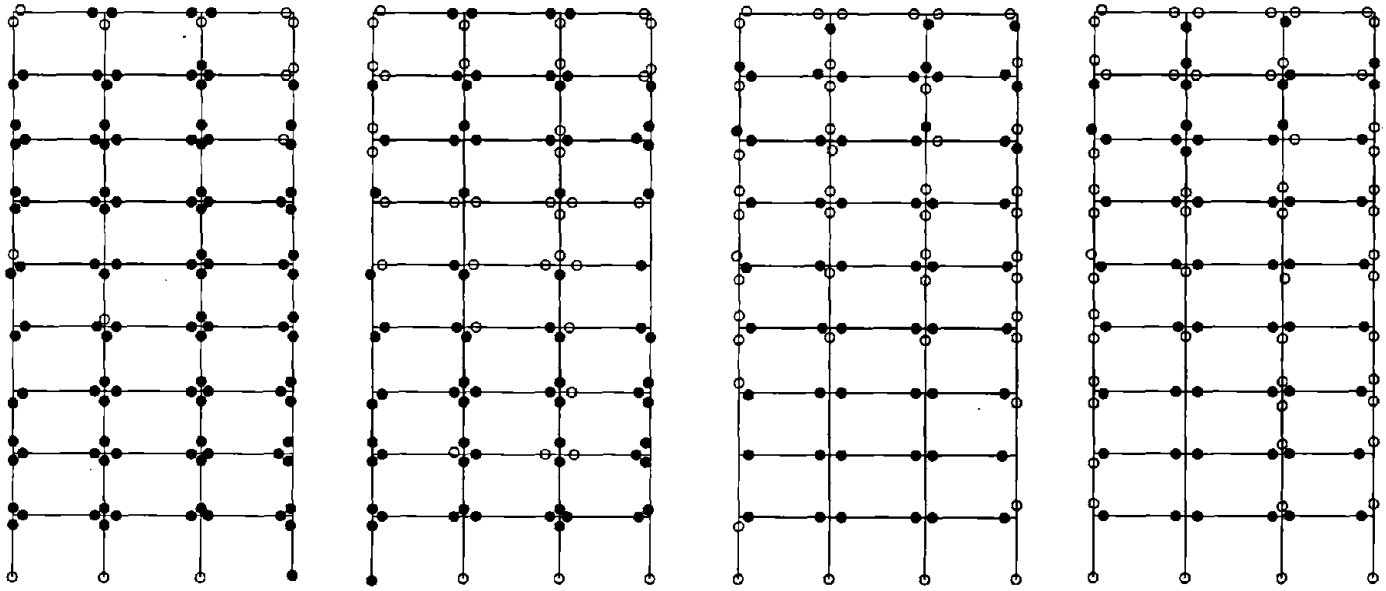

9REAL 6CPR 9DPR 9JSP

(c) 9 Story Frames

Figure 7.1 Final State of Frames Subjected to Taft (PGA = 0.20 g)

Story drifts resulting from the Nahanni earthquake and the Taft earthquake are presented in Figures 7.2 and 7.3. The effect of higher modes is noticeable particularly in the 9-story frame. For the Taft earthquake, only the 6 and 9 story frames are shown since the results of the 3-story frame did not reveal any distinguishing feature of each detailing scheme. In fact, in most of the runs, the responses of the three story frame did not show any significant variation or trend to merit detailed discussion. The responses of the 6 and 9 story frames, on the other hand, showed a clearer pattern of behavior. Consequently, the remaining results presented in this Section are confined to the 6 and 9 story frames. It is, however, felt that the conclusions drawn from the results of the six and nine story frames will also apply to three story frames.

Story shears resulting from the analyses using the two earthquakes are displayed in Figures 7.4 and 7.5. Damage statistics for the same earthquakes for beams and columns at a story level are shown in Figures 7.6 - 7.9.

Results not shown in figures are tabulated in Appendix B.

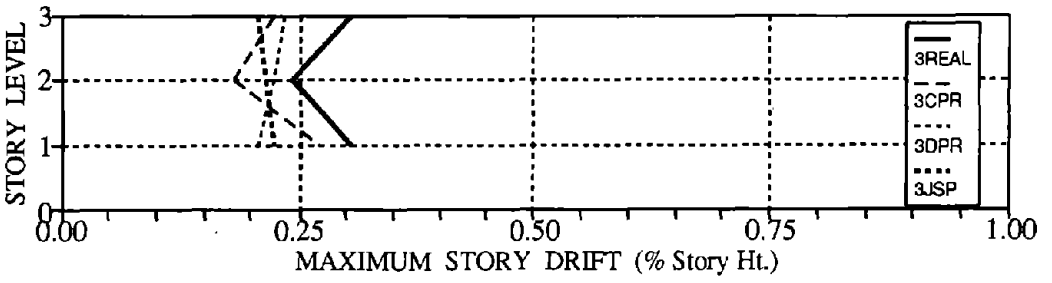

a) 3 STORY FRAME

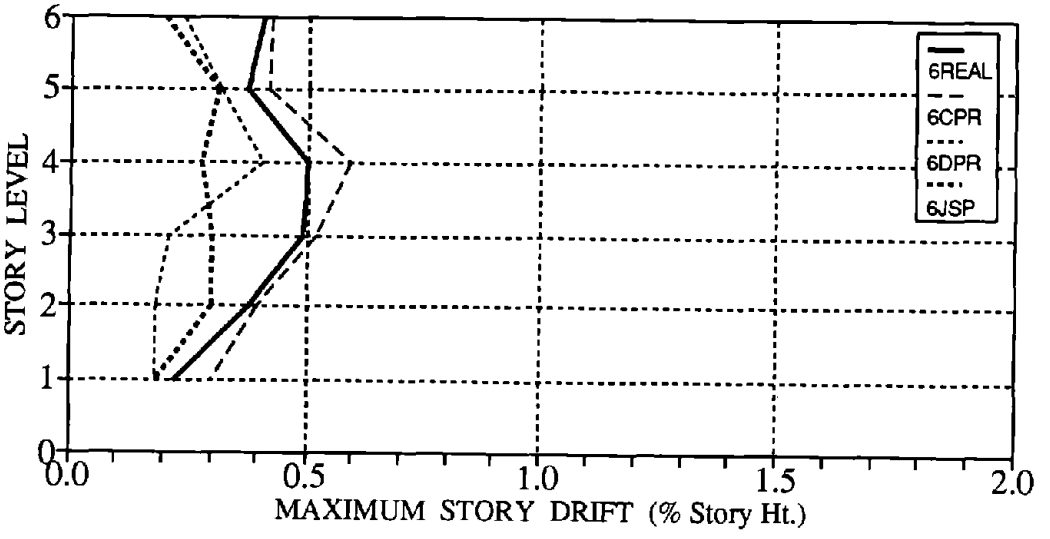

b) 6 STORY FRAME

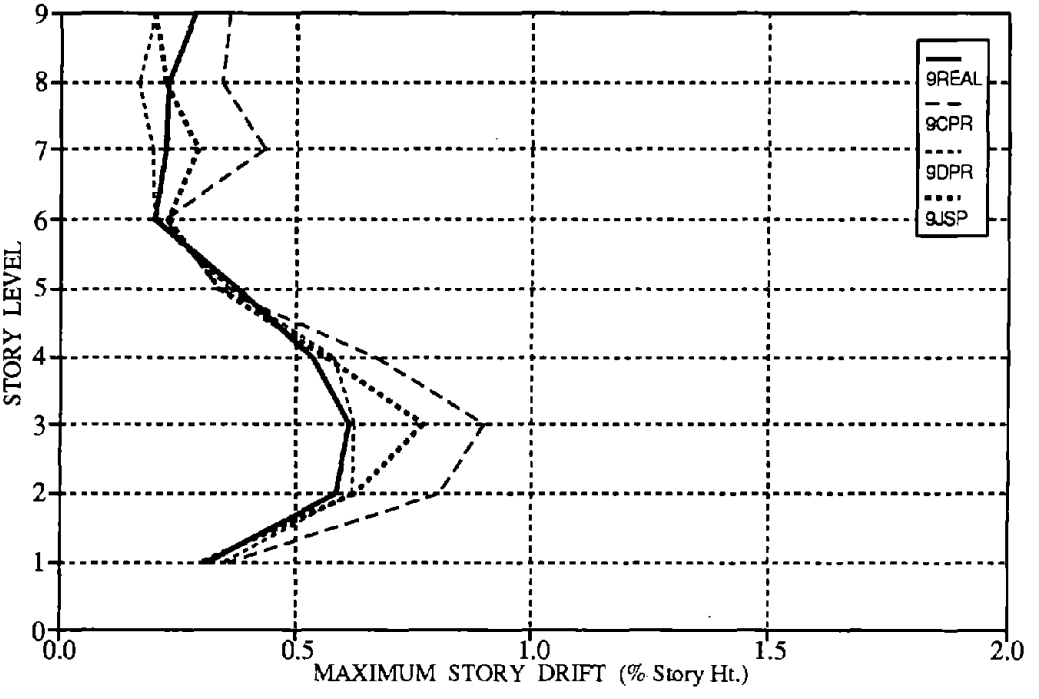

c) 9 STORY FRAME

Figure 7.2 Story Drift Distribution for Frames Subjected to Nahanni (PGA = 0.20 g)

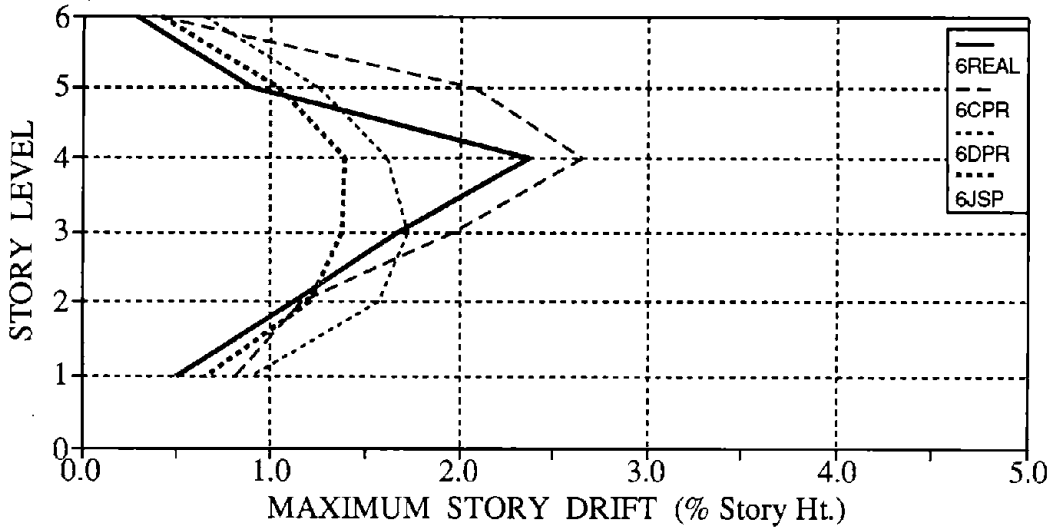

6 STORY FRAME

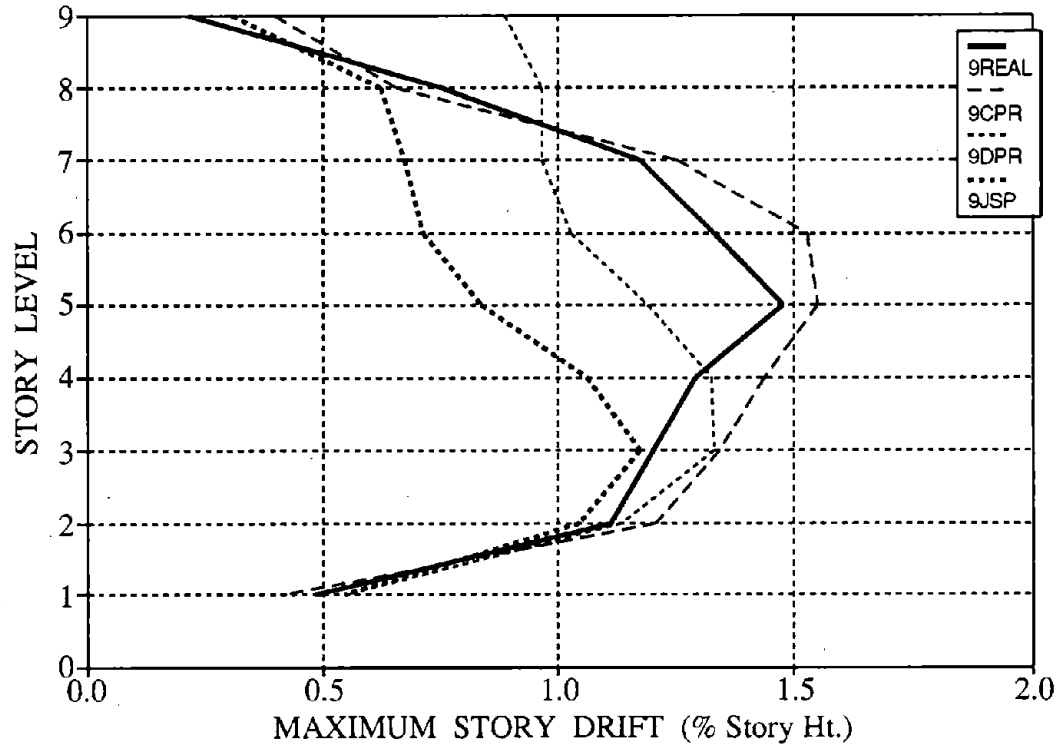

9 STORY FRAME

Figure 7.3 Story Drift Distribution for Frames Subjected to Taft (PGA = 0.20 g)

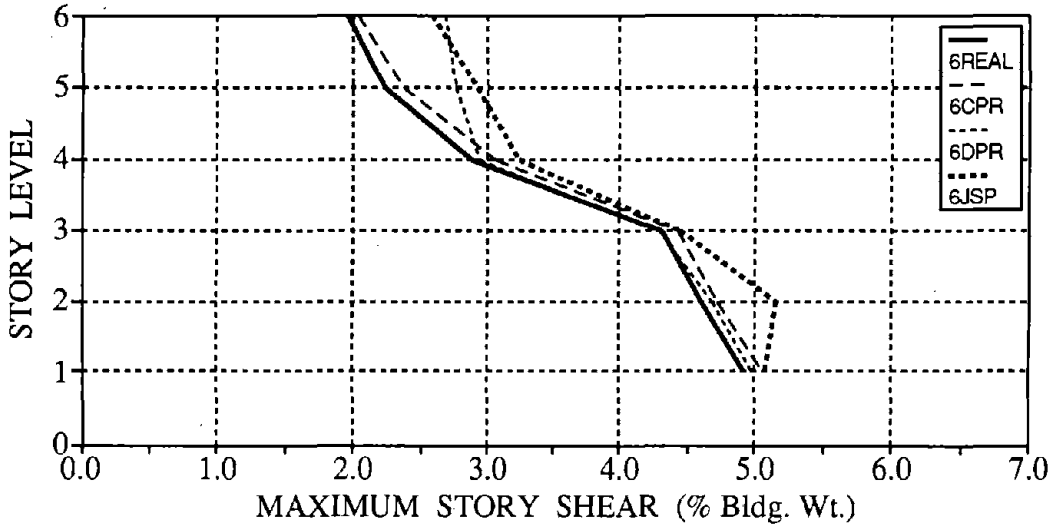

6 STORY FRAME

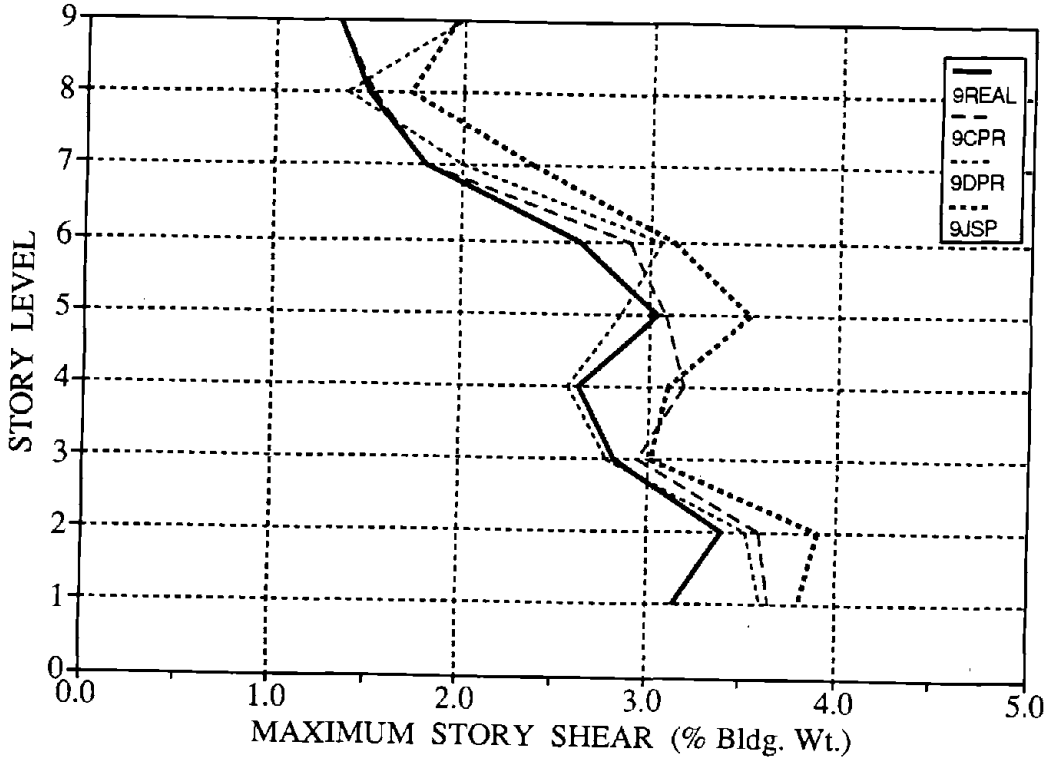

9 STORY FRAME

Figure 7.4 Story Shear Distribution for Frames Subjected to Nahanni (PGA = 0.20 g)

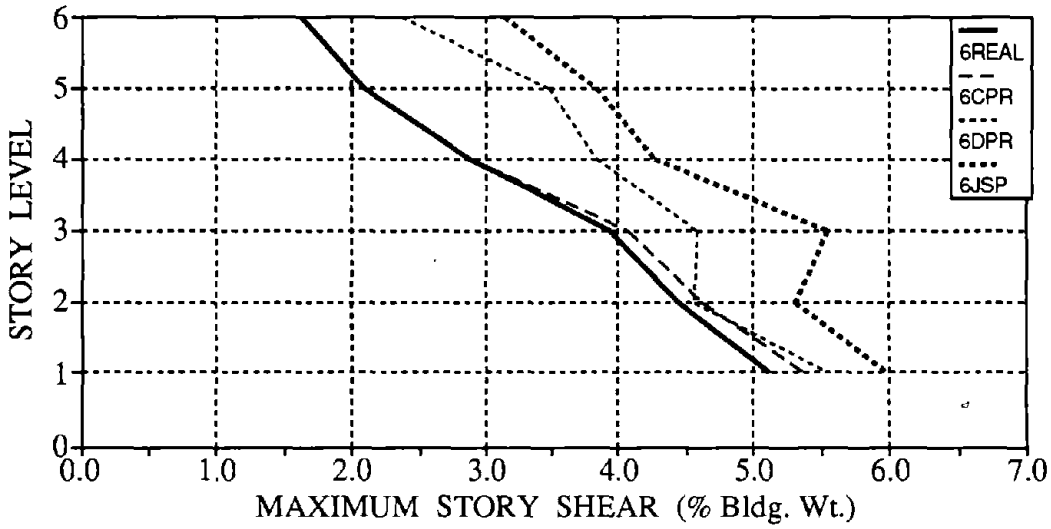

6 STORY FRAME

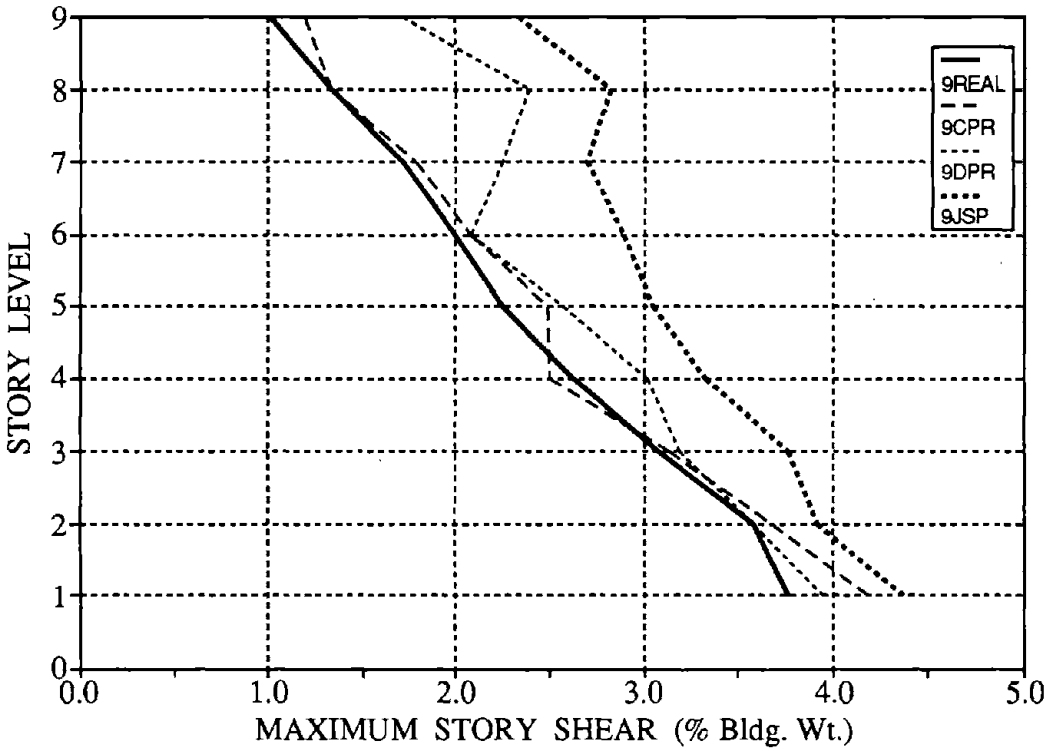

9 STORY FRAME

Figure 7.5 Story Shear Distribution for Frames Subjected to Taft (PGA = 0.20 g)

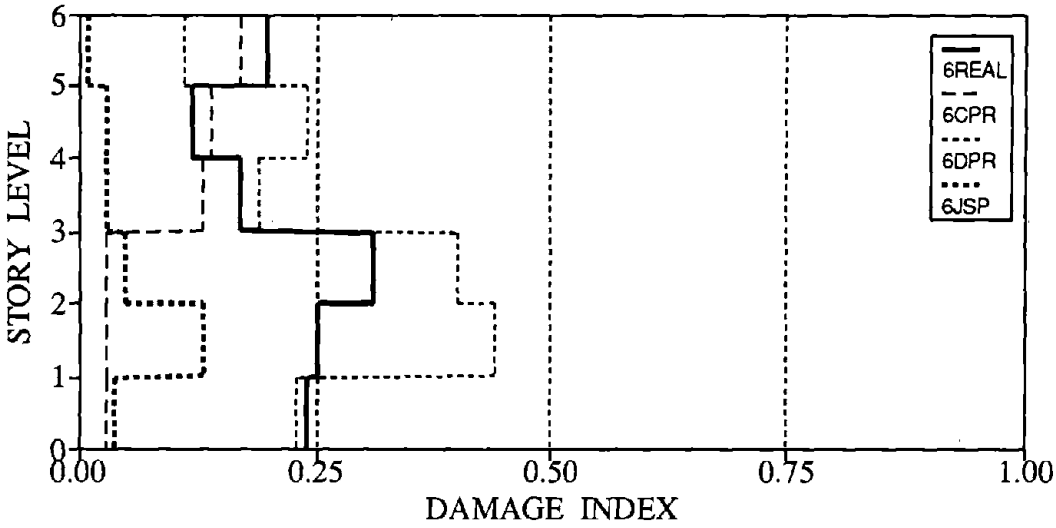

a) 6 STORY FRAME

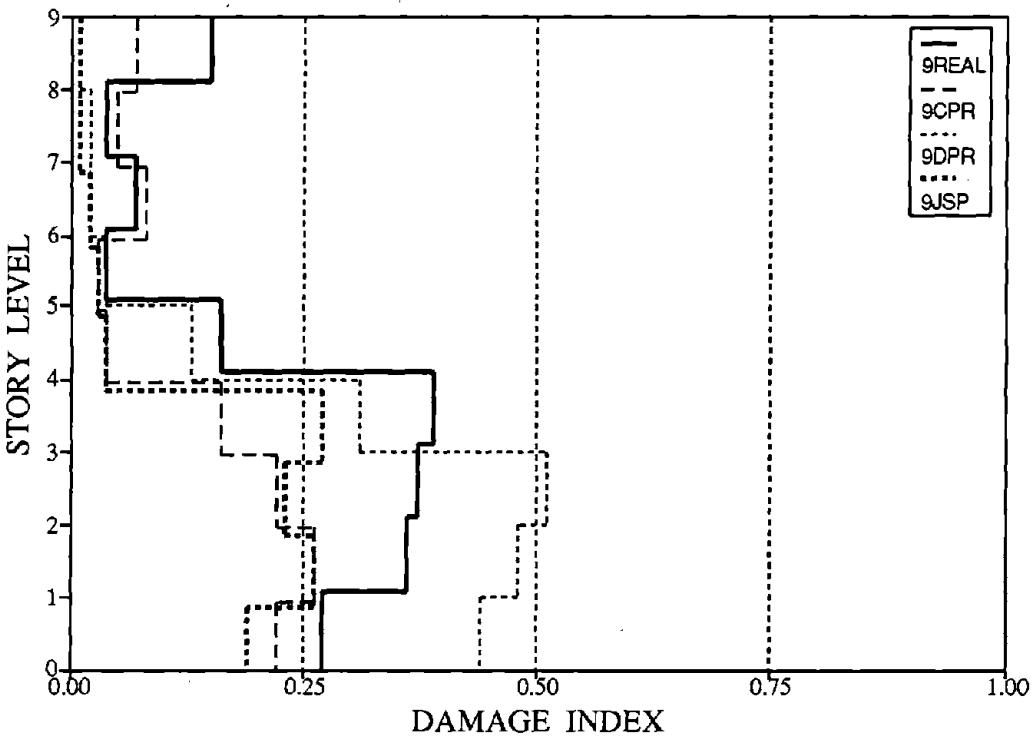

b) 9 STORY FRAME

Figure 7.6 Beam Damage Distribution for Frames Subjected to Nahanni (PGA = 0.20 g)

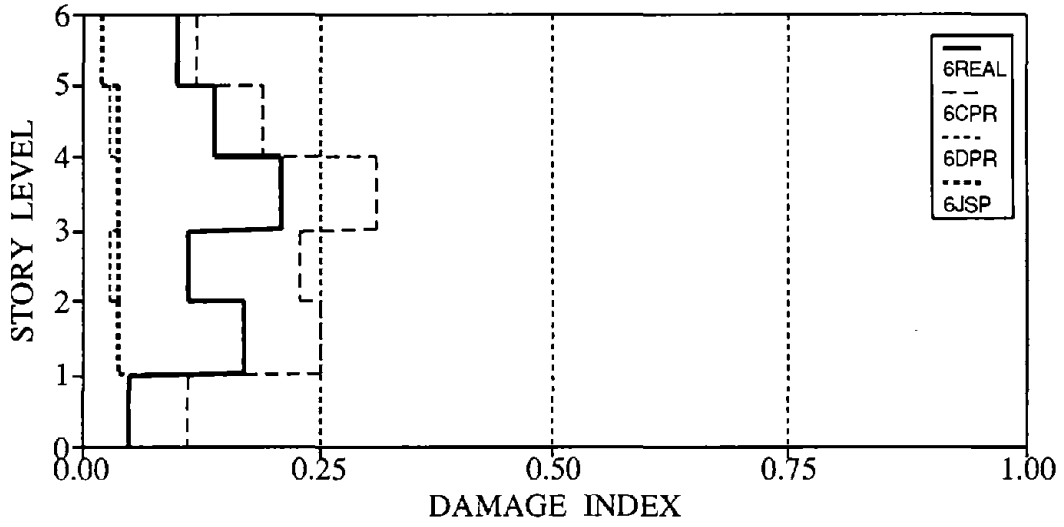

a) 6 STORY FRAME

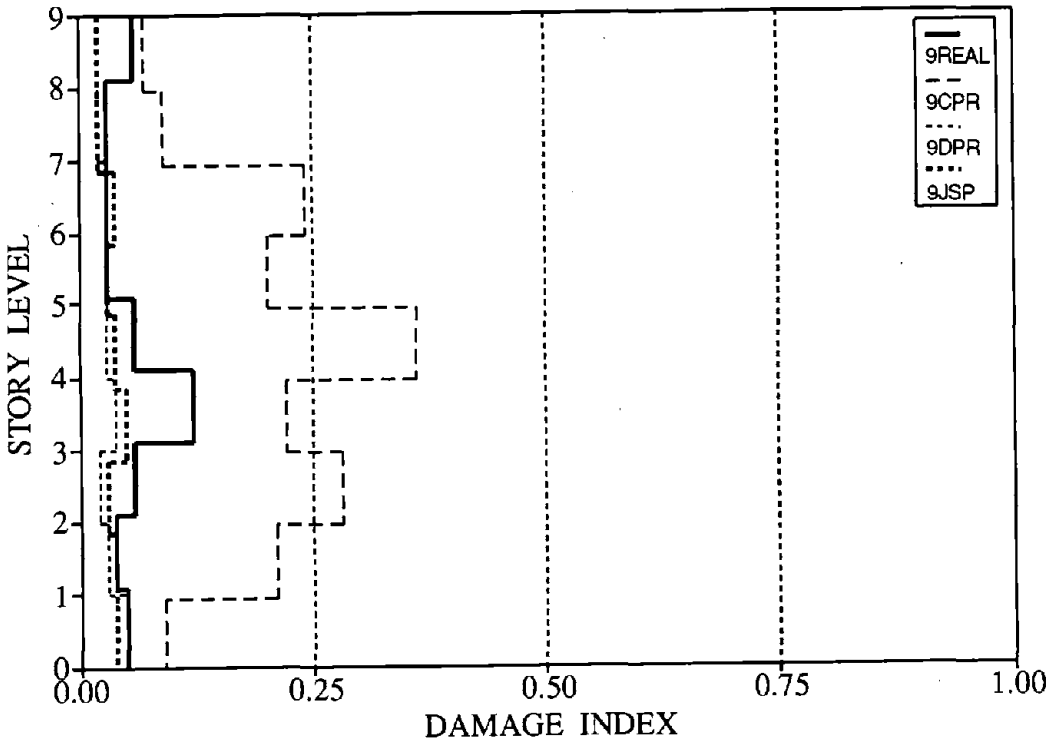

b) 9 STORY FRAME

Figure 7.7 Column Damage Distribution for Frames Subjected to Nahanni (PGA = 0.20 g)

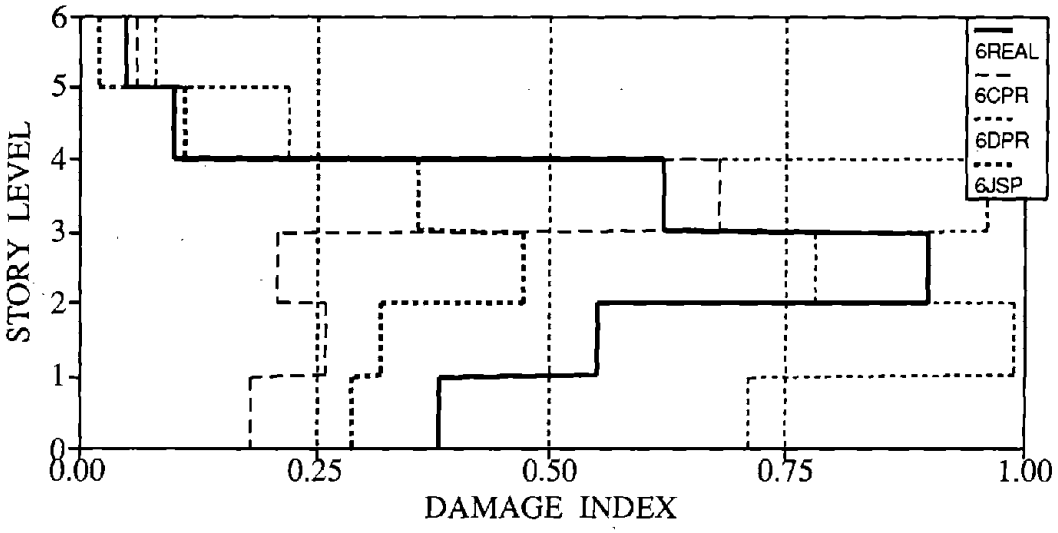

a) 6 STORY FRAME

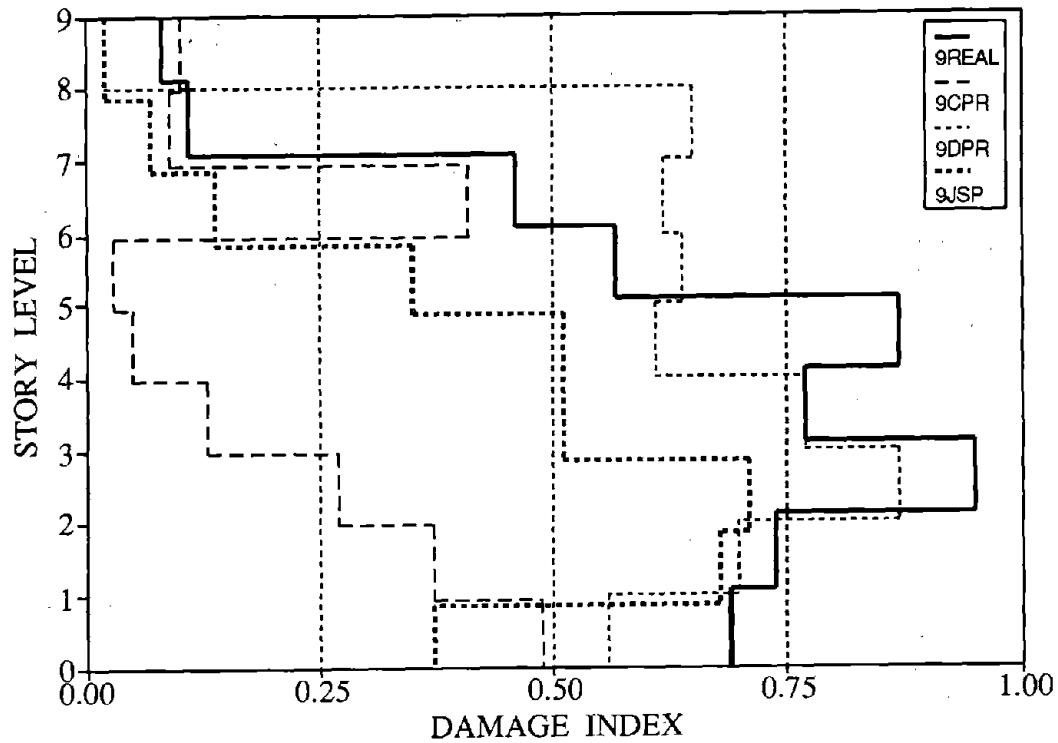

b) 9 STORY FRAME

Figure 7.8 Beam Damage Distribution for Frames Subjected to Taft (PGA = 0.20 g)

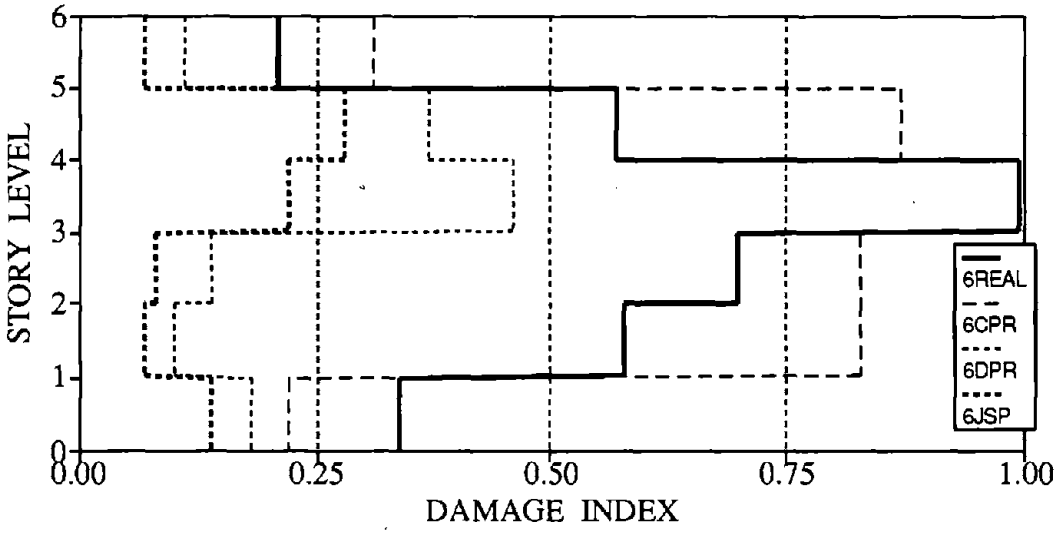

a) 6 STORY FRAME

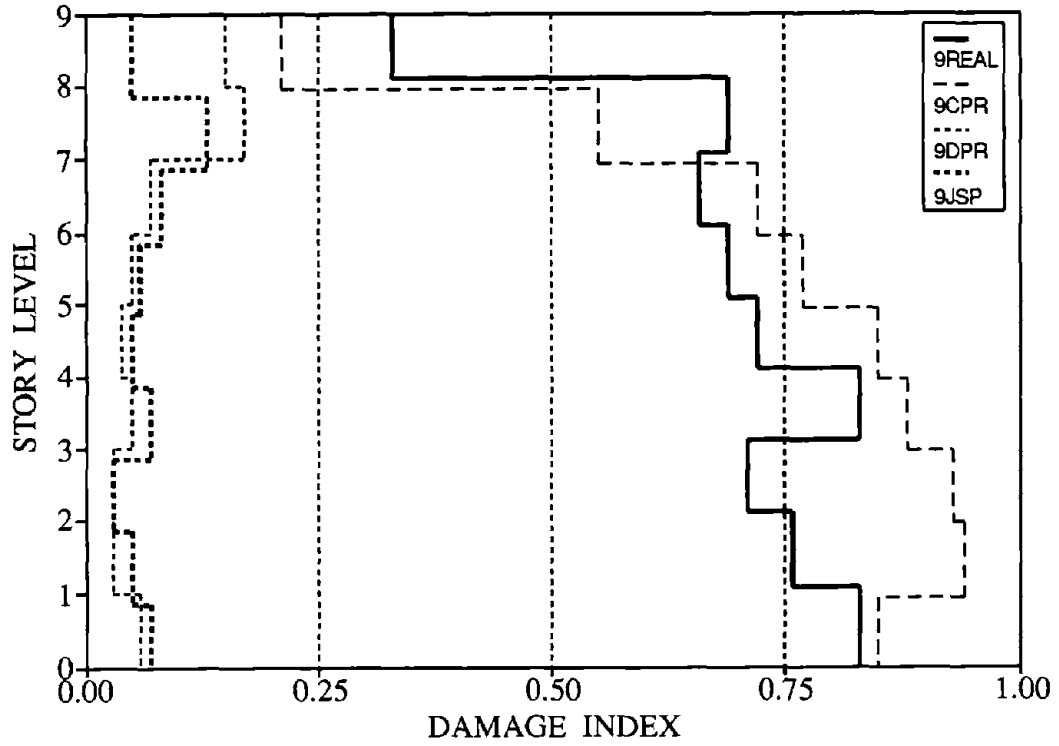

b) 9 STORY FRAME

Figure 7.9 Column Damage Distribution for Frames Subjected to Taft (PGA = 0.20 g)

7.2.1 Effect of Continuing Positive Reinforcement in Beams (CPR vs REAL)

The final damaged state of each structure subjected to 0.2 PGA Taft is shown in Figure 7.1. This display which indicates whether members have cracked, yielded or remained elastic at the end of the dynamic analysis, failed to reveal any discernible trends in the behavior or any shift of the failure mechanism as a result of providing continuity to the bottom flexural reinforcement in the beams. This is because, for both detailing arrangements, a high majority of the members had yielded before a failure mechanism had developed.

However, Figure 7.2 and Figure 7.3, which display inter-story drifts, illustrate quite clearly the effect of added beam strength. The drifts are seen to increase indicating a shift in the damage distribution from beams to columns. This is further evidenced in Figures 7.6 - 7.9 which show the distribution of damage across story levels. Damage in beams are seen to decrease with a corresponding increase in column damage. Since the results are more clearly visible in the six and nine story frames, only these are presented as typical responses. It is also noted that this shift in behavior is more obvious for the moderate earthquakes, whereas the severe motions caused fairly extensive damage in both the original frame and the modified frame with detail CPR.

It is, therefore, concluded that this detailing arrangement (CPR), **if utilized alone**, without other modifications, would likely produce more damage than the original non-seismically detailed structure.

7.2.2 Effect of Ensuring Joint Shear Capacity (DPR vs REAL)

It was observed that structures containing the two detailing arrangements that dont provide for adequate joint shear strength form a story mechanism starting at the first story level, not at the base as one would expect. This is because joint shear failure occurs at the first story level before the base column section reaches its yield moment, resulting in an undesirable soft story effect. The base of the 1st story column is monolithic with the foundation and this region was modelled to have adequate shear strength to develop the moment capacity of this column. Thus, the weakest link was the shear capacity at the first floor joint and the base region is alleviated of any additional forces.

It is seen from Figure 7.1 that the provision of joint shear reinforcement clearly results in a change in failure mechanism from a sporadic combination of beam and column hinging to a more uniform

beam-sidesway mechanism. This is especially true for the bottom stories of the 6 story frame where column yielding is restricted to the hinges that normally develop at the base region. This can be explained by the fact that the provision of joint steel enhances the column strength, restoring the full yield strength while only restoring the negative bending capacity of the beams. In this structural model (DPR), the positive bending capacity of the beams is still restricted by the discontinuous bottom reinforcement reaching its *pullout* capacity. Hence, a weak beam-strong column structure is created.

The inter-story drifts shown in Figures 7.2 and 7.3 show a definite pattern of reduced drift demands. While the shears do increase as seen in Figures 7.4 and 7.5, the relative increase compared to the original configuration is not significant. Plots of column and beam damage (Figures 7.6-7.9) also confirm the conclusions drawn from the hinging pattern and reduced drift demands.

Summarizing, the provision of joint steel shifts the failure mechanism to a more favorable beam-sidesway mechanism, preventing excessive deformations, and significantly reducing column damage. It is seen that providing this detail alone will indeed produce substantial benefits in the overall structural performance of the building. However, due to the substantial beam damage that results and the large inter-story drifts that remain, this detail may not be satisfactory for serviceability criteria for critical facilities.

7.2.3 Effect of Ensuring Full Joint Strength (JSP vs REAL)

As with the previous detail, it is observed from Figure 7.1 that a beam-sidesway mechanism will again develop as the governing failure mechanism. However, a slight amount of column hinging is detected in the upper floors in all 3 frames for the analyses performed using the Taft earthquake. Also, despite the overall damage reductions, it can be seen from the final damage statistics that several beams still come close to their critical capacity.

The overall response is similar to the DPR detail, with a few exceptions. Of the four detailing configurations investigated in this part, the JSP detail experiences the highest story shear forces. This is the obvious result of the joint steel and bottom bar continuity in the beams assuring that the full flexural strength of the members is reached before load redistribution. The increase in story shear experienced by the structure with fully reinforced joints (JSP) compared to the structure with no special detailing (REAL) is in the order of 20% for structures subjected to low to moderate earthquakes and 30% for those subjected to the moderate to severe earthquakes. The story drifts for this detail is clearly the smallest, making it the most favorable of the four details studied so far.

7.3 Effect of Beam and Column Confinement

Results of analyses on the initial four detailing strategies point to the fact that the JSP detail performs relatively better than the others. In this next part of the investigation, the JSP detail is studied further with additional enhancements by way of increasing confinement effectiveness.

The next set of Figures show the relative effects of confinement on the damage distribution to beams and columns. Damage statistics for the JSP detail and the REAL detail are also included in each plot for comparison.

Members were modelled as being poorly confined (say 12-15" hoop spacing), fairly confined (8" hoop spacing) and well confined (4" hoop spacing).

At this point, it should be noted that transverse reinforcement has almost no effect on member strength or stiffness. Its primary effect is in enhancing deformation capacity. Thus, the relative difference in damage distribution among story levels will not change. Analyses of this nature may be used to determine at what level of confinement does the damage decrease to a tolerable level so as to indicate that the structure may be serviceable after a seismic event.

Of the twenty-four separate cases involving all the frames, only a few representative results are shown.

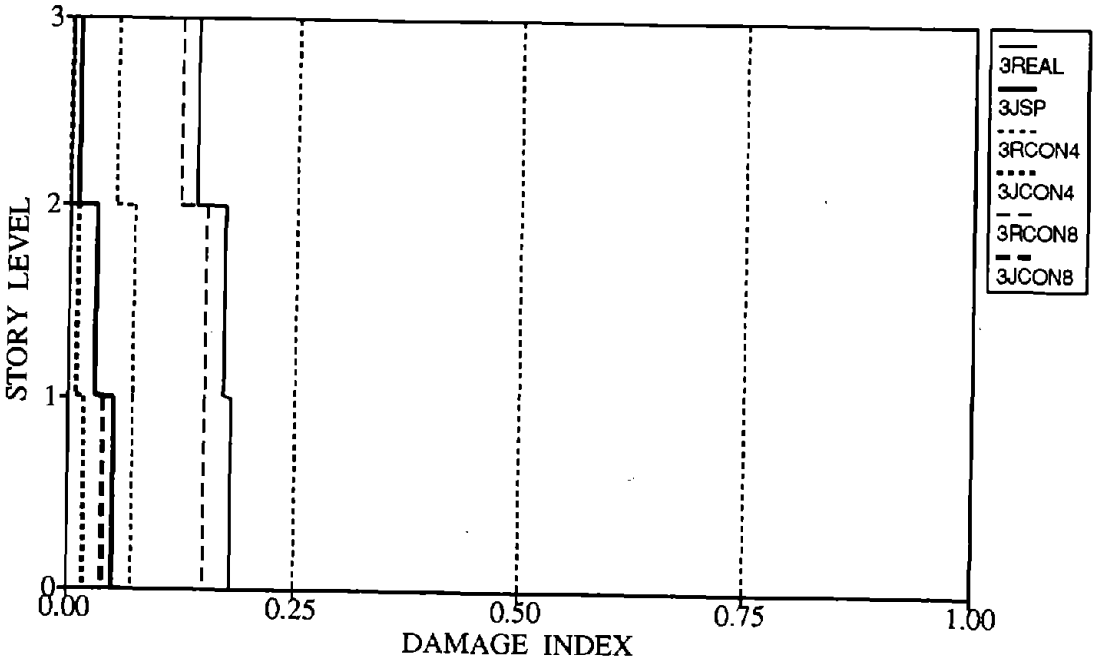

Figure 7.10 Effect of Confinement on Beam Damage Distribution for 3-Story Frames Subjected to Spectrum-Compatible Earthquake (PGA = 0.15 g)

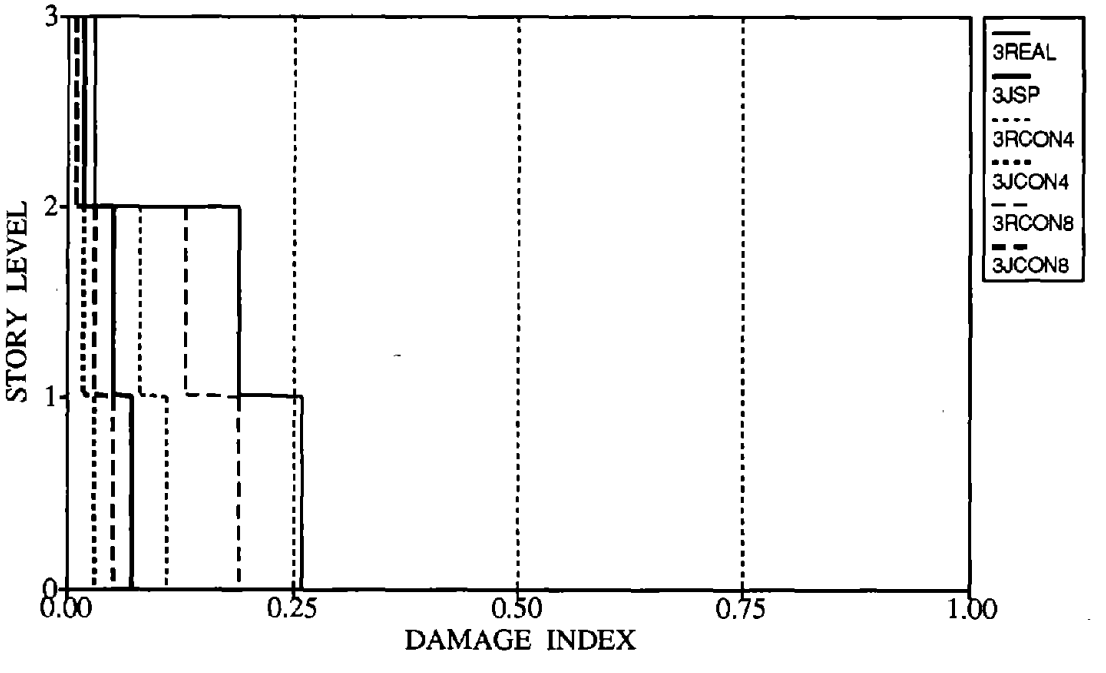

Figure 7.11 Effect of Confinement on Column Damage Distribution for Frames Subjected to Spectrum-Compatible Earthquake (PGA = 0.15 g)

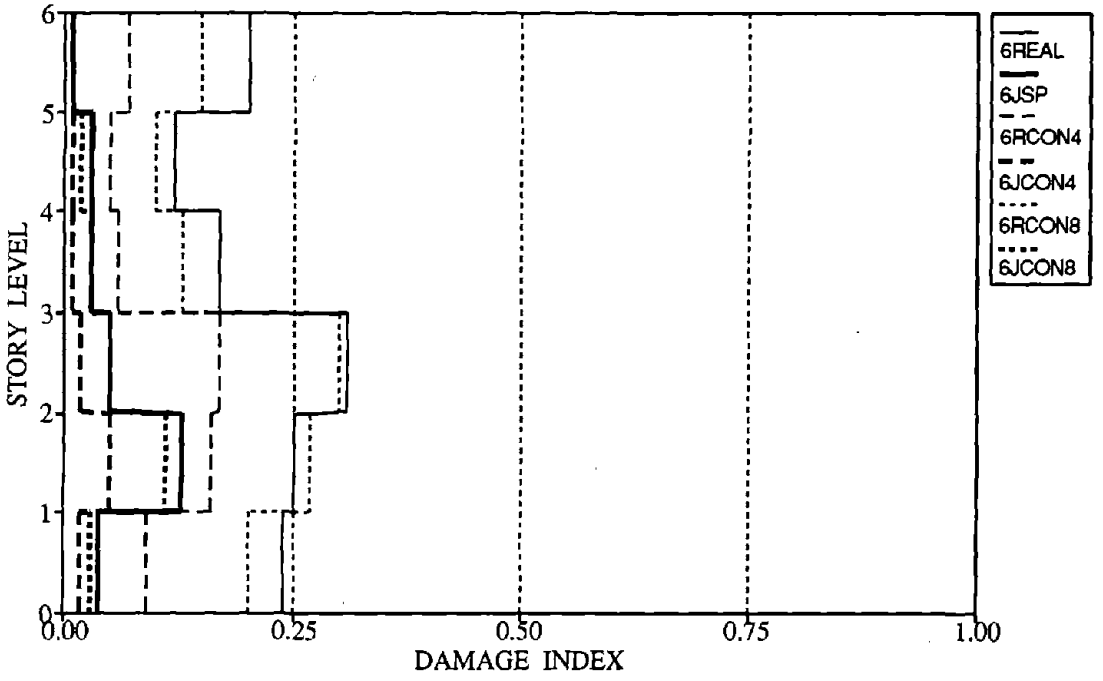

Figure 7.12 Effect of Confinement on Beam Damage Distribution for 6-Story Frames Subjected to Nahanni (PGA = 0.20 g)

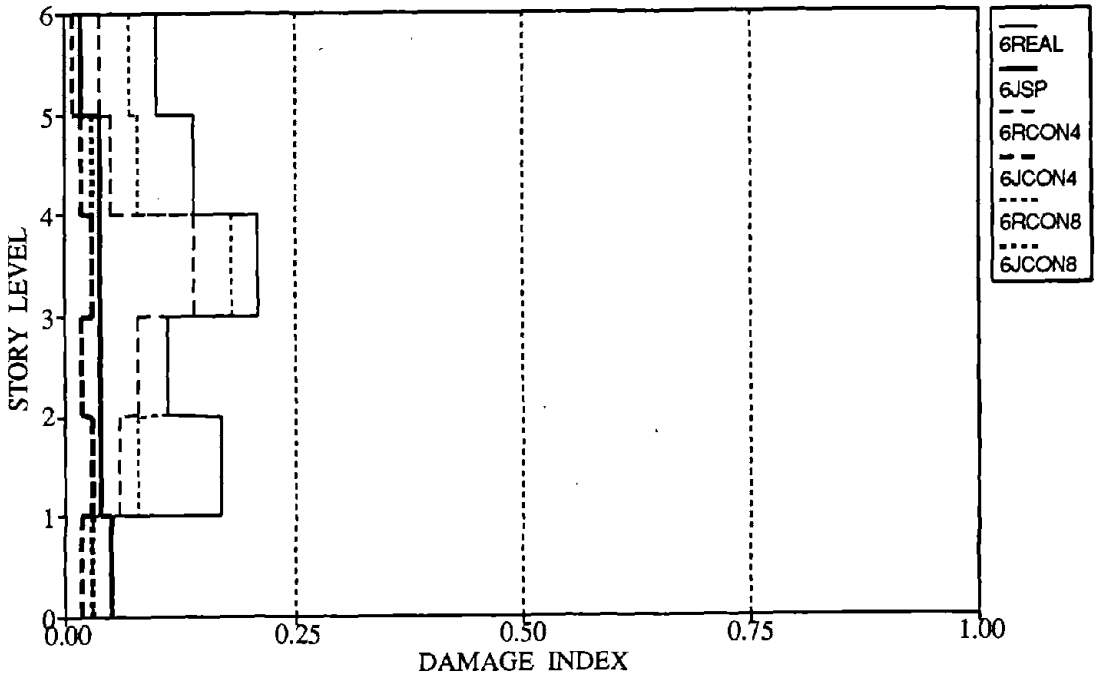

Figure 7.13 Effect of Confinement on Column Damage Distribution for 6-Story Frames Subjected to Nahanni (PGA = 0.20 g)

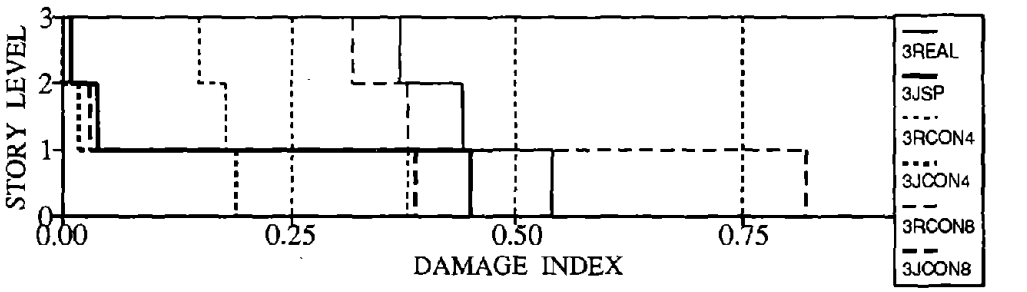

a) 3 STORY FRAME

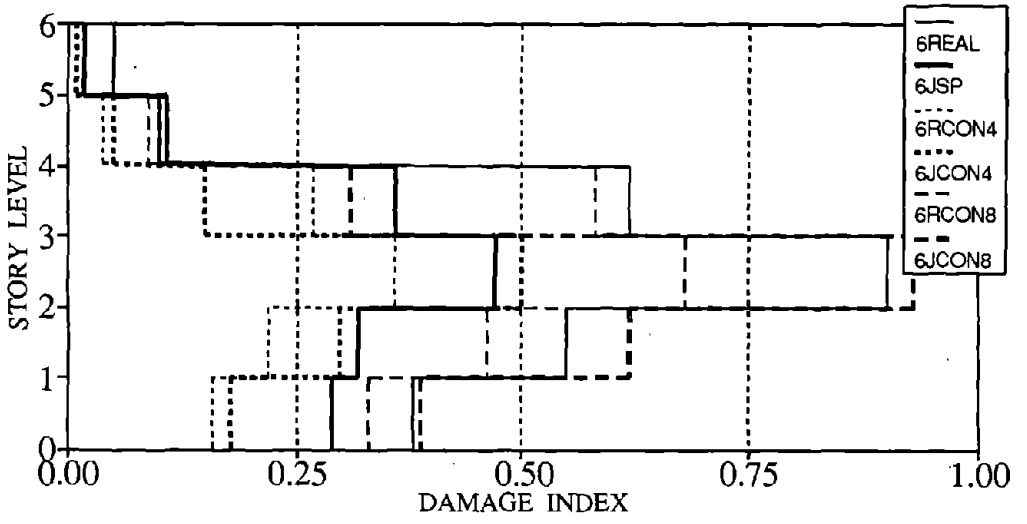

b) 6 STORY FRAME

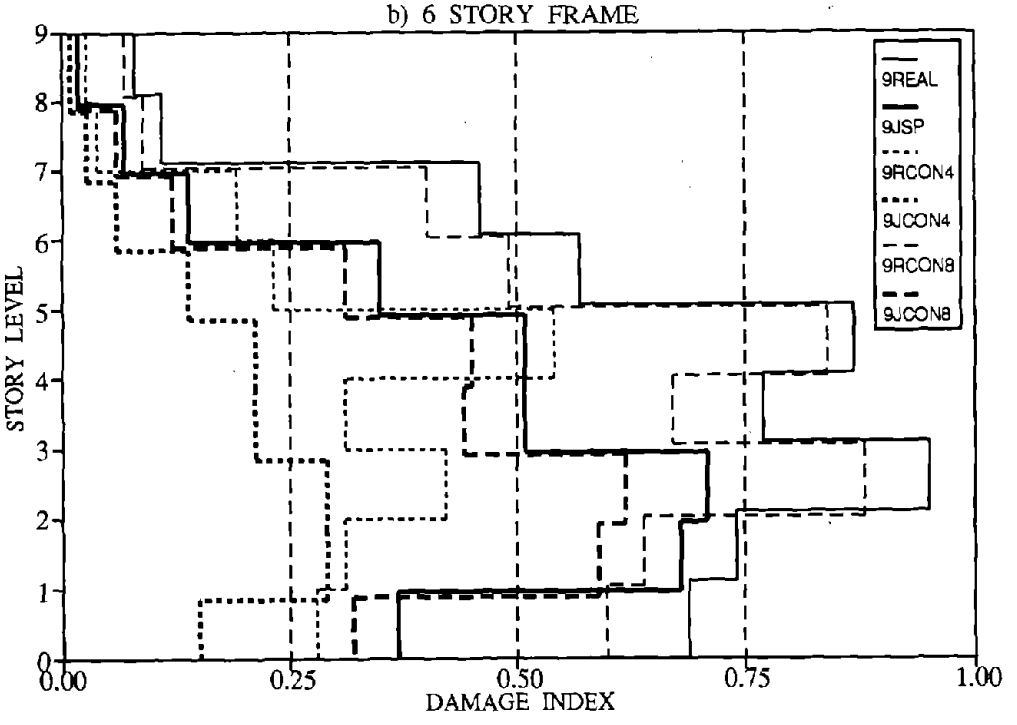

c) 9 STORY FRAME

Figure 7.14 Effect of Confinement on Beam Damage Distribution for Frames Subjected to Taft (PGA = 0.20 g)

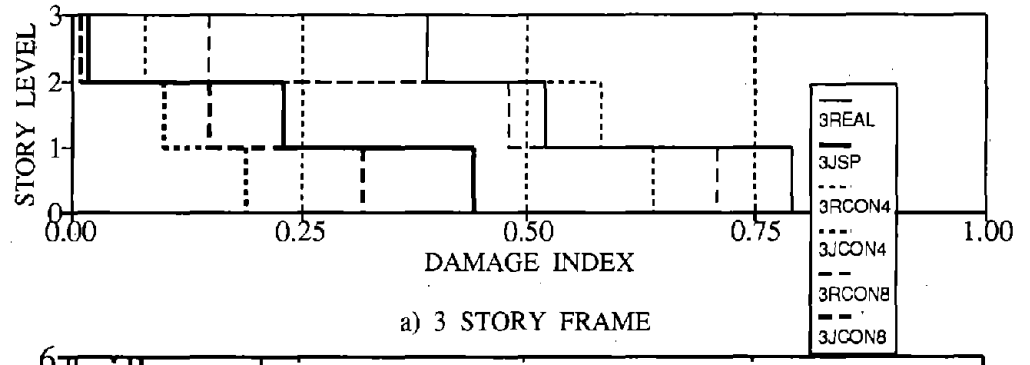

a) 3 STORY FRAME

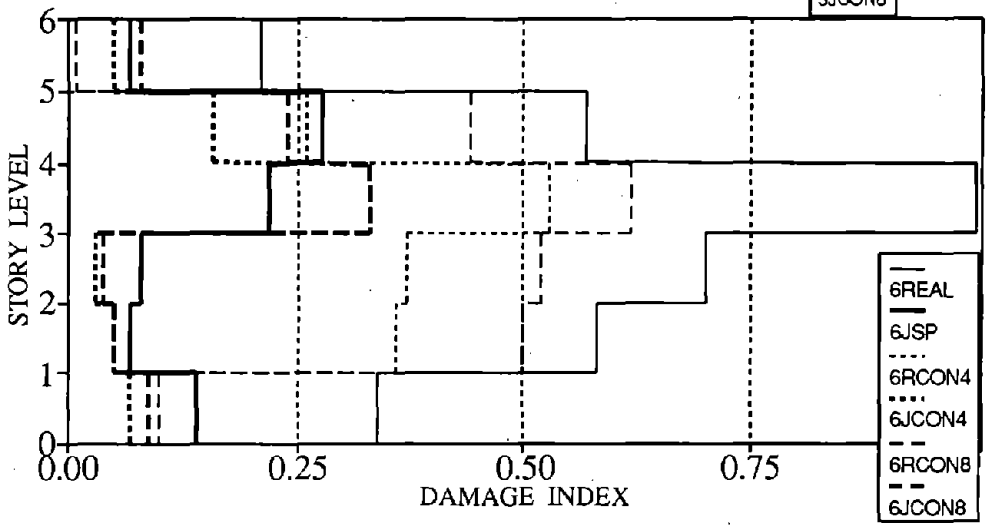

b) 6 STORY FRAME

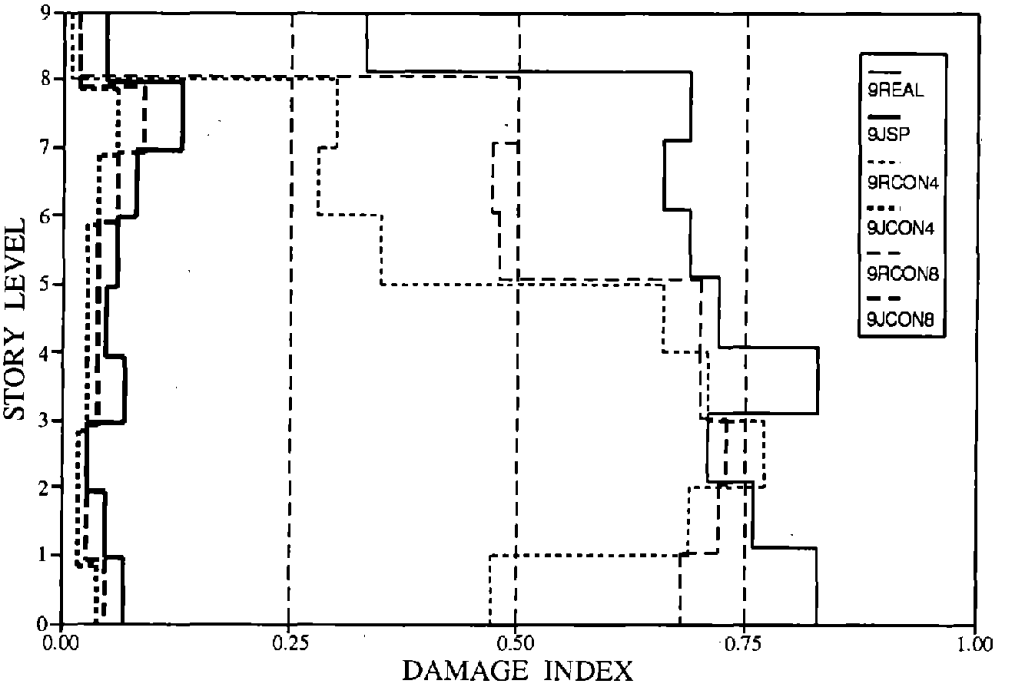

c) 9 STORY FRAME

Figure 7.15 Effect of Confinement on Column Damage Distribution for Frames Subjected to Taft (PGA = 0.20 g)

7.3.1 Effect of Increasing Level of Confinement

In general, for moderate earthquakes, the provision of additional transverse reinforcement in the columns does not have a substantial influence on the computed damage in the structure. This is primarily due to the fact that the confinement levels in the original columns were adequate to keep them within serviceable limit states. The minimal damage (for mild to moderate earthquakes) is a result of the axial load on the columns enhancing their strength.

Figures 7.10 - 7.13 illustrate the effects of confinement on three and six story frames subject to moderate seismic motions. Within the relative context of the damage levels, the enhanced confinement is clearly shown to improve behavior. As explained earlier, the increased confinement translates directly into additional ductility in the hinge regions, which in turn diminishes the structural damage.

For structures subjected to El Centro and Taft ground motions respectively, more pronounced damage reductions were observed. Modest reductions in beam damage in the order of 5-10% were observed from the provision of hoops at 8" spacing, while the provision of transverse steel at 4" spacing resulted in damage reductions in the order of 50%.

The provision of additional transverse steel can be considered more critical for severe earthquakes in which added ductility capacity is crucial to keep damage within acceptable limits.

7.4 Summary and Comparison of Member Damage

Tables 7.1 and 7.2 summarize the effects of the significant detailing strategies investigated in this study. These tables present values of average damage for beams and columns. The average member damage index is compared to that of the benchmark structure to examine the shift in damage and to ascertain the overall level of benefit provided from employment of the particular detailing strategy. Tables are provided for analyses performed using the Artificial Earthquake and the Taft Earthquake only. It was seen that the Nahanni Earthquake produced similar trends in average damage as the Artificial Earthquake. The same observation was made between the analyses performed using El Centro and Taft ground motions.

It can be observed that continuing positive beam reinforcement (case CPR) reduces the damage in the beams by 20% to as much as 60%, but increases the damage in the columns by far greater percentages. This detail, if adopted, should be complemented by joint steel reinforcement and enhanced confinement that reduces both beam and column damage. This was achieved in the detail JCON4.

From examination of all the results presented in this section, it is obvious that the frame utilizing the JCON4 detail provided the best seismic performance in terms of drift limitation, and damage reduction. The only question is whether the lower story columns, other than at the base of the first story, require such a tight spacing of transverse reinforcement. Since the columns in the lower story levels possess much greater flexural capacity than the corresponding beams, it appears unlikely that these columns will yield, thus never utilizing the additional ductility provided by the additional hoops. However, to prevent the remote possibility of longitudinal bars buckling and brittle crushing of poorly confined core concrete, a reasonable level of transverse reinforcement should be provided. As will be seen in the next section, the added cost of providing the additional steel is small in comparison to the added assurance against non-ductile failure.

Table 7.1 Average Beam and Column Damage Indices For Frames Subjected to Artificial Earthquake (PGA = 0.15g)

Detailing Strategy	Average Beam Damage Index	Percent Change in Damage	Average Column Damage Index	Percent Change in Damage
3REAL	0.11	-	0.07	-
3CPR	0.08	-22%	0.09	33%
3DPR	0.07	-34%	0.03	-62%
3JSP	0.02	-84%	0.03	-57%
3RCON4	0.04	-63%	0.03	-57%
3RCON8	0.09	-16%	0.05	-33%
3CPCON4	0.03	-75%	0.02	-71%
3CPCON8	0.07	-31%	0.03	-52%
3DCON4	0.03	-72%	0.01	-81%
3DCON8	0.06	-44%	0.02	-67%
3JCON4	0.01	-91%	0.01	-81%
3JCON8	0.02	-84%	0.02	-67%
6REAL	0.22	-	0.13	-
6CPR	0.09	-59%	0.20	55%
6DPR	0.27	25%	0.04	-73%
6JSP	0.05	-78%	0.04	-71%
6RCON4	0.10	-53%	0.07	-49%
6RCON8	0.21	-1%	0.09	-29%
6CPCON4	0.04	-84%	0.04	-71%
6CPCON8	0.08	-64%	0.06	-53%
6DCON4	0.10	-53%	0.02	-86%
6DCON8	0.22	0%	0.03	-79%
6JCON4	0.02	-91%	0.02	-83%
6JCON8	0.04	-81%	0.03	-79%
9REAL	0.21	-	0.05	-
9CPR	0.13	-39%	0.20	267%
9DPR	0.22	6%	0.03	-44%
9JSP	0.12	-43%	0.03	-35%
9RCON4	0.09	-55%	0.03	-50%
9RCON8	0.20	-3%	0.04	-25%
9CPCON4	0.07	-65%	0.10	83%
9CPCON8	0.16	-24%	0.15	175%
9DCON4	0.09	-56%	0.02	-71%
9DCON8	0.18	-13%	0.02	-58%
9JCON4	0.07	-64%	0.02	-71%
9JCON8	0.16	-24%	0.03	-52%

Table 7.2 Average Beam and Column Damage Indices For Frames Subjected to Taft Earthquake (PGA = 0.20g)

Detailing Strategy	Average Beam Damage Index	Percent Change in Damage	Average Column Damage Index	Percent Change in Damage
3REAL	0.45	-	0.57	-
3CPR	0.39	-13%	0.69	22%
3DPR	0.49	9%	0.30	-47%
3JSP	0.17	-63%	0.23	-59%
3RCON4	0.24	-47%	0.43	-24%
3RCON8	0.51	13%	0.45	-21%
3CPCON4	0.30	-33%	0.46	-19%
3CPCON8	0.31	-31%	0.63	12%
3DCON4	0.25	-44%	0.12	-78%
3DCON8	0.47	5%	0.21	-64%
3JCON4	0.07	-84%	0.10	-82%
3JCON8	0.14	-68%	0.16	-72%
6REAL	0.43	-	0.57	-
6CPR	0.25	-43%	0.68	19%
6DPR	0.62	44%	0.23	-60%
6JSP	0.26	-40%	0.14	-75%
6RCON4	0.18	-59%	0.27	-53%
6RCON8	0.37	-16%	0.37	-36%
6CPCON4	0.10	-77%	0.40	-30%
6CPCON8	0.21	-51%	0.54	-5%
6DCON4	0.34	-22%	0.08	-86%
6DCON8	0.66	53%	0.10	-82%
6JCON4	0.20	-54%	0.12	-80%
6JCON8	0.40	-9%	0.14	-76%
9REAL	0.58	-	0.69	-
9CPR	0.22	-63%	0.74	8%
9DPR	0.60	4%	0.07	-90%
9JSP	0.37	-36%	0.07	-91%
9RCON4	0.26	-55%	0.47	-32%
9RCON8	0.52	-11%	0.56	-20%
9CPCON4	0.10	-83%	0.37	-46%
9CPCON8	0.18	-69%	0.41	-41%
9DCON4	0.25	-57%	0.04	-95%
9DCON8	0.53	-10%	0.06	-92%
9JCON4	0.15	-73%	0.03	-95%
9JCON8	0.33	-44%	0.04	-94%

SECTION 8

COSTS & CONSEQUENCES OF IMPROVED DETAILING IN NEW CONSTRUCTION

Building owners and consulting engineers are generally most concerned about the cost of implementation, in addition to other factors such as feasibility, possible delay in construction time, and product or system availability. Most often, benefits of seismic resistance systems are put in terms of inter-story drift reduction, damage index reduction or decreased story shears. While this is necessary to illustrate behavioral enhancements of system implementation, design engineers, especially those outside the mandate of rigorous seismic codes, are afraid to investigate the possible utilization of these solutions from a cost point of view. Since this study concerns buildings that dont necessarily require seismic performance adequacy, it was decided to investigate costs associated with the suggested detailing alternatives, so as to evaluate the feasibility of such schemes.

Table 8.1 is a summary of the estimated total reinforcement and concrete required and associated material and placement costs involved of the sixteen detailing arrangements examined in this study as they would be implemented in the six story model. Comparisons of the added costs for the detailing strategies are made to the basic gravity-load-designed structure for total structural cost (excluding footing and excavation). *Only the six story building was evaluated for cost considerations as a representative sample.* The same trends would be obvious for the other buildings as well. Material and construction costs were estimated from data obtained from regional contractors and fabricators. Since the unit price data obtained was only pertinent to estimating concrete and reinforcement material and placement costs, comparisons made to total building cost were estimated by simple rule of thumb approximations of the ratio of total structural cost (excluding nonstructural walls) to total building cost. Calculation of concrete placement costs including formwork were based on the following unit price scale.

Slabs & Beams:	$\$200/yd^3$
Structural Walls:	$\$250/yd^3$
Columns:	$\$300/yd^3$

Calculations of reinforcement material and placement costs were estimated based on a basic unit price of \$0.60 per pound for easy-to-place typical structural detailing such as that in gravity-load-designed buildings.

Table 8.1 Summary of Estimated Material and Placement Costs For 6-Story Building

Detailing Designation	Total Concrete (yd^3)	Concrete Cost ($)	Total Reinforcement (lb.)	Approx. Unit Price ($/lb.)	Reinforcement Cost ($)	Percent Change From GLD Structural Cost	Percent Change From Total Bldg. Cost
(1)	(2)	(3)	(4)	(5)	(6)	(7)	(8)
6REAL	490	135,000	88,900	0.60	53,400	-	-
6CPR	490	135,000	89,500	0.60	53,700	0.2%	0%
6DPR	490	135,000	91,200	0.75	68,500	8.0%	1%
6JSP	490	135,000	91,800	0.75	68,900	8.2%	1%
6RCON4	490	135,000	93,300	0.80	74,700	11.3%	1.5%
6RCON8	490	135,000	91,500	0.75	68,700	8.1%	1%
6CPCON4	490	135,000	93,900	0.80	75,100	11.5%	1.5%
6CPCON8	490	135,000	92,100	0.75	69,100	8.3%	1%
6DCON4	490	135,000	95,600	0.95	90,800	19.9%	2.5%
6DCON8	490	135,000	93,800	0.90	84,500	16.5%	2%
6JCON4	490	135,000	96,200	0.95	91,400	20.2%	2.5%
6JCON8	490	135,000	94,400	0.90	85,000	16.8%	2%
6CCON4	490	135,000	93,300	0.80	74,700	11.3%	1.5%
6CCON8	490	135,000	91,500	0.75	68,700	8.1%	1%
6BCON4	490	135,000	93,300	0.80	74,700	11.3%	1.5%
6BCON8	490	135,000	91,500	0.80	68,700	8.1%	1%

However, due to the labor intensive nature of providing a tight configuration of reinforcement, contractors are likely to not be satisfied with proportionally applying their normal unit price for typical reinforcement placement to this additional reinforcement. Thus, the basic unit price was adjusted to reflect this disproportional labor required and the construction difficulties that are inherent in the revised detailing configurations. Added to the basic unit price of $0.60/lb. was $0.15/lb. for providing a medium level of hoop spacing (fairly confined) or $0.20/lb. for requiring a very tight spacing of hoops (well confined). Also, providing the required joint shear steel was estimated to increase the basic unit price by $0.15/lb. due to the added construction difficulty involved in tying transverse hoops within the joint region. It was assumed that no adjustment in the unit price would be made for the required bar splices needed to provide continuity of the bottom steel through the joint, other than the basic cost of the additional steel required from overlapping these bars in the low moment regions of the beam instead of termination within the interior joints.

These additional unit costs were intended to be rather conservative so as not to underestimate the placement problems that would inevitably arise from the high concentration of reinforcement in the joint region, especially for structures with more complicated framing arrangements.

The study indicates that no significant cost increase will result from implementing such changes. The maximum increase in steel cost alone from the lightly reinforced base detail (6REAL) to the most concentrated detailing arrangement (6JSP) is a mere 8% (not tabulated). However, due to the differing unit costs assumed, when comparing these two detailing strategies in terms of total structural cost, the increase appears to be much more significant at just over 20%. But, one must remember that the structural cost is a small portion of the actual building cost. Column (8) in Table 2 is a very rough estimate of the increase in total building cost due to implementation of the various detailing arrangements. It was roughly approximated that for simple R/C frames, the structural cost was anywhere from 8%-15% of the total building costs depending on it's intended usage. Conservatively, values in this table were computed using the higher end of this approximation and rounded to the nearest half percent. Hence we see from the table that the maximum increase in total building cost from utilizing any of the detailing arrangements is conservatively estimated at 2.5%.

Given the small additional cost to the structural portion of the building cost for a newly constructed building, the utilization of the best detailing arrangement should be considered as the *minimum* provision in newly designed R/C frames for seismic protection.

SECTION 9

CONCLUDING REMARKS

9.1 Existing GLD Structures

The first phase of this research was concerned with the performance of gravity load designed (GLD) RC structures under the action of seismic loads. In summary, the evaluation considered two types of earthquakes: one pair representing a design or typical earthquake of low to moderate energy content; and the other pair of records representing a maximum credible event with higher energy content. An overview of the damage plots (Section 5) and computed maximum story drift for each of the buildings indicate that:

- the buildings will perform satisfactorily when subject to a moderate earthquake with low energy content, though some degree of repairable damage may be inflicted throughout the structure.

- the buildings are susceptible to severe damage if subject to an intense ground-shaking at peak ground accelerations within the design spectra but with an energy content comparable to typical west coast earthquakes.

Some of the main problems associated with the performance of GLD structures are described below.

1) Most of the damage at the top and bottom of columns was generated by the failure of the joint panel. The cyclic load reversals in the joint severely weaken its limited shear capacity due to the grinding away of the concrete at the shear crack plane.

2) Beams suffered moderate damage in general. Those beams that suffered large damage did so due to inadequate rotational capacity. Lack of rotational capacity is due to inadequate anchorage of positive reinforcement and concrete confinement.

3) The failure mechanisms, in general, are a random combination of yielded columns and beams with column sidesway mechanisms developing at the lower levels (soft story mechanisms). These column mechanisms developed as a result of horizontal joint shear failures that prevented the column from reaching their full capacity. Such non-ductile failures, more likely during a severe earthquake, can lead to sudden or progressive collapse of the structure.

4) Interstory drifts in excess of 2.0% were observed in structures subjected to severe ground motions. In most cases, the drifts observed in the GLD structure were well in excess of the code prescribed limits.

It should be noted that in the above study, being a two-dimensional frame analysis, the full three-dimensional influence of the slabs was not able to be included, despite the stiffness and strength contributions of the slab being included in the beam elements. It is expected that additional slab contribution would further accentuate the column sidesway mechanism that developed. *Therefore, the conclusions presented above would not be contradicted if a more rigorous three-dimensional analysis was performed.*

Seismic design in general will require that: (1) the failure mechanism be such to maintain service load capacity; (2) members fail in a ductile manner and avoid a brittle fracture type of failure; (3) ductility capacity in plastic hinge zones be such as to withstand large rotations without the crushing of concrete in the compression zone.

It is unlikely that a gravity-load designed building will meet the above criteria if subject to a maximum credible event. However, given the expected return period and probability of occurrence of such an earthquake, it may not be economically viable to upgrade existing RC buildings unless they are critical to maintain essential services to the community following such an event.

Finally, it must be pointed out that site characteristics were not explicitly considered in the evaluations. In this case, two separate issues may also need to be addressed: (1) if the building is located on soft soil, the spectral characteristics of the earthquake will be vastly different with higher amplitudes in the longer period ranges, resulting in a different damage scenario; (2) the proximity of the building to other tall structures may dictate special requirements since otherwise acceptable drifts of 0.5-1.0% may still lead to problems of pounding with adjacent structures.

9.2 Enhanced Detailing for New Construction and Principles of Seismic Retrofit

The detailing strategies investigated in this concluding phase of the study was directed at simple enhancements in rebar details at hinge locations and beam-column joints without resorting to a full

seismic design. Similar detailing improvements, in a qualitative sense, can be achieved by retrofit techniques applied to reinforced concrete members and joints such as jacketing. The following observations were made:

1) **The provision of continuity of bottom bars of the beams** significantly reduced the beam damage by reducing the amount of hinge rotation. However, this transferred the majority of the damage to the columns. The restoration of beam capacity resulted in even a greater number of joint failures. This obviously magnified the soft story effect of the structures. Due to the non-ductile failure mechanism that remained, it was evident that the *provision of bottom bar continuity alone would be detrimental to the structural performance.*

2) **The provision of transverse steel to restore joint shear capacity** had a tendency of shifting the damage from the columns into the beams. Since joint shear failure was eliminated, the failure mechanism transferred into a favorable beam-sidesway mechanism. However, due to the significant undercapacity of the beams, story drifts were still at an unfavorable level.

3) **The provision of additional confinement in the plastic hinge regions** of members provided just a limited benefit by itself. Since the confinement does not appreciably affect the deformation demand of the structure, the non-ductile failure mechanism remained, as well as the large drifts and member rotations. The confinement did provide appreciable benefits in that member rotational capacity was significantly enhanced by the additional hoops.

4) **The combination of the three detailing strategies** proved to yield the best benefits. By restoring both beam and joint capacities, overall structure behavior was more uniform and story drifts were reduced to nearly those stipulated by building codes. A beam-sidesway mechanism will form under this detailing arrangement and since rotational capacities are much higher (compared to those in the GLD structure), member damages are drastically decreased.

Since the additional cost to the structural portion of the building resulting from the use of detail JCON4 is around 2.5% for a newly constructed building, the utilization of the best detailing arrangement (JCON4) should be considered as the minimum provision in newly designed R/C frames for seismic protection. These strategies can also serve as the qualitative basis for development of retrofit techniques of existing structures. Such techniques must deal with the following issues *simultaneously:* improvement of continuity of positive reinforcement (or a proper anchorage); strengthening of beam-column joints; and increasing the confinement in the new critical sections.

9.3 Recommendations for Newly Designed Structures

Although gravity-load-designed methods can still be used in low to moderate seismicity regions, the detailing of reinforcement must follow rational guidelines. The following recommendations can be made based on the analysis and observations obtained from this research:

1) A portion of the positive flexural reinforcement should remain continuous through the joint. Providing full yield strength in the beam is not a problem in lower story levels where column strengths are enhanced from large axial loads. To avoid a possible strong beam condition in upper floors, it is suggested that an increased number of smaller diameter flexural bars, as opposed to a small number of large bars, should be used for bottom reinforcement in the beam with some (say one-half) of them being continuous. For example, the 2-#6 bars (A_s = 0.88 in^2) used for bottom bars near the joint in the original frame examined in this study, could be easily replaced with 2-#4 bars and 2-#5 bars (A_s = 1.00 in^2) and either pair of bars could be left continuous as required by the strength of the column they frame into. This would only be required in upper story levels to assure the weak beam-strong column system remained. It is pointed out that continuity of all bars may be detrimental. A capacity check of adjoining beams and columns must be required for low rise buildings or upper stories in high rise buildings.

2) The transverse reinforcement in the joint should be such maintain joint integrity and assure framing members may develop their full flexural capacity. Such reinforcement can be a natural continuation of column hoops or some transverse diagonal bars from the beams.

3) At present, the ACI-318 code specifies the volumetric ratio of the transverse reinforcement through the joint (ACI 21.4.4) as minimum which is based on the joint confinement required and not the necessary transmission of joint shear forces. Further, code estimations of joint shear strength are only a function of concrete strength and effective joint area (ACI 21.6.3). The provisions are independent of axial load and level of transverse or longitudinal reinforcement. Should designers be faced with the problem of having a trial design in which joint shear forces are larger than the code calculated capacity, their only option, according to the code, is to increase the joint size. The code does not address the option of increasing the shear steel volume.

   Common design practice is to assume that the required joint shear strength is equal to the maximum shear force occurring in any member at the joint face. However, this is generally not adequate, since for lateral loading, the actual shear transmitted through the joint by the

longitudinal reinforcement is usually much greater. Instead, the actual shear force acting on the joint from the transfer axial forces through the joint should be determined. This could be done, by assuming the maximum shear force on the joint is that which would correspond to the flexural yielding of the members framing into it.

4) Additional transverse reinforcement should be provided in all potential plastic hinge regions to assure that the large strains associated with plastic rotations may develop without crushing of the concrete core.

SECTION 10

REFERENCES

1. ACI Committee 318, Building Code Requirements for Reinforced Concrete, (ACI 318-89), Including Commentary, American Concrete Institute, Detroit, 1989.

2. ACI-ASCE Committee 352, "Recommendations for Design of Beam-Column Joints in Monolithic Structures", *Journal of ACI*, 73, July, 1976.

3. American National Standards Institute Inc., "American National Standard: Minimum Design Loads for Buildings and Other Structures", ANSI A58.1-1982, New York.

4. Anagostopolous, S.A., Petrovski, J. and Bouwkamp, J.G., "Emergency Earthquake Damage and Usability Assessment of Buildings", *EERI/Earthqake Spectra*, Vol. 5, No. 3, August, pp. 461-476, 1989.

5. Applied Technology Council, "A Handbook for Seismic Evaluation of Existing Buildings", ATC-22, Redwood City, California, 1989.

6. Bracci, J.M., Reinhorn, A.M. and Mander J.B., "Experimental Evaluation of One-Third Scale Three Story Gravity-Load-Designed R/C Frame Structure", Technical Report for the National Center for Earthquake Engineering Research, State University of New York at Buffalo, Publication Pending.

7. Bracci, J.M., Reinhorn A.M., Mander J.B. and Kunnath, S.K., "Deterministic Model For Seismic Damage Evaluation of Reinforced Concrete Structures", Technical Report NCEER-89-0033, State University of New York at Buffalo, 1989.

8. Chung, Y.S., Meyer, C. and Shinozuka, M., "Seismic Damage Assessment of Reinforced Concrete Members," Technical Report NCEER-87-0022, State University of New York at Buffalo, 1987.

9. Gasparini, D.A. and Vanmarke, E.H., "Simulated Earthquake Motions Compatible With Prescribed Response Spectra", Massachusetts Institute of Technology Department of Civil Engineering Research Report R76-4, 1976.

10. Ghali, A. and Neville, A.M., "Structural Analysis: A Unified Classical and Matrix Approach", Chapman and Hall, New York, 1989.

11. Kaanan, A.E. and Powell, G.H., "DRAIN-2D, A General Purpose Computer Program for Dynamic Analysis of Planar Structures", UCB/EERC Report 73-6, University of California, Berkeley, 1973.

12. Kunnath, S.K., Mander, J.B. and Reinhorn, A.M., "Seismic Response and Damageability of Gravity-Load (Non-Seismic) Designed Buildings", Proceedings: 9th European Conference on Earthquake Engineering, Vol. 9, pp. 323-332, Moscow, 1990.

13. Lao F.L., "The Effect of Detailing on the Seismic Performance of Gravity Load Dominated Reinforced Concrete Frames", M.S. Thesis, Department of Civil Engineering, State University of New York at Buffalo, 1990.

14. Mander, J.B., "Seismic Design of Bridge Piers", Ph.d. Thesis, Department of Civil Engineering, University of Canterbury, Christchurch, New Zealand, 1983.

15. Newmark, N.M. and Rosenbleuth, E., Fundamentals of Earthquake Engineering, Prentice Hall, 1974.

16. Otani, S., Kitayama, K. and Hiroyaki, A., "Beam Bar Bond Stress and Behavior of Reinforced Concrete Interior Beam-Column Connections", A paper presented during second U.S.-New Zealand-Japan Seminar on Design of Reinforced Concrete Beam-Column Joints, Tokyo, Japan, May, 1985.

17. Otani, S., Kobayashi, Y. and Hiroyaki, A., "Reinforced Concrete Interior Beam-Column Joints Under Simulated Earthquake Loading", A paper presented during first U.S.-New Zealand-Japan Seminar on Design of Reinforced Concrete Beam-Column Joints, Monterey, California, July, 1984.

18. Papageorgiou, A.S., "Estimation of Earthquake Strong Ground-Motion In Eastern North America: Preliminary Estimates Vis-A-Vis Existing Data", Proceedings: Symposium on Seismic Hazards, Ground Motions, Soil-Liquefaction and Engineering and Engineering Practice in Eastern North America, October 20-22, 1987, Technical Report NCEER-87-0025, pp 282-299.

19. Park, R. and Paulay, T., Reinforced Concrete Structures, John-Wiley and Sons, New York, 1974.

20. Park, Y.J., Ang, A. H-S. and Wen, Y.K., "Mechanistic Seismic Damage Model for Reinforced Concrete", *ASCE/Journal of Structural Engineering*, Vol. 111, No. 4, pp. 722-739, 1985.

21. Park, Y.J., Ang, A.H-S. and Wen, Y.K., "Seismic Damage Analysis and Damage-Limiting Design of R/C Buildings", Civil Engineering Studies, SRS No. 516, University of Illinois, Urbana, 1984.

22. Park, Y.J., Reinhorn, A.M. and Kunnath, S.K., "IDARC: Inelastic Damage Analysis of Reinforced Concrete Frame-Shear Wall Structures", Technical Report NCEER-87-0008, State University of New York at Buffalo, 1987.

23. Paulay, T., "Equilibrium Criteria for Reinforced Concrete Beam-Column Joints", *ACI Structural Journal*, Vol. 86, No. 6, November-December 1989.

24. Pessiki, S.P., Conley C.H., Gergely, P. and White, R.N., "Seismic Behavior of Lightly Reinforced Concrete Column and Beam-Column Joint Details", Technical Report NCEER-90-0014, State University of New York at Buffalo, 1990.

25. Reinhorn, A.M., Seidel, M.J., Kunnath, S.K. and Park, Y.J., "Damage Assessment of Reinforced Concrete Structures in Eastern United States", Technical Report NCEER-88-0016, State University of New York at Buffalo, 1988.

26. Uniform Building Code, International Conference of Building Officials, Whittier, California, 1988.

27. Winters, C.W., Hoffmann, G.W., Symans, M.D. and Wood, T.L., "An Experimental Study of Four Beam-Column Joint Assemblages", Special Study Report, Department of Civil Engineering, State University of New York at Buffalo, 1991.

APPENDIX A

MEMBER SECTION PROPERTIES

General Notes Pertaining to All Tables:

1. All units are in kips and inches unless otherwise noted.
2. Column types and beam types are designated using the following notation:

   E - exterior
   I - interior
   C - column
   B - beam
   1st number - story number starting from top floor
   2nd number - spacing of transverse reinforcement
   (top) - indicates that properties correspond to top of column only
   (bot) - indicates that properties correspond to bottom of column only

   Figure A-1 further illustrates the location of all the column and beam types.
3. Exterior beams refer to the exterior section of the outside beam.
4. Interior beams refer to both ends of interior beams as well as interior ends of exterior beams.
5. Unless noted, it is assumed that the properties at the top of a column are the same as those at the bottom of a column.
6. EIo represents the initial composite stiffness of a member.
7. The post-yield stiffness (EI3) of members has been expressed as a percent of the initial composite stiffness of the member.
8. Values represent properties calculated based on the cross-sections and material properties outlined in Sections 2.

Notes Specific to Individual Table(s):

Table A-1 Exterior Column Properties with Sufficient Joint Steel Provided
Table A-2 Interior Column Properties with Sufficient Joint Steel Provided

1. *Tables give section properties of exterior and interior columns assuming that the corresponding joints in which they frame are sufficiently reinforced to allow full transfer of the shear forces induced by the transfer of column moments.*

Table A-3 Exterior Column Properties Reduced to Reflect Joint Capacity
Table A-4 Interior Column Properties Reduced to Reflect Joint Capacity

1. *Tables give section properties of exterior and interior columns that have been adjusted to model the behavior corresponding to an unreinforced beam-column joint. That is, the moment capacities have been adjusted, if necessary, to correspond to the column moment*

that would cause the unreinforced joint to fail in shear prior to the column reaching its full yield capacity. Obviously, if the joint has sufficient strength to transfer the full yield moment, then no adjustment is necessary. Yield curvatures and ultimate curvatures of members have also been adjusted to maintain the proper cracked stiffness as well as to model the reduction in ductility to some extent. See Section 3 for the development of this joint shear failure model.

2. *Post cracking stiffness has been adjusted to assure that the cracked curvature and yield curvature are not too close as to cause program instability during dynamic analysis. If cracked curvature is too close to the value of yield curvature, the analysis could go from elastic to post-yield in one time step, leading occasionally to large unbalanced forces. The adjustment is superficial and does not affect member capacities or ductilities.*
3. *Special attention has been given to the top floors and the bottom floors to ensure accurate modelling. It is justly assumed that the bottom of the first story column need not be adjusted for joint shear failure since it is typically framed into the foundation. The "N/A" that appears in columns (6) and (7) for the bottom of the 1st floor column (9) indicates that the shear strength of this "joint" does not influence the capacity of this column and is not applicable for this table.*
4. *Referring to columns (4) and (5) in the tables, b' and d' respectively, represent the effective width and depth of the beam-column in shear. See Fig. 3.9 for illustration of these dimensions.*
5. *Referring to column (6), V_{jv} represents the vertical shear capacity of the beam-column joint. See Section 3 for discussion on joint shear strength.*
6. *Referring to column (7), M_j represents the corresponding moment in the column that would induce the failure of the beam-column joint in shear. If lower than the calculated yield capacity of the column (M_y) this value of equivalent moment to induce joint shear failure (M_j) is used in place of the yield moment. See Section 3 for development of these equivalent moment capacities.*

Table A-5 Beam Properties With Sufficient Joint Steel and Development Length Provided

1. *This Table gives section properties of exterior and interior beam assuming that the corresponding joints in which they frame joint are sufficiently reinforced to allow full transfer of the shear forces induced by the transfer of beam moments. Values in this table are also based on the assumption that proper development length exists to ensure that "pullout" does not occur.*
2. *Values are provided for one exterior beam and one interior beam for various levels of confinement (hoop spacing). This is simply because if the conditions in note 1 regarding sufficient joint strength are met, all the exterior beams will have the same properties regardless of story level. The same is true for all interior beams.*

Table A-6 Beam Properties Reduced to Reflect Discontinuous Positive Reinforcement

1. *This Table gives section properties of exterior and interior beams that have been adjusted to correspond to the behavior that would be a result of inadequate development length. The existing embedment length and the required development length are shown in columns (3) and (4). The yield moment in column (7) has been adjusted to correspond with the moment that would correspond to bar "pullout". The cracking moment has also been adjusted to ensure a trilinear moment curvature diagram as required by the dynamic analysis program. Curvatures have been similarly adjusted to assure proper stiffness and ductility that result from this type of failure.*
2. *Values are provided for positive bending since this phenomenon does not occur in negative bending due to the continuity of the top reinforcing steel.*
3. *Beams at only two story levels have been included in the table because beams framing into 12" columns (top 3 floors) have the same properties regardless of story level. The same holds true for beams framing into 15" columns (stories supporting 3 or more floors).*
4. *Interior and exterior beams have essentially the same positive flexural properties as can be seen from the table.*

Table A-7 Exterior Beam Properties Reduced to Reflect Joint Capacity
Table A-8 Interior Beam Properties Reduced to Reflect Joint Capacity

1. *Tables give section properties of exterior and interior beams that have been adjusted to model the behavior corresponding to an unreinforced beam-column joint. That is, the moment capacities have been adjusted, if necessary, to correspond to the beam moment that would cause the unreinforced joint to fail in shear prior to the beam reaching its full yield capacity. Obviously, if the joint has sufficient strength to transfer the full yield moment, then no adjustment is necessary. Yield curvatures and ultimate curvatures of members have also been adjusted to maintain the proper cracked stiffness as well as to model the reduction in ductility to some extent. See Section 3 for the development of this joint shear failure model.*
2. *Values of the effective dimensions of the joint in horizontal shear have not been tabulated, however they can be easily obtained from Fig. 3.9.*
3. *Referring to column (2), V_{jh} represents the horizontal shear capacity of the beam-column joint. See Section 3 for discussion on joint shear strength.*
4. *Column (3): M_j represents the corresponding moment in the column that would induce the failure of the beam-column joint in shear. If lower than the calculated yield capacity of the column (M_y) this value of equivalent moment to induce joint shear failure (M_j) is used in place of the yield moment. See Section 3 for development of these equivalent moment capacities.*

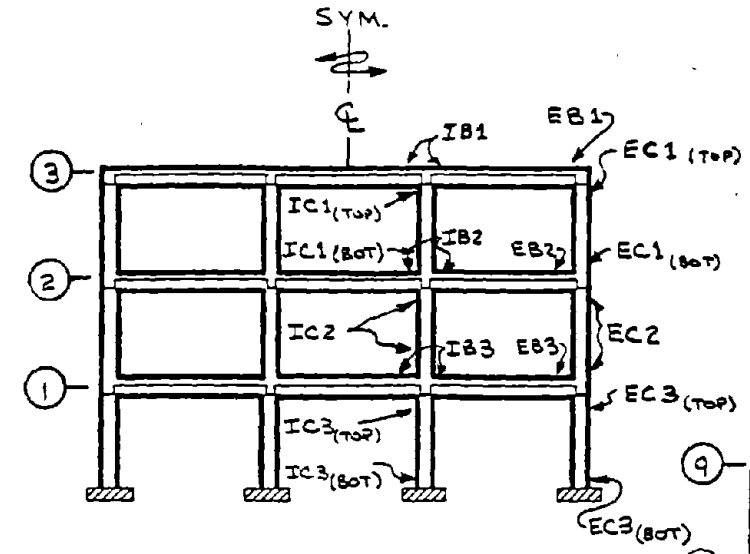

(a) 3 Story Frames

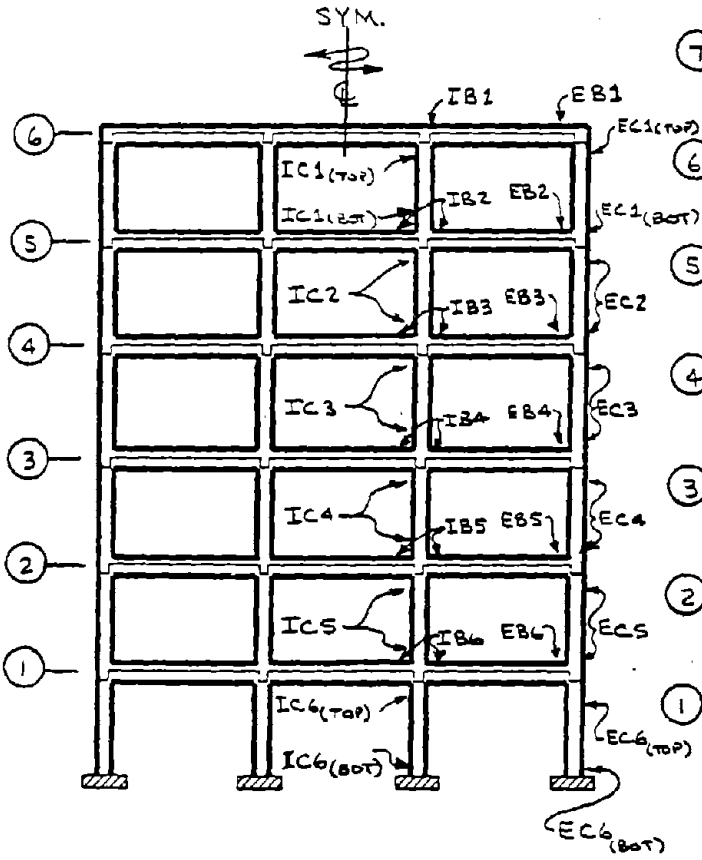

(b) 6 Story Frames

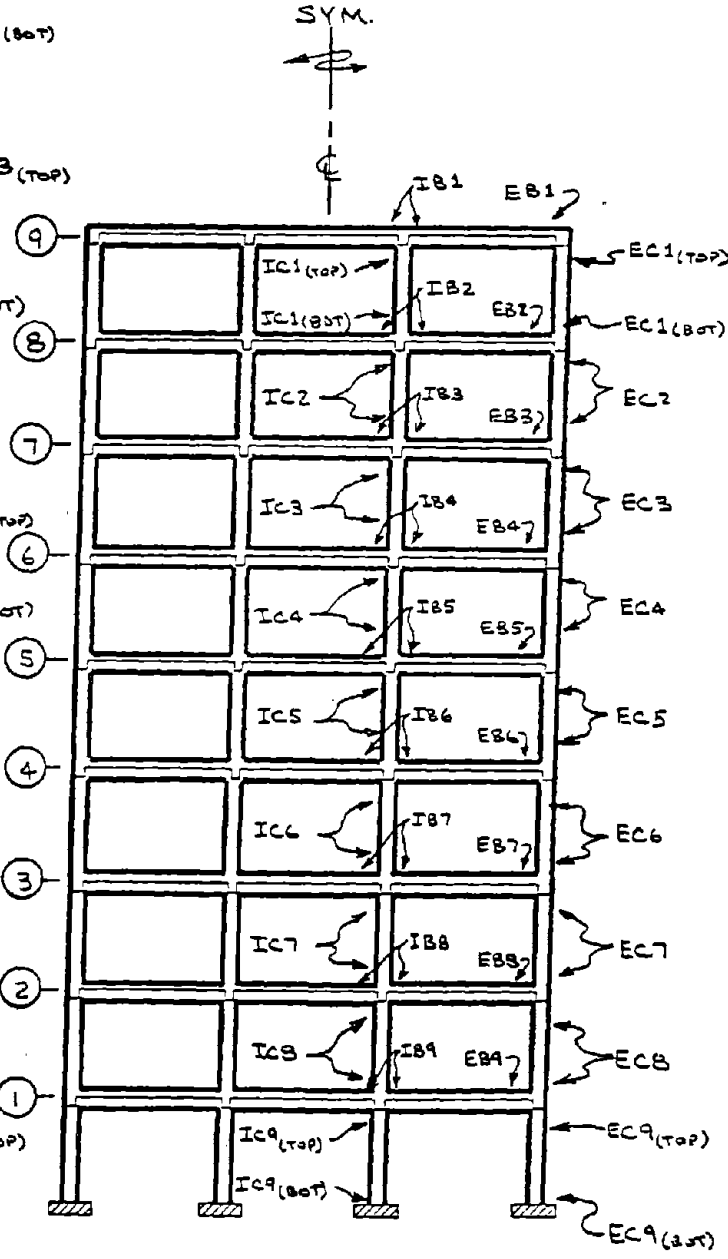

(c) 9 Story Frames

Figure A-1 Member Designation

Table A-1 Exterior Column Properties with Sufficient Joint Steel

COLUM TYPE	SIZE (in)	LONG. REINF.	HOOP SPA.	AXIAL LOAD (kips)	Elo (x 10^6) (k-in^2)	Mcr (k-in)	My (k-in)	PHIy (x 10^-3) (1/in)	PHIu (x 10^-3) (1/in)	EI3/Elo (%)	EA/L (k/in)	GA (x 10^6) (k)
(1)	(2)	(3)	(4)	(5)	(6)	(7)	(8)	(9)	(10)	(11)	(12)	(13)
EC1_3	12x12	4 # 6	#3 @ 3"	28	7.2	258	485	0.117	18.0	0.20	3915	0.186
EC1_4	12x12	4 # 6	#3 @ 4"	28	7.2	258	485	0.117	14.0	0.20	3915	0.182
EC1_6	12x12	4 # 6	#3 @ 6"	28	7.2	258	485	0.117	8.5	0.20	3915	0.178
EC1_8	12x12	4 # 6	#3 @ 8"	28	7.2	258	485	0.117	7.6	0.20	3915	0.175
EC1_12	12x12	4 # 6	#3 @ 12	28	7.2	258	485	0.117	7.0	0.20	3915	0.173
EC2_3	12x12	4 # 6	#3 @ 3"	56	7.2	316	618	0.152	10.0	0.20	3915	0.186
EC2_4	12x12	4 # 6	#3 @ 4"	56	7.2	316	618	0.152	8.0	0.20	3915	0.182
EC2_6	12x12	4 # 6	#3 @ 6"	56	7.2	316	618	0.152	5.8	0.20	3915	0.178
EC2_8	12x12	4 # 6	#3 @ 8"	56	7.2	316	618	0.152	5.3	0.20	3915	0.175
EC2_12	12x12	4 # 6	#3 @ 12	56	7.2	316	618	0.152	4.6	0.20	3915	0.173
EC3_3	12x12	4 # 6	#3 @ 3"	83	7.2	373	730	0.176	8.4	0.20	3915	0.186
EC3_4	12x12	4 # 6	#3 @ 4"	83	7.2	373	730	0.176	7.0	0.20	3915	0.182
EC3_6	12x12	4 # 6	#3 @ 6"	83	7.2	373	730	0.176	5.6	0.20	3915	0.178
EC3_8	12x12	4 # 6	#3 @ 8"	83	7.2	373	730	0.176	4.8	0.20	3915	0.175
EC3_12	12x12	4 # 6	#3 @ 12	83	7.2	373	730	0.176	4.0	0.20	3915	0.173
EC4_4	15x15	4 # 8	#3 @ 4"	111	18.0	700	1430	0.140	5.1	0.27	6186	0.269
EC4_6	15x15	4 # 8	#3 @ 6"	111	18.0	700	1430	0.140	4.1	0.27	6186	0.263
EC4_8	15x15	4 # 8	#3 @ 8"	111	18.0	700	1430	0.140	3.8	0.27	6186	0.260
EC4_12	15x15	4 # 8	#3 @ 12	111	18.0	700	1430	0.140	3.6	0.27	6186	0.257
EC4_15	15x15	4 # 8	#3 @ 15	111	18.0	700	1430	0.140	2.8	0.27	6186	0.256
EC5_4	15x15	4 # 8	#3 @ 4"	139	18.0	776	1575	0.154	4.9	0.27	6186	0.269
EC5_6	15x15	4 # 8	#3 @ 6"	139	18.0	776	1575	0.154	3.9	0.27	6186	0.263
EC5_8	15x15	4 # 8	#3 @ 8"	139	18.0	776	1575	0.154	3.5	0.27	6186	0.260
EC5_12	15x15	4 # 8	#3 @ 12	139	18.0	776	1575	0.154	3.1	0.27	6186	0.257
EC5_15	15x15	4 # 8	#3 @ 15	139	18.0	776	1575	0.154	2.1	0.27	6186	0.256
EC6_4	15x15	4 # 8	#3 @ 4"	167	18.0	851	1720	0.168	3.6	0.27	6186	0.269
EC6_6	15x15	4 # 8	#3 @ 6"	167	18.0	851	1720	0.168	3.1	0.27	6186	0.263
EC6_8	15x15	4 # 8	#3 @ 8"	167	18.0	851	1720	0.168	2.6	0.27	6186	0.260
EC6_12	15x15	4 # 8	#3 @ 12	167	18.0	851	1720	0.168	2.1	0.27	6186	0.257
EC6_15	15x15	4 # 8	#3 @ 15	167	18.0	851	1720	0.168	1.9	0.27	6186	0.256
EC7_4	15x15	8 # 8	#3 @ 4"	195	20.0	954	2350	0.182	3.9	0.30	8608	0.269
EC7_6	15x15	8 # 8	#3 @ 6"	195	20.0	954	2350	0.182	3.4	0.30	8608	0.263
EC4_8	15x15	8 # 8	#3 @ 8"	195	20.0	954	2350	0.182	2.6	0.30	8608	0.260
EC7_12	15x15	8 # 8	#3 @ 12	195	20.0	954	2350	0.182	2.4	0.30	8608	0.257
EC7_15	15x15	8 # 8	#3 @ 15	195	20.0	954	2350	0.182	2.2	0.30	8608	0.256
EC8_4	15x15	8 # 8	#3 @ 4"	222	20.0	1026	2425	0.191	3.8	0.30	8608	0.269
EC8_6	15x15	8 # 8	#3 @ 6"	222	20.0	1026	2425	0.191	3.1	0.30	8608	0.263
EC8_8	15x15	8 # 8	#3 @ 8"	222	20.0	1026	2425	0.191	2.6	0.30	8608	0.260
EC8_12	15x15	8 # 8	#3 @ 12	222	20.0	1026	2425	0.191	2.3	0.30	8608	0.257
EC8_15	15x15	8 # 8	#3 @ 15	222	20.0	1026	2425	0.191	2.1	0.30	8608	0.256
EC9_4	15x15	8 # 8	#3 @ 4"	250	20.0	1101	2500	0.195	3.7	0.30	8608	0.269
EC9_6	15x15	8 # 8	#3 @ 6"	250	20.0	1101	2500	0.195	2.8	0.30	8608	0.263
EC9_8	15x15	8 # 8	#3 @ 8"	250	20.0	1101	2500	0.195	2.6	0.30	8608	0.260
EC9_12	15x15	8 # 8	#3 @ 12	250	20.0	1101	2500	0.195	2.3	0.30	8608	0.257
EC9_15	15x15	8 # 8	#3 @ 15	250	20.0	1101	2500	0.195	2.0	0.30	8608	0.256

Table A-2 Interior Column Properties with Sufficient Joint Steel

COLUM TYPE	SIZE (in)	LONG. REINF.	HOOP SPA.	AXIAL LOAD (kips)	EIo (x 10^6) (k-in^2)	Mcr (k-in)	My (k-in)	PHIy (x 10^-3) (1/in)	PHIu (x 10^-3) (1/in)	EI3/EIo (%)	EA/L (k/in)	.GA (x 10^6) (k)
(1)	(2)	(3)	(4)	(5)	(6)	(7)	(8)	(9)	(10)	(11)	(12)	(13)
IC1_3	12x12	4 # 6	#3 @ 3"	44	7.2	291	560	0.134	12.0	0.20	3915	0.186
IC1_4	12x12	4 # 6	#3 @ 4"	44	7.2	291	560	0.134	10.4	0.20	3915	0.182
IC1_6	12x12	4 # 6	#3 @ 6"	44	7.2	291	560	0.134	8.0	0.20	3915	0.178
IC1_8	12x12	4 # 6	#3 @ 8"	44	7.2	291	560	0.134	6.8	0.20	3915	0.175
IC1_12	12x12	4 # 6	#3 @ 12	44	7.2	291	560	0.134	5.6	0.20	3915	0.173
IC2_3	12x12	4 # 6	#3 @ 3"	89	7.2	386	758	0.183	8.2	0.20	3915	0.186
IC2_4	12x12	4 # 6	#3 @ 4"	89	7.2	386	758	0.183	6.1	0.20	3915	0.182
IC2_6	12x12	4 # 6	#3 @ 6"	89	7.2	386	758	0.183	5.3	0.20	3915	0.178
IC2_8	12x12	4 # 6	#3 @ 8"	89	7.2	386	758	0.183	4.3	0.20	3915	0.175
IC2_12	12x12	4 # 6	#3 @ 12	89	7.2	386	758	0.183	3.4	0.20	3915	0.173
IC3_3	12x12	4 # 6	#3 @ 3"	133	7.2	481	915	0.217	6.0	0.20	3915	0.186
IC3_4	12x12	4 # 6	#3 @ 4"	133	7.2	481	915	0.217	4.8	0.20	3915	0.182
IC3_6	12x12	4 # 6	#3 @ 6"	133	7.2	481	915	0.217	3.6	0.20	3915	0.178
IC3_8	12x12	4 # 6	#3 @ 8"	133	7.2	481	915	0.217	2.8	0.20	3915	0.175
IC3_12	12x12	4 # 6	#3 @ 12	133	7.2	481	915	0.217	2.6	0.20	3915	0.173
IC4_4	15x15	4 # 8	#3 @ 4"	177	18.0	879	1770	0.173	3.6	0.27	6186	0.269
IC4_6	15x15	4 # 8	#3 @ 6"	177	18.0	879	1770	0.173	3.0	0.27	6186	0.263
IC4_8	15x15	4 # 8	#3 @ 8"	177	18.0	879	1770	0.173	2.5	0.27	6186	0.260
IC4_12	15x15	4 # 8	#3 @ 12	177	18.0	879	1770	0.173	1.7	0.27	6186	0.257
IC4_15	15x15	4 # 8	#3 @ 15	177	18.0	879	1770	0.173	1.6	0.27	6186	0.256
IC5_4	15x15	4 # 8	#3 @ 4"	222	18.0	999	1960	0.189	2.8	0.27	6186	0.269
IC5_6	15x15	4 # 8	#3 @ 6"	222	18.0	999	1960	0.189	2.5	0.27	6186	0.263
IC5_8	15x15	4 # 8	#3 @ 8"	222	18.0	999	1960	0.189	2.0	0.27	6186	0.260
IC5_12	15x15	4 # 8	#3 @ 12	222	18.0	999	1960	0.189	1.6	0.27	6186	0.257
IC5_15	15x15	4 # 8	#3 @ 15	222	18.0	999	1960	0.189	1.5	0.27	6186	0.256
IC6_4	15x15	4 # 8	#3 @ 4"	260	18.0	1119	2100	0.198	2.6	0.27	6186	0.269
IC6_6	15x15	4 # 8	#3 @ 6"	260	18.0	1119	2100	0.198	2.0	0.27	6186	0.263
IC6_8	15x15	4 # 8	#3 @ 8"	260	18.0	1119	2100	0.198	1.9	0.27	6186	0.260
IC6_12	15x15	4 # 8	#3 @ 12	260	18.0	1119	2100	0.198	1.5	0.27	6186	0.257
IC6_15	15x15	4 # 8	#3 @ 15	260	18.0	1119	2100	0.198	1.2	0.27	6186	0.256
IC7_4	15x15	8 # 8	#3 @ 4"	310	20.0	1261	2640	0.201	3.4	0.30	8608	0.269
IC7_6	15x15	8 # 8	#3 @ 6"	310	20.0	1261	2640	0.201	2.6	0.30	8608	0.263
IC4_8	15x15	8 # 8	#3 @ 8"	310	20.0	1261	2640	0.201	2.4	0.30	8608	0.260
IC7_12	15x15	8 # 8	#3 @ 12	310	20.0	1261	2640	0.201	2.1	0.30	8608	0.257
IC7_15	15x15	8 # 8	#3 @ 15	310	20.0	1261	2640	0.201	1.9	0.30	8608	0.256
IC8_4	15x15	8 # 8	#3 @ 4"	354	20.0	1378	2730	0.204	3.2	0.30	8608	0.269
IC8_6	15x15	8 # 8	#3 @ 6"	354	20.0	1378	2730	0.204	2.5	0.30	8608	0.263
IC8_8	15x15	8 # 8	#3 @ 8"	354	20.0	1378	2730	0.204	2.3	0.30	8608	0.260
IC8_12	15x15	8 # 8	#3 @ 12	354	20.0	1378	2730	0.204	1.8	0.30	8608	0.257
IC8_15	15x15	8 # 8	#3 @ 15	354	20.0	1378	2730	0.204	1.7	0.30	8608	0.256
IC9_4	15x15	8 # 8	#3 @ 4"	399	20.0	1499	2800	0.205	2.8	0.30	8608	0.269
IC9_6	15x15	8 # 8	#3 @ 6"	399	20.0	1499	2800	0.205	2.4	0.30	8608	0.263
IC9_8	15x15	8 # 8	#3 @ 8"	399	20.0	1499	2800	0.205	2.2	0.30	8608	0.260
IC9_12	15x15	8 # 8	#3 @ 12	399	20.0	1499	2800	0.205	1.7	0.30	8608	0.257
IC9_15	15x15	8 # 8	#3 @ 15	399	20.0	1499	2800	0.205	1.6	0.30	8608	0.256

Table A-3 Factored Exterior Column Properties to Reflect Joint Capacity

COLUMN TYPE	SIZE	AXIAL LOAD	b'	h'	(Vjv)	(Mjv)	Elo (x 10^6)	Mcr	My	PHIy (x 10^-3	PHIu (x 10^-3	EI3/EIo
	(in)	(kips)	(in)	(in)	(kips)	(k-in)	(k-in^2)	(k-in)	(k-in)	(1/in)	(1/in)	(%)
(1)	(2)	(3)	(4)	(5)	(6)	(7)	(8)	(9)	(10)	(11)	(13)	(14)
EC1_3 (top)	12x12	28	9.0	16.5	71.6	659	7.2	258	485	0.117	18.0	0.20
EC1_3 (bot)	12x12	28	9.0	16.5	71.6	329	7.2	258	329	0.051	18.0	0.01
EC1_4 (top)	12x12	28	9.0	16.5	71.6	659	7.2	258	485	0.117	14.0	0.20
EC1_4 (bot)	12x12	28	9.0	16.5	71.6	329	7.2	258	329	0.051	14.0	0.01
EC1_6 (top)	12x12	28	9.0	16.5	71.6	659	7.2	258	485	0.117	8.5	0.20
EC1_6 (bot)	12x12	28	9.0	16.5	71.6	329	7.2	258	329	0.051	8.5	0.01
EC1_8 (top)	12x12	28	9.0	16.5	71.6	659	7.2	258	485	0.117	7.6	0.20
EC1_8 (bot)	12x12	28	9.0	16.5	71.6	329	7.2	258	329	0.051	7.6	0.01
EC1_1 (top)	12x12	28	9.0	16.5	71.6	659	7.2	258	485	0.117	7.0	0.20
EC1_1 (bot)	12x12	28	9.0	16.5	71.6	329	7.2	258	329	0.051	7.0	0.01
EC2_3	12x12	56	9.0	16.5	81.0	373	7.2	316	373	0.056	10.0	0.01
EC2_4	12x12	56	9.0	16.5	81.0	373	7.2	316	373	0.056	8.0	0.01
EC2_6	12x12	56	9.0	16.5	81.0	373	7.2	316	373	0.056	5.8	0.01
EC2_8	12x12	56	9.0	16.5	81.0	373	7.2	316	373	0.056	5.3	0.01
EC2_12	12x12	56	9.0	16.5	81.0	373	7.2	316	373	0.056	4.6	0.01
EC3_3	12x12	83	9.0	16.5	89.1	410	7.2	373	410	0.061	8.4	0.01
EC3_4	12x12	83	9.0	16.5	89.1	410	7.2	373	410	0.061	7.0	0.01
EC3_6	12x12	83	9.0	16.5	89.1	410	7.2	373	410	0.061	5.6	0.01
EC3_8	12x12	83	9.0	16.5	89.1	410	7.2	373	410	0.061	4.8	0.01
EC3_12	12x12	83	9.0	16.5	89.1	410	7.2	373	410	0.061	4.0	0.01
EC4_4	15x15	111	12.0	16.5	107.2	665	18.0	650	665	0.040	5.1	0.01
EC4_6	15x15	111	12.0	16.5	107.2	665	18.0	650	665	0.040	4.1	0.01
EC4_8	15x15	111	12.0	16.5	107.2	665	18.0	650	665	0.040	3.8	0.01
EC4_12	15x15	111	12.0	16.5	107.2	665	18.0	650	665	0.040	3.6	0.01
EC4_15	15x15	111	12.0	16.5	107.2	665	18.0	650	665	0.040	2.8	0.01
EC5_4	15x15	139	12.0	16.5	113.8	706	18.0	690	706	0.042	4.9	0.01
EC5_6	15x15	139	12.0	16.5	113.8	706	18.0	690	706	0.042	3.9	0.01
EC5_8	15x15	139	12.0	16.5	113.8	706	18.0	690	706	0.042	3.5	0.01
EC5_12	15x15	139	12.0	16.5	113.8	706	18.0	690	706	0.042	3.1	0.01
EC5_15	15x15	139	12.0	16.5	113.8	706	18.0	690	706	0.042	2.1	0.01
EC6_4	15x15	167	12.0	16.5	119.9	743	18.0	730	743	0.044	3.6	0.01
EC6_6	15x15	167	12.0	16.5	119.9	743	18.0	730	743	0.044	3.1	0.01
EC6_8	15x15	167	12.0	16.5	119.9	743	18.0	730	743	0.044	2.6	0.01
EC6_12	15x15	167	12.0	16.5	119.9	743	18.0	730	743	0.044	2.1	0.01
EC6_15	15x15	167	12.0	16.5	119.9	743	18.0	730	743	0.044	1.9	0.01
EC7_4	15x15	195	12.0	16.5	125.8	780	20.0	765	780	0.042	3.9	0.01
EC7_6	15x15	195	12.0	16.5	125.8	780	20.0	765	780	0.042	3.4	0.01
EC4_8	15x15	195	12.0	16.5	125.8	780	20.0	765	780	0.042	2.6	0.01
EC7_12	15x15	195	12.0	16.5	125.8	780	20.0	765	780	0.042	2.4	0.01
EC7_15	15x15	195	12.0	16.5	125.8	780	20.0	765	780	0.042	2.2	0.01
EC8_4	15x15	222	12.0	16.5	131.2	813	20.0	800	813	0.043	3.8	0.01
EC8_6	15x15	222	12.0	16.5	131.2	813	20.0	800	813	0.043	3.1	0.01
EC8_8	15x15	222	12.0	16.5	131.2	813	20.0	800	813	0.043	2.6	0.01
EC8_12	15x15	222	12.0	16.5	131.2	813	20.0	800	813	0.043	2.3	0.01
EC8_15	15x15	222	12.0	16.5	131.2	813	20.0	800	813	0.043	2.1	0.01
EC9_4 (top)	15x15	250	12.0	16.5	136.6	847	20.0	835	847	0.045	3.7	0.01
EC9_4 (bot)	15x15	250	12.0	16.5	N/A	N/A	20.0	1101	2500	0.195	3.7	0.30
EC9_6 (top)	15x15	250	12.0	16.5	136.6	847	20.0	835	847	0.045	2.8	0.01
EC9_6 (bot)	15x15	250	12.0	16.5	N/A	N/A	20.0	1101	2500	0.195	2.8	0.30
EC9_8 (top)	15x15	250	12.0	16.5	136.6	847	20.0	835	847	0.045	2.6	0.01
EC9_8 (bot)	15x15	250	12.0	16.5	N/A	N/A	20.0	1101	2500	0.195	2.6	0.30
EC9_1 (top)	15x15	250	12.0	16.5	136.6	847	20.0	835	847	0.045	2.3	0.01
EC9_1 (bot)	15x15	250	12.0	16.5	N/A	N/A	20.0	1101	2500	0.195	2.3	0.30
EC9_1 (top)	15x15	250	12.0	16.5	136.6	847	20.0	835	847	0.045	2.0	0.01
EC9_1 (bot)	15x15	250	12.0	16.5	N/A	N/A	20.0	1101	2500	0.195	2.0	0.30

Table A-4 Factored Interior Column Properties to Reflect Joint Capacity

COLUMN TYPE	SIZE	AXIAL LOAD	b'	h'	(Vjv)	(Mjv)	Elo (x 10^6)	Mcr	My	PHIy (x 10^-3	PHIu (x 10^-3	EI3/Elo
	(in)	(kips)	(in)	(in)	(kips)	(k-in)	(k-in^2)	(k-in)	(k-in)	(1/in)	(1/in)	(%)
(1)	(2)	(3)	(4)	(5)	(6)	(7)	(8)	(9)	(10)	(11)	(13)	(14)
IC1_3 (top)	12x12	44	9.0	16.5	77.1	732	7.2	291	560	0.134	12.0	0.20
IC1_3 (bot)	12x12	44	9.0	16.5	77.1	362	7.2	291	362	0.055	12.0	0.01
IC1_4 (top)	12x12	44	9.0	16.5	77.1	732	7.2	291	560	0.134	10.4	0.20
IC1_4 (bot)	12x12	44	9.0	16.5	77.1	362	7.2	291	362	0.055	10.4	0.01
IC1_6 (top)	12x12	44	9.0	16.5	77.1	732	7.2	291	560	0.134	8.0	0.20
IC1_6 (bot)	12x12	44	9.0	16.5	77.1	362	7.2	291	362	0.055	8.0	0.01
IC1_8 (top)	12x12	44	9.0	16.5	77.1	732	7.2	291	560	0.134	6.8	0.20
IC1_8 (bot)	12x12	44	9.0	16.5	77.1	362	7.2	291	362	0.055	6.8	0.01
IC1_12 (top)	12x12	44	9.0	16.5	77.1	732	7.2	291	560	0.134	5.6	0.20
IC1_12 (bot)	12x12	44	9.0	16.5	77.1	362	7.2	291	362	0.055	5.6	0.01
IC2_3	12x12	89	9.0	16.5	90.8	427	7.2	386	427	0.063	8.2	0.01
IC2_4	12x12	89	9.0	16.5	90.8	427	7.2	386	427	0.063	6.1	0.01
IC2_6	12x12	89	9.0	16.5	90.8	427	7.2	386	427	0.063	5.3	0.01
IC2_8	12x12	89	9.0	16.5	90.8	427	7.2	386	427	0.063	4.3	0.01
IC2_12	12x12	89	9.0	16.5	90.8	427	7.2	386	427	0.063	3.4	0.01
IC3_3	12x12	133	9.0	16.5	102.5	482	7.2	475	482	0.071	6.0	0.01
IC3_4	12x12	133	9.0	16.5	102.5	482	7.2	475	482	0.071	4.8	0.01
IC3_6	12x12	133	9.0	16.5	102.5	482	7.2	475	482	0.071	3.6	0.01
IC3_8	12x12	133	9.0	16.5	102.5	482	7.2	475	482	0.071	2.8	0.01
IC3_12	12x12	133	9.0	16.5	102.5	482	7.2	475	482	0.071	2.6	0.01
IC4_4	15x15	177	12.0	16.5	122.1	781	18.0	770	781	0.051	3.6	0.01
IC4_6	15x15	177	12.0	16.5	122.1	781	18.0	770	781	0.051	3.0	0.01
IC4_8	15x15	177	12.0	16.5	122.1	781	18.0	770	781	0.051	2.5	0.01
IC4_12	15x15	177	12.0	16.5	122.1	781	18.0	770	781	0.051	1.7	0.01
IC4_15	15x15	177	12.0	16.5	122.1	781	18.0	770	781	0.051	1.6	0.01
IC5_4	15x15	222	12.0	16.5	131.2	840	18.0	830	840	0.054	2.8	0.01
IC5_6	15x15	222	12.0	16.5	131.2	840	18.0	830	840	0.054	2.5	0.01
IC5_8	15x15	222	12.0	16.5	131.2	840	18.0	830	840	0.054	2.0	0.01
IC5_12	15x15	222	12.0	16.5	131.2	840	18.0	830	840	0.054	1.6	0.01
IC5_15	15x15	222	12.0	16.5	131.2	840	18.0	830	840	0.054	1.5	0.01
IC6_4	15x15	266	12.0	16.5	139.6	893	18.0	880	893	0.055	2.6	0.01
IC6_6	15x15	266	12.0	16.5	139.6	893	18.0	880	893	0.055	2.0	0.01
IC6_8	15x15	266	12.0	16.5	139.6	893	18.0	880	893	0.055	1.9	0.01
IC6_12	15x15	266	12.0	16.5	139.6	893	18.0	880	893	0.055	1.5	0.01
IC6_15	15x15	266	12.0	16.5	139.6	893	18.0	880	893	0.055	1.2	0.01
IC7_4	15x15	310	12.0	16.5	147.5	944	20.0	930	944	0.055	3.4	0.01
IC7_6	15x15	310	12.0	16.5	147.5	944	20.0	930	944	0.055	2.6	0.01
IC4_8	15x15	310	12.0	16.5	147.5	944	20.0	930	944	0.055	2.4	0.01
IC7_12	15x15	310	12.0	16.5	147.5	944	20.0	930	944	0.055	2.1	0.01
IC7_15	15x15	310	12.0	16.5	147.5	944	20.0	930	944	0.055	1.9	0.01
IC8_4	15x15	354	12.0	16.5	154.9	991	20.0	980	991	0.055	3.2	0.01
IC8_6	15x15	354	12.0	16.5	154.9	991	20.0	980	991	0.055	2.5	0.01
IC8_8	15x15	354	12.0	16.5	154.9	991	20.0	980	991	0.055	2.3	0.01
IC8_12	15x15	354	12.0	16.5	154.9	991	20.0	980	991	0.055	1.8	0.01
IC8_15	15x15	354	12.0	16.5	154.9	991	20.0	980	991	0.055	1.7	0.01
IC9_4 (top)	15x15	399	12.0	16.5	162.2	1038	20.0	1025	1038	0.055	2.8	0.01
IC9_4 (bot)	15x15	399	12.0	16.5	N/A	N/A	20.0	1499	2800	0.205	2.8	0.30
IC9_6 (top)	15x15	399	12.0	16.5	162.2	1038	20.0	1025	1038	0.055	2.4	0.01
IC9_6 (bot)	15x15	399	12.0	16.5	N/A	N/A	20.0	1499	2800	0.205	2.4	0.30
IC9_8 (top)	15x15	399	12.0	16.5	162.2	1038	20.0	1025	1038	0.055	2.2	0.01
IC9_8 (bot)	15x15	399	12.0	16.5	N/A	N/A	20.0	1499	2800	0.205	2.2	0.30
IC9_12 (top)	15x15	399	12.0	16.5	162.2	1038	20.0	1025	1038	0.055	1.7	0.01
IC9_12 (bot)	15x15	399	12.0	16.5	N/A	N/A	20.0	1499	2800	0.205	1.7	0.30
IC9_15 (top)	15x15	399	12.0	16.5	162.2	1038	20.0	1025	1038	0.055	1.6	0.01
IC9_15 (bot)	15x15	399	12.0	16.5	N/A	N/A	20.0	1499	2800	0.205	1.6	0.30

Table A-5 Beam Properties with Sufficient Joint Steel and Development Length

BEAM TYPE	HOOP SPA.	Elo (x 10^6)	POSITIVE BENDING PROPERTIES					NEGATIVE BENDING PROPERTIES					AXIAL	SHEAR
			Mcr	My	PHIy (x 10^-3)	PHIu (x 10^-3)	Elo/El3	Mcr	My	PHIy (x 10^-3)	PHIu (x 10^-3)	Elo/El3	EA/L	GA (x 10^6)
		(k-in^2)	(k-in)	(k-in)	(1/in)	(1/in)	(%)	(k-in)	(k-in)	(1/in)	(1-in)	(%)	(k/in)	(kips)
(1)	(2)	(3)	(4)	(5)	(6)	(7)	(8)	(9)	(10)	(11)	(12)	(13)	(14)	(15)
EB1_4	#3 @ 4"	69.6	391	540	0.047	30.0	0.07	-556	-970	-0.10	-6.0	0.38	3726	0.200
EB1_6	#3 @ 6"	69.6	391	540	0.047	24.0	0.07	-556	-970	-0.10	-5.0	0.38	3726	0.194
EB1_8	#3 @ 8"	69.6	391	540	0.047	20.0	0.07	-556	-970	-0.10	-3.0	0.38	3726	0.191
EB1_12	#3 @ 12"	69.6	391	540	0.047	15.0	0.07	-556	-970	-0.10	-2.6	0.38	3726	0.187
IB1_4	#3 @ 4"	72.5	391	540	0.046	32.0	0.07	-565	-1250	-0.15	-5.0	0.45	3798	0.200
IB1_6	#3 @ 6"	72.5	391	540	0.046	26.0	0.07	-565	-1250	-0.15	-3.5	0.45	3798	0.194
IB1_8	#3 @ 8"	72.5	391	540	0.046	21.0	0.07	-565	-1250	-0.15	-2.3	0.45	3798	0.191
IB1_12	#3 @ 12"	72.5	391	540	0.046	17.0	0.07	-565	-1250	-0.15	-2.0	0.45	3798	0.187

Table A-6 Beam Properties to Reflect Discontinuous Positive Reinforcement

BEAM TYPE	HOOP SPA.	EMBEDMENT LENGTH	DEVELOPMENT LENGTH	Elo (x 10^6)	Mcr	My	PHIy (x 10^-3)	PHIu (x 10^-3)	EI3/Elo
		(in)	(in)	(k-in^2)	(k-in)	(k-in)	(1/in)	(1/in)	(%)
(1)	(2)	(3)	(4)	(5)	(6)	(7)	(8)	(9)	(10)
EB1_4	#3 @ 4"	6"	12.0"	69.6	270	284	0.017	30.0	0.035
EB1_6	#3 @ 6"	6"	12.0"	69.6	270	284	0.017	24.0	0.035
EB1_8	#3 @ 8"	6"	12.0"	69.6	270	284	0.017	20.0	0.035
EB1_12	#3 @ 12"	6"	12.0"	69.6	270	284	0.017	15.0	0.035
IB1_4	#3 @ 4"	6"	12.0"	72.5	270	284	0.017	32.0	0.035
IB1_6	#3 @ 6"	6"	12.0"	72.5	270	284	0.017	26.0	0.035
IB1_8	#3 @ 8"	6"	12.0"	72.5	270	284	0.017	21.0	0.035
IB1_12	#3 @ 12"	6"	12.0"	72.5	270	284	0.017	17.0	0.035
EB4_4	#3 @ 4"	7.5"	12.0"	69.6	360	372	0.021	30.0	0.044
EB4_6	#3 @ 6"	7.5"	12.0"	69.6	360	372	0.021	24.0	0.044
EB4_8	#3 @ 8"	7.5"	12.0"	69.6	360	372	0.021	20.0	0.044
EB4_12	#3 @ 12"	7.5"	12.0"	69.6	360	372	0.021	15.0	0.044
IB4_4	#3 @ 4"	7.5"	12.0"	72.5	360	372	0.021	32.0	0.044
IB4_6	#3 @ 6"	7.5"	12.0"	72.5	360	372	0.021	26.0	0.044
IB4_8	#3 @ 8"	7.5"	12.0"	72.5	360	372	0.021	21.0	0.044
IB4_12	#3 @ 12"	7.5"	12.0"	72.5	360	372	0.021	17.0	0.044

Table A-7 Factored Exterior Beam Properties to Reflect Joint Capacity

				POSITIVE BENDING PROPERTIES					NEGATIVE BENDING PROPERTIES				
BEAM TYPE	(Vjh)	(Mjh)	Elo (x 10^6)	Mcr	My	PHIy (x 10^-3)	PHIu (x 10^-3)	Elo/EI3	Mcr	My	PHIy (x 10^-3)	PHIu (x 10^-3)	Elo/EI3
	(kips)	(k-in)	(k-in^2)	(k-in)	(k-in)	(1/in)	(1/in)	(%)	(k-in)	(k-in)	(1/in)	(1/in)	(%)
(1)	(2)	(3)	(4)	(5)	(6)	(7)	(8)	(9)	(10)	(11)	(12)	(13)	(14)
EB1_4	45.6	821	69.0	391	540	0.047	30.0	0.07	-556	-821	-0.074	-6.0	0.01
EB1_6	45.6	821	69.0	391	540	0.047	24.0	0.07	-556	-821	-0.074	-5.0	0.01
EB1_8	45.6	821	69.0	391	540	0.047	20.0	0.07	-556	-821	-0.074	-3.0	0.01
EB1_12	45.6	821	69.0	391	540	0.047	15.0	0.07	-556	-821	-0.074	-2.6	0.01
EB2_4	51.5	927	69.0	391	540	0.047	30.0	0.07	-556	-927	-0.093	-6.0	0.01
EB2_6	51.5	927	69.0	391	540	0.047	24.0	0.07	-556	-927	-0.093	-5.0	0.01
EB2_8	51.5	927	69.0	391	540	0.047	20.0	0.07	-556	-927	-0.093	-3.0	0.01
EB2_12	51.5	927	69.0	391	540	0.047	15.0	0.07	-556	-927	-0.093	-2.6	0.01
EB3_4	56.7	1021	69.0	391	540	0.047	30.0	0.07	-556	-970	-0.100	-6.0	0.38
EB3_6	56.7	1021	69.0	391	540	0.047	24.0	0.07	-556	-970	-0.100	-5.0	0.38
EB3_8	56.7	1021	69.0	391	540	0.047	20.0	0.07	-556	-970	-0.100	-3.0	0.38
EB3_12	56.7	1021	69.0	391	540	0.047	15.0	0.07	-556	-970	-0.100	-2.6	0.38
EB4_4	87.7	1579	69.0	391	540	0.047	30.0	0.07	-556	-970	-0.100	-6.0	0.38
EB4_6	87.7	1579	69.0	391	540	0.047	24.0	0.07	-556	-970	-0.100	-5.0	0.38
EB4_8	87.7	1579	69.0	391	540	0.047	20.0	0.07	-556	-970	-0.100	-3.0	0.38
EB4_12	87.7	1579	69.0	391	540	0.047	15.0	0.07	-556	-970	-0.100	-2.6	0.38
EB5_4	93.1	1676	69.0	391	540	0.047	30.0	0.07	-556	-970	-0.100	-6.0	0.38
EB5_6	93.1	1676	69.0	391	540	0.047	24.0	0.07	-556	-970	-0.100	-5.0	0.38
EB5_8	93.1	1676	69.0	391	540	0.047	20.0	0.07	-556	-970	-0.100	-3.0	0.38
EB5_12	93.1	1676	69.0	391	540	0.047	15.0	0.07	-556	-970	-0.100	-2.6	0.38
EB6_4	98.1	1766	69.0	391	540	0.047	30.0	0.07	-556	-970	-0.100	-6.0	0.38
EB6_6	98.1	1766	69.0	391	540	0.047	24.0	0.07	-556	-970	-0.100	-5.0	0.38
EB6_8	98.1	1766	69.0	391	540	0.047	20.0	0.07	-556	-970	-0.100	-3.0	0.38
EB6_12	98.1	1766	69.0	391	540	0.047	15.0	0.07	-556	-970	-0.100	-2.6	0.38
EB7_4	102.9	1852	69.0	391	540	0.047	30.0	0.07	-556	-970	-0.100	-6.0	0.38
EB7_6	102.9	1852	69.0	391	540	0.047	24.0	0.07	-556	-970	-0.100	-5.0	0.38
EB7_8	102.9	1852	69.0	391	540	0.047	20.0	0.07	-556	-970	-0.100	-3.0	0.38
EB7_12	102.9	1852	69.0	391	540	0.047	15.0	0.07	-556	-970	-0.100	-2.6	0.38
EB8_4	107.3	1931	69.0	391	540	0.047	30.0	0.07	-556	-970	-0.100	-6.0	0.38
EB8_6	107.3	1931	69.0	391	540	0.047	24.0	0.07	-556	-970	-0.100	-5.0	0.38
EB8_8	107.3	1931	69.0	391	540	0.047	20.0	0.07	-556	-970	-0.100	-3.0	0.38
EB8_12	107.3	1931	69.0	391	540	0.047	15.0	0.07	-556	-970	-0.100	-2.6	0.38
EB9_4	111.8	2012	69.0	391	540	0.047	30.0	0.07	-556	-970	-0.100	-6.0	0.38
EB9_6	111.8	2012	69.0	391	540	0.047	24.0	0.07	-556	-970	-0.100	-5.0	0.38
EB9_8	111.8	2012	69.0	391	540	0.047	20.0	0.07	-556	-970	-0.100	-3.0	0.38
EB9_12	111.8	2012	69.0	391	540	0.047	15.0	0.07	-556	-970	-0.100	-2.6	0.38

Table A-8 Factored Interior Beam Properties to Reflect Joint Capacity

				POSITIVE BENDING PROPERTIES					NEGATIVE BENDING PROPERTIES				
BEAM TYPE	(Vjh)	(Mjh)	Elo (x 10^6)	Mcr	My	PHIy (x 10^-3)	PHIu (x 10^-3)	Elo/El3	Mcr	My	PHIy (x 10^-3)	PHIu (x 10^-3)	Elo/El3
	(kips)	(k-in)	(k-in^2)	(k-in)	(k-in)	(1/in)	(1/in)	(%)	(k-in)	(k-in)	(1/in)	(1/in)	(%)
(1)	(2)	(3)	(4)	(5)	(6)	(7)	(8)	(9)	(10)	(11)	(12)	(13)	(14)
IB1_4	49.1	417	72.5	391	417	0.024	32.0	0.01	-400	-417	-0.022	-5.0	0.01
IB1_6	49.1	417	72.5	391	417	0.024	26.0	0.01	-400	-417	-0.022	-3.5	0.01
IB1_8	49.1	417	72.5	391	417	0.024	21.0	0.01	-400	-417	-0.022	-2.3	0.01
IB1_12	49.1	417	72.5	391	417	0.024	17.0	0.01	-400	-417	-0.022	-2.0	0.01
IB2_4	57.8	520	72.5	391	520	0.043	32.0	0.01	-500	-520	-0.027	-5.0	0.01
IB2_6	57.8	520	72.5	391	520	0.043	26.0	0.01	-500	-520	-0.027	-3.5	0.01
IB2_8	57.8	520	72.5	391	520	0.043	21.0	0.01	-500	-520	-0.027	-2.3	0.01
IB2_12	57.8	520	72.5	391	520	0.043	17.0	0.01	-500	-520	-0.027	-2.0	0.01
IB3_4	65.2	587	72.5	391	540	0.046	32.0	0.07	-565	-587	-0.029	-5.0	0.01
IB3_6	65.2	587	72.5	391	540	0.046	26.0	0.07	-565	-587	-0.029	-3.5	0.01
IB3_8	65.2	587	72.5	391	540	0.046	21.0	0.07	-565	-587	-0.029	-2.3	0.01
IB3_12	65.2	587	72.5	391	540	0.046	17.0	0.07	-565	-587	-0.029	-2.0	0.01
IB4_4	99.9	909	72.5	391	540	0.046	32.0	0.07	-565	-909	-0.087	-5.0	0.01
IB4_6	99.9	909	72.5	391	540	0.046	26.0	0.07	-565	-909	-0.087	-3.5	0.01
IB4_8	99.9	909	72.5	391	540	0.046	21.0	0.07	-565	-909	-0.087	-2.3	0.01
IB4_12	99.9	909	72.5	391	540	0.046	17.0	0.07	-565	-909	-0.087	-2.0	0.01
IB5_4	107.3	976	72.5	391	540	0.046	32.0	0.07	-565	-976	-0.099	-5.0	0.01
IB5_6	107.3	976	72.5	391	540	0.046	26.0	0.07	-565	-976	-0.099	-3.5	0.01
IB5_8	107.3	976	72.5	391	540	0.046	21.0	0.07	-565	-976	-0.099	-2.3	0.01
IB5_12	107.3	976	72.5	391	540	0.046	17.0	0.07	-565	-976	-0.099	-2.0	0.01
IB6_4	114.2	1039	72.5	391	540	0.046	32.0	0.07	-565	-1039	-0.110	-5.0	0.01
IB6_6	114.2	1039	72.5	391	540	0.046	26.0	0.07	-565	-1039	-0.110	-3.5	0.01
IB6_8	114.2	1039	72.5	391	540	0.046	21.0	0.07	-565	-1039	-0.110	-2.3	0.01
IB6_12	114.2	1039	72.5	391	540	0.046	17.0	0.07	-565	-1039	-0.110	-2.0	0.01
IB7_4	120.7	1098	72.5	391	540	0.046	32.0	0.07	-565	-1098	-0.120	-5.0	0.01
IB7_6	120.7	1098	72.5	391	540	0.046	26.0	0.07	-565	-1098	-0.120	-3.5	0.01
IB7_8	120.7	1098	72.5	391	540	0.046	21.0	0.07	-565	-1098	-0.120	-2.3	0.01
IB7_12	120.7	1098	72.5	391	540	0.046	17.0	0.07	-565	-1098	-0.120	-2.0	0.01
IB8_4	126.7	1153	72.5	391	540	0.046	32.0	0.07	-565	-1153	-0.129	-5.0	0.01
IB8_6	126.7	1153	72.5	391	540	0.046	26.0	0.07	-565	-1153	-0.129	-3.5	0.01
IB8_8	126.7	1153	72.5	391	540	0.046	21.0	0.07	-565	-1153	-0.129	-2.3	0.01
IB8_12	126.7	1153	72.5	391	540	0.046	17.0	0.07	-565	-1153	-0.129	-2.0	0.01
IB9_4	132.7	1208	72.5	391	540	0.046	32.0	0.07	-565	-1208	-0.139	-5.0	0.01
IB9_6	132.7	1208	72.5	391	540	0.046	26.0	0.07	-565	-1208	-0.139	-3.5	0.01
IB9_8	132.7	1208	72.5	391	540	0.046	21.0	0.07	-565	-1208	-0.139	-2.3	0.01
IB9_12	132.7	1208	72.5	391	540	0.046	17.0	0.07	-565	-1208	-0.139	-2.0	0.01

APPENDIX B

BEAM AND COLUMN DAMAGE INDICES

General Notes Pertaining to Tables:

1. Tables represent the damage indices corresponding to beams and columns for each story level as computed by the IDARC program.

2. The damage index typically has a range from 0.00 to 1.00 with 0.00 representing no damage and 1.00 representing collapse. For further background or interpretation of the damage index refer to Section 4 and to References 20-22.

3. Results from the analysis of 3, 6 & 9 story buildings for all detailing strategies are tabulated separately for the following four input ground motions:
   - 1940 El Centro (S 00 E): (PGA = 0.20 g)
   - Spectrum-Compatible Accelerogram: (PGA = 0.15 g)
   - 1985 Nahanni (N 00 W): (PGA = 0.20 g)
   - 1952 Taft (N 21 E): (PGA = 0.20 g)

4. Representative illustrations of the specific reinforcing details which were modeled in the analysis are presented again for quick reference in Figure B-1. Figures shown are for interior beam column joints. Exterior beam-column joints were modeled in the same manner (see Section 3 for details). Larger scale illustrations can be found in Appendix C. Complete descriptions of the individual details are presented in Section 6.

5. These tables are presented to show the general trend in the damage in columns and beams and between story levels. While some irregularities are inherent in some of the responses due to the complexity of the response, the overall behavior is well represented. The conclusions in Section 7 are directly derived from this summary.

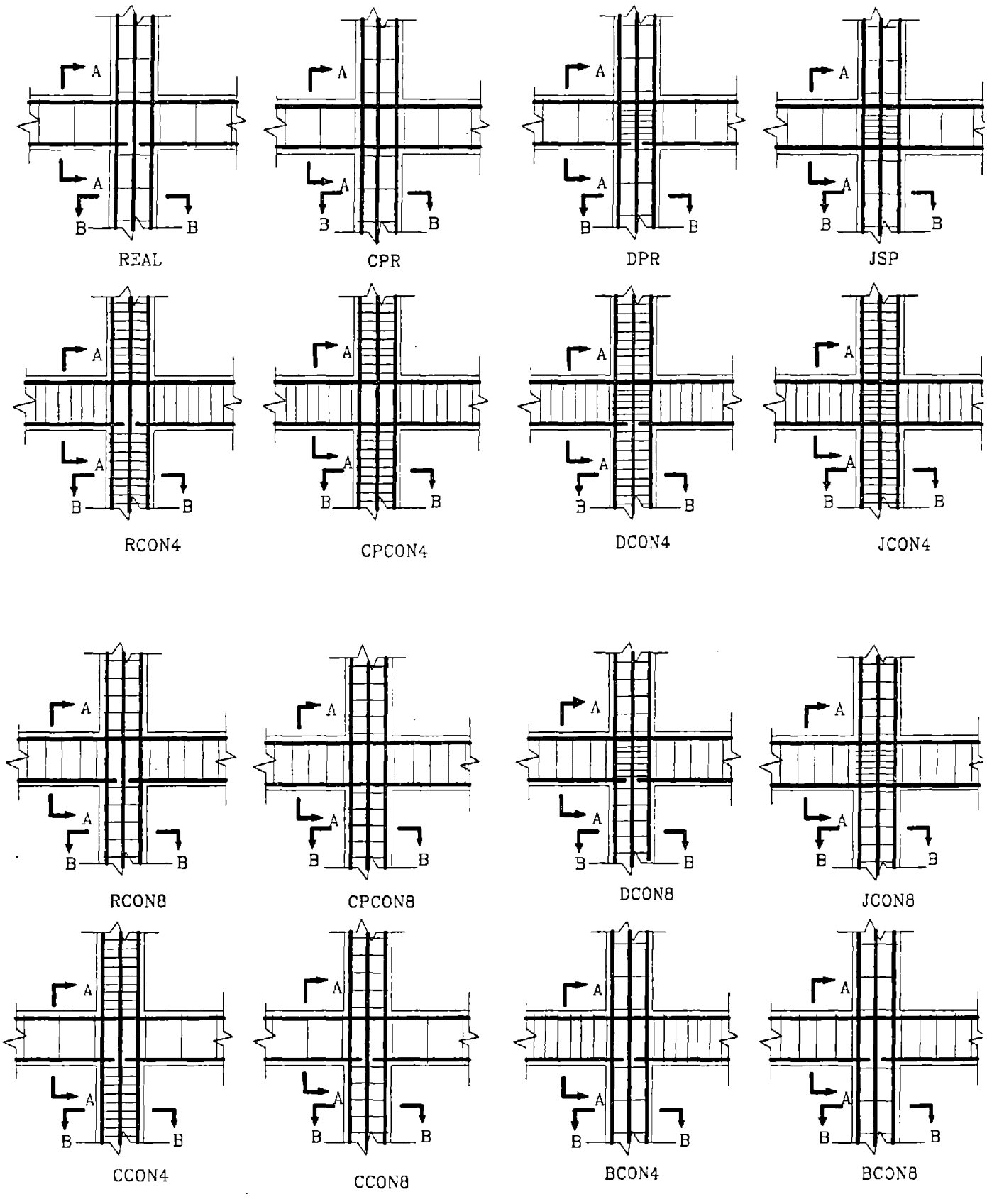

Figure B-1 Representative Beam-Column Joint Reinforcing Details

Table B-1 Beam and Column Damage Indices for Three Story Frames (El-Centro, PGA = 0.20 g)

STORY	3REAL		3CPR		3DPR		3JSP	
	BEAMS	COLUMN	BEAMS	COLUMN	BEAMS	COLUMN	BEAMS	COLUMN
3	0.55	0.48	0.67	0.38	0.02	0.13	0.01	0.02
2	0.47	0.31	0.40	0.37	0.76	0.27	0.05	0.34
1	0.41	0.62	0.47	0.57	0.82	0.18	0.47	0.49
STORY	3RCON4		3CPCON4		3DCON4		3JCON4	
	BEAMS	COLUMN	BEAMS	COLUMN	BEAMS	COLUMN	BEAMS	COLUMN
3	0.32	0.20	0.27	0.16	0.01	0.06	0.01	0.01
2	0.19	0.14	0.16	0.17	0.31	0.13	0.02	0.14
1	0.16	0.27	0.19	0.25	0.34	0.08	0.20	0.21
STORY	3RCON8		3CPCON8		3DCON8		3JCON8	
	BEAMS	COLUMN	BEAMS	COLUMN	BEAMS	COLUMN	BEAMS	COLUMN
3	0.69	0.42	0.58	0.32	0.02	0.09	0.01	0.02
2	0.41	0.24	0.35	0.32	0.66	0.22	0.04	0.21
1	0.35	0.44	0.41	0.41	0.71	0.13	0.41	0.36
STORY	3CCON4		3CCON8		3BCON4		3BCON8	
	BEAMS	COLUMN	BEAMS	COLUMN	BEAMS	COLUMN	BEAMS	COLUMN
3	0.80	0.20	0.80	0.42	0.32	0.48	0.69	0.48
2	0.47	0.14	0.47	0.24	0.19	0.31	0.41	0.31
1	0.41	0.27	0.41	0.44	0.16	0.62	0.35	0.62

Table B-2 Beam and Column Damage Indices for Six Story Frames (El-Centro, PGA = 0.20 g)

STORY	6REAL BEAMS	6REAL COLUMN	6CPR BEAMS	6CPR COLUMN	6DPR BEAMS	6DPR COLUMN	6JSP BEAMS	6JSP COLUMN
6	0.11	0.02	0.09	0.03	0.02	0.34	0.02	0.03
5	0.11	0.82	0.10	0.91	0.90	0.14	0.05	0.15
4	0.54	0.83	0.67	0.92	0.97	0.22	0.45	0.26
3	0.60	0.87	0.13	0.46	0.45	0.04	0.61	0.05
2	0.41	0.76	0.27	0.81	0.59	0.04	0.82	0.05
1	0.37	0.43	0.23	0.20	0.71	0.13	0.43	0.12

STORY	6RCON4 BEAMS	6RCON4 COLUMN	6CPCON4 BEAMS	6CPCON4 COLUMN	6DCON4 BEAMS	6DCON4 COLUMN	6JCON4 BEAMS	6JCON4 COLUMN
6	0.04	0.01	0.04	0.01	0.01	0.15	0.01	0.02
5	0.04	0.48	0.04	0.47	0.44	0.07	0.02	0.06
4	0.20	0.58	0.27	0.61	0.49	0.11	0.19	0.19
3	0.37	0.85	0.05	0.20	0.18	0.03	0.24	0.04
2	0.17	0.41	0.11	0.46	0.29	0.03	0.36	0.03
1	0.15	0.24	0.09	0.10	0.30	0.06	0.18	0.06

STORY	6RCON8 BEAMS	6RCON8 COLUMN	6CPCON8 BEAMS	6CPCON8 COLUMN	6DCON8 BEAMS	6DCON8 COLUMN	6JCON8 BEAMS	6JCON8 COLUMN
6	0.09	0.01	0.08	0.02	0.02	0.25	0.01	0.02
5	0.10	0.72	0.09	0.79	0.88	0.11	0.04	0.10
4	0.44	0.74	0.58	0.81	0.93	0.08	0.39	0.19
3	0.56	0.90	0.11	0.29	0.37	0.03	0.53	0.03
2	0.37	0.57	0.23	0.64	0.40	0.03	0.74	0.03
1	0.33	0.34	0.20	0.14	0.61	0.08	0.37	0.08

STORY	6CCON4 BEAMS	6CCON4 COLUMN	6CCON8 BEAMS	6CCON8 COLUMN	6BCON4 BEAMS	6BCON4 COLUMN	6BCON8 BEAMS	6BCON8 COLUMN
6	0.11	0.01	0.11	0.01	0.04	0.02	0.09	0.02
5	0.11	0.48	0.11	0.72	0.04	0.82	0.10	0.82
4	0.50	0.58	0.50	0.74	0.20	0.83	0.44	0.83
3	0.59	0.85	0.59	0.90	0.37	0.88	0.56	0.88
2	0.42	0.41	0.42	0.57	0.17	0.75	0.37	0.75
1	0.37	0.24	0.37	0.34	0.15	0.46	0.33	0.46

Table B-3 Beam and Column Damage Indices for Nine Story Frames (El-Centro, PGA = 0.20 g)

STORY	9REAL BEAMS	9REAL COLUMN	9CPR BEAMS	9CPR COLUMN	9DPR BEAMS	9DPR COLUMN	9JSP BEAMS	9JSP COLUMN
9	0.22	0.16	0.13	0.02	0.02	0.07	0.02	0.11
8	0.15	0.29	0.07	0.31	0.61	0.07	0.05	0.13
7	0.29	0.35	0.35	0.81	0.53	0.07	0.28	0.07
6	0.33	0.31	0.03	0.34	0.82	0.03	0.37	0.05
5	0.47	0.32	0.06	0.27	0.67	0.03	0.53	0.04
4	0.54	0.72	0.10	0.40	0.50	0.04	0.46	0.05
3	0.61	0.69	0.21	0.49	0.63	0.02	0.44	0.03
2	0.74	0.77	0.45	0.67	0.50	0.03	0.36	0.04
1	0.55	0.85	0.30	0.43	0.44	0.05	0.27	0.05

STORY	9RCON4 BEAMS	9RCON4 COLUMN	9CPCON4 BEAMS	9CPCON4 COLUMN	9DCON4 BEAMS	9DCON4 COLUMN	9JCON4 BEAMS	9JCON4 COLUMN
9	0.09	0.06	0.05	0.01	0.01	0.03	0.01	0.05
8	0.06	0.12	0.03	0.13	0.25	0.03	0.02	0.05
7	0.11	0.16	0.14	0.37	0.21	0.03	0.11	0.03
6	0.14	0.14	0.01	0.15	0.34	0.02	0.15	0.02
5	0.19	0.16	0.03	0.14	0.27	0.02	0.22	0.02
4	0.22	0.38	0.04	0.18	0.21	0.02	0.18	0.02
3	0.25	0.48	0.09	0.28	0.27	0.01	0.18	0.01
2	0.32	0.63	0.18	0.37	0.21	0.02	0.15	0.02
1	0.22	0.46	0.12	0.23	0.18	0.03	0.11	0.03

STORY	9RCON8 BEAMS	9RCON8 COLUMN	9CPCON8 BEAMS	9CPCON8 COLUMN	9DCON8 BEAMS	9DCON8 COLUMN	9JCON8 BEAMS	9JCON8 COLUMN
9	0.19	0.16	0.10	0.10	0.02	0.05	0.02	0.07
8	0.13	0.21	0.05	0.23	0.53	0.05	0.04	0.08
7	0.25	0.27	0.37	0.62	0.46	0.05	0.24	0.05
6	0.29	0.20	0.03	0.04	0.72	0.02	0.32	0.03
5	0.41	0.23	0.06	0.21	0.58	0.02	0.46	0.03
4	0.47	0.52	0.09	0.36	0.43	0.03	0.40	0.03
3	0.53	0.72	0.17	0.40	0.54	0.02	0.38	0.02
2	0.67	0.73	0.30	0.69	0.43	0.02	0.31	0.03
1	0.47	0.66	0.35	0.50	0.38	0.04	0.24	0.04

STORY	9CCON4 BEAMS	9CCON4 COLUMN	9CCON8 BEAMS	9CCON8 COLUMN	9BCON4 BEAMS	9BCON4 COLUMN	9BCON8 BEAMS	9BCON8 COLUMN
9	0.22	0.06	0.22	0.14	0.09	0.16	0.19	0.16
8	0.15	0.12	0.15	0.20	0.06	0.29	0.13	0.29
7	0.29	0.16	0.29	0.25	0.11	0.35	0.25	0.35
6	0.33	0.14	0.33	0.20	0.14	0.31	0.29	0.31
5	0.47	0.16	0.47	0.23	0.19	0.32	0.41	0.32
4	0.54	0.38	0.54	0.52	0.22	0.72	0.47	0.72
3	0.61	0.48	0.61	0.72	0.25	0.69	0.53	0.69
2	0.74	0.63	0.74	0.73	0.32	0.70	0.67	0.70
1	0.55	0.46	0.55	0.66	0.22	0.85	0.47	0.85

Table B-4 Beam and Column Damage Indices for Three Story Frames (Simulated Earthquake, PGA = 0.15 g)

STORY	3REAL BEAMS	3REAL COLUMN	3CPR BEAMS	3CPR COLUMN	3DPR BEAMS	3DPR COLUMN	3JSP BEAMS	3JSP COLUMN
3	0.14	0.03	0.16	0.02	0.01	0.02	0.01	0.02
2	0.17	0.19	0.18	0.07	0.37	0.04	0.03	0.05
1	0.18	0.26	0.17	0.25	0.43	0.05	0.05	0.07

STORY	3RCON4 BEAMS	3RCON4 COLUMN	3CPCON4 BEAMS	3CPCON4 COLUMN	3DCON4 BEAMS	3DCON4 COLUMN	3JCON4 BEAMS	3JCON4 COLUMN
3	0.05	0.01	0.06	0.01	0.00	0.01	0.00	0.01
2	0.07	0.08	0.07	0.03	0.15	0.02	0.01	0.02
1	0.07	0.11	0.07	0.11	0.17	0.02	0.02	0.03

STORY	3RCON8 BEAMS	3RCON8 COLUMN	3CPCON8 BEAMS	3CPCON8 COLUMN	3DCON8 BEAMS	3DCON8 COLUMN	3JCON8 BEAMS	3JCON8 COLUMN
3	0.12	0.02	0.14	0.01	0.01	0.01	0.01	0.01
2	0.15	0.13	0.15	0.04	0.32	0.02	0.03	0.03
1	0.15	0.19	0.14	0.18	0.38	0.04	0.04	0.05

STORY	3CCON4 BEAMS	3CCON4 COLUMN	3CCON8 BEAMS	3CCON8 COLUMN	3BCON4 BEAMS	3BCON4 COLUMN	3BCON8 BEAMS	3BCON8 COLUMN
3	0.14	0.01	0.14	0.02	0.05	0.03	0.12	0.03
2	0.17	0.08	0.17	0.13	0.07	0.19	0.15	0.19
1	0.18	0.11	0.18	0.19	0.07	0.26	0.15	0.26

Table B-5 Beam and Column Damage Indices for Six Story Frames (Simulated Earthquake, PGA = 0.15 g)

STORY	6REAL BEAMS	6REAL COLUMN	6CPR BEAMS	6CPR COLUMN	6DPR BEAMS	6DPR COLUMN	6JSP BEAMS	6JSP COLUMN
6	0.15	0.09	0.15	0.02	0.01	0.01	0.01	0.02
5	0.30	0.18	0.24	0.63	0.02	0.02	0.02	0.03
4	0.24	0.30	0.43	0.53	0.28	0.03	0.04	0.05
3	0.37	0.05	0.03	0.12	0.36	0.03	0.40	0.04
2	0.27	0.03	0.06	0.05	0.35	0.03	0.50	0.03
1	0.22	0.04	0.09	0.05	0.26	0.06	0.33	0.07

STORY	6RCON4 BEAMS	6RCON4 COLUMN	6CPCON4 BEAMS	6CPCON4 COLUMN	6DCON4 BEAMS	6DCON4 COLUMN	6JCON4 BEAMS	6JCON4 COLUMN
6	0.06	0.04	0.06	0.01	0.00	0.01	0.00	0.01
5	0.12	0.08	0.09	0.27	0.01	0.01	0.01	0.01
4	0.10	0.13	0.17	0.23	0.11	0.02	0.01	0.04
3	0.15	0.03	0.01	0.05	0.15	0.02	0.17	0.02
2	0.11	0.01	0.02	0.03	0.14	0.02	0.20	0.02
1	0.09	0.02	0.04	0.02	0.11	0.03	0.13	0.04

STORY	6RCON8 BEAMS	6RCON8 COLUMN	6CPCON8 BEAMS	6CPCON8 COLUMN	6DCON8 BEAMS	6DCON8 COLUMN	6JCON8 BEAMS	6JCON8 COLUMN
6	0.13	0.06	0.13	0.02	0.01	0.01	0.01	0.01
5	0.26	0.12	0.21	0.44	0.02	0.02	0.02	0.02
4	0.21	0.22	0.37	0.38	0.24	0.02	0.03	0.04
3	0.32	0.03	0.03	0.08	0.45	0.02	0.35	0.02
2	0.24	0.02	0.05	0.04	0.29	0.02	0.43	0.02
1	0.19	0.03	0.08	0.03	0.22	0.04	0.29	0.05

STORY	6CCON4 BEAMS	6CCON4 COLUMN	6CCON8 BEAMS	6CCON8 COLUMN	6BCON4 BEAMS	6BCON4 COLUMN	6BCON8 BEAMS	6BCON8 COLUMN
6	0.15	0.04	0.15	0.06	0.06	0.09	0.13	0.09
5	0.30	0.08	0.30	0.12	0.12	0.18	0.26	0.18
4	0.24	0.13	0.24	0.22	0.10	0.30	0.21	0.30
3	0.37	0.03	0.37	0.03	0.15	0.05	0.32	0.05
2	0.27	0.01	0.27	0.02	0.11	0.03	0.24	0.03
1	0.22	0.02	0.22	0.03	0.09	0.04	0.19	0.04

Table B-6 Beam and Column Damage Indices for Nine Story Frames (Simulated Earthquake, PGA = 0.15 g)

STORY	9REAL BEAMS	9REAL COLUMN	9CPR BEAMS	9CPR COLUMN	9DPR BEAMS	9DPR COLUMN	9JSP BEAMS	9JSP COLUMN
9	0.09	0.01	0.09	0.01	0.01	0.01	0.01	0.01
8	0.09	0.06	0.13	0.25	0.02	0.02	0.02	0.03
7	0.14	0.05	0.29	0.70	0.03	0.03	0.03	0.04
6	0.03	0.09	0.04	0.07	0.17	0.03	0.06	0.03
5	0.21	0.04	0.06	0.03	0.34	0.03	0.23	0.03
4	0.29	0.03	0.05	0.06	0.54	0.03	0.35	0.03
3	0.40	0.03	0.19	0.16	0.60	0.02	0.45	0.02
2	0.28	0.02	0.27	0.07	0.33	0.02	0.32	0.03
1	0.44	0.04	0.22	0.04	0.25	0.05	0.24	0.05

STORY	9RCON4 BEAMS	9RCON4 COLUMN	9CPCON4 BEAMS	9CPCON4 COLUMN	9DCON4 BEAMS	9DCON4 COLUMN	9JCON4 BEAMS	9JCON4 COLUMN
9	0.04	0.01	0.04	0.01	0.00	0.01	0.00	0.01
8	0.03	0.02	0.05	0.10	0.01	0.01	0.01	0.01
7	0.05	0.02	0.12	0.36	0.01	0.01	0.01	0.02
6	0.01	0.04	0.02	0.03	0.07	0.01	0.02	0.01
5	0.08	0.02	0.02	0.01	0.14	0.01	0.09	0.01
4	0.12	0.02	0.02	0.03	0.22	0.01	0.14	0.02
3	0.16	0.02	0.08	0.09	0.25	0.01	0.19	0.01
2	0.11	0.01	0.11	0.04	0.13	0.01	0.14	0.02
1	0.18	0.02	0.09	0.02	0.10	0.03	0.09	0.03

STORY	9RCON8 BEAMS	9RCON8 COLUMN	9CPCON8 BEAMS	9CPCON8 COLUMN	9DCON8 BEAMS	9DCON8 COLUMN	9JCON8 BEAMS	9JCON8 COLUMN
9	0.08	0.01	0.08	0.01	0.01	0.01	0.01	0.01
8	0.08	0.04	0.12	0.17	0.02	0.01	0.02	0.02
7	0.12	0.04	0.25	0.60	0.02	0.02	0.03	0.03
6	0.03	0.06	0.04	0.05	0.14	0.02	0.05	0.02
5	0.18	0.02	0.05	0.02	0.30	0.02	0.20	0.02
4	0.25	0.02	0.04	0.04	0.47	0.02	0.30	0.02
3	0.35	0.03	0.16	0.12	0.52	0.02	0.39	0.02
2	0.24	0.02	0.23	0.05	0.28	0.02	0.28	0.02
1	0.38	0.03	0.19	0.03	0.21	0.04	0.21	0.03

STORY	9CCON4 BEAMS	9CCON4 COLUMN	9CCON8 BEAMS	9CCON8 COLUMN	9BCON4 BEAMS	9BCON4 COLUMN	9BCON8 BEAMS	9BCON8 COLUMN
9	0.09	0.01	0.09	0.01	0.04	0.01	0.08	0.01
8	0.09	0.02	0.09	0.04	0.03	0.06	0.08	0.06
7	0.14	0.02	0.14	0.04	0.05	0.05	0.12	0.05
6	0.03	0.04	0.03	0.06	0.01	0.09	0.03	0.09
5	0.21	0.02	0.21	0.02	0.08	0.04	0.18	0.04
4	0.29	0.02	0.29	0.02	0.12	0.03	0.25	0.03
3	0.40	0.02	0.40	0.03	0.16	0.03	0.35	0.03
2	0.28	0.01	0.28	0.02	0.11	0.02	0.24	0.02
1	0.44	0.02	0.44	0.03	0.18	0.04	0.38	0.04

Table B-7 Beam and Column Damage Indices for Three Story Frames (Nahanni, PGA = 0.20 g)

STORY	3REAL BEAMS	3REAL COLUMN	3CPR BEAMS	3CPR COLUMN	3DPR BEAMS	3DPR COLUMN	3JSP BEAMS	3JSP COLUMN
3	0.19	0.12	0.15	0.07	0.01	0.02	0.01	0.02
2	0.07	0.06	0.05	0.06	0.18	0.02	0.02	0.03
1	0.06	0.03	0.05	0.03	0.02	0.04	0.02	0.04
STORY	3RCON4 BEAMS	3RCON4 COLUMN	3CPCON4 BEAMS	3CPCON4 COLUMN	3DCON4 BEAMS	3DCON4 COLUMN	3JCON4 BEAMS	3JCON4 COLUMN
3	0.07	0.06	0.06	0.03	0.01	0.01	0.01	0.01
2	0.03	0.02	0.02	0.02	0.07	0.01	0.01	0.01
1	0.02	0.01	0.02	0.01	0.01	0.02	0.01	0.02
STORY	3RCON8 BEAMS	3RCON8 COLUMN	3CPCON8 BEAMS	3CPCON8 COLUMN	3DCON8 BEAMS	3DCON8 COLUMN	3JCON8 BEAMS	3JCON8 COLUMN
3	0.16	0.08	0.13	0.05	0.01	0.02	0.01	0.02
2	0.06	0.04	0.04	0.03	0.15	0.02	0.02	0.02
1	0.05	0.02	0.05	0.02	0.02	0.03	0.02	0.03
STORY	3CCON4 BEAMS	3CCON4 COLUMN	3CCON8 BEAMS	3CCON8 COLUMN	3BCON4 BEAMS	3BCON4 COLUMN	3BCON8 BEAMS	3BCON8 COLUMN
3	0.19	0.06	0.19	0.08	0.07	0.12	0.16	0.12
2	0.07	0.02	0.07	0.04	0.03	0.06	0.06	0.06
1	0.06	0.01	0.06	0.02	0.02	0.03	0.05	0.03

Table B-8 Beam and Column Damage Indices for Six Story Frames (Nahanni, PGA = 0.20 g)

STORY	6REAL BEAMS	6REAL COLUMN	6CPR BEAMS	6CPR COLUMN	6DPR BEAMS	6DPR COLUMN	6JSP BEAMS	6JSP COLUMN
6	0.20	0.10	0.17	0.12	0.11	0.02	0.01	0.02
5	0.12	0.14	0.14	0.19	0.24	0.03	0.03	0.04
4	0.17	0.21	0.13	0.31	0.19	0.04	0.03	0.04
3	0.31	0.11	0.03	0.23	0.40	0.03	0.05	0.04
2	0.25	0.17	0.03	0.25	0.44	0.04	0.13	0.04
1	0.24	0.05	0.03	0.11	0.23	0.05	0.04	0.05

STORY	6RCON4 BEAMS	6RCON4 COLUMN	6CPCON4 BEAMS	6CPCON4 COLUMN	6DCON4 BEAMS	6DCON4 COLUMN	6JCON4 BEAMS	6JCON4 COLUMN
6	0.07	0.04	0.07	0.05	0.01	0.01	0.01	0.01
5	0.05	0.05	0.06	0.02	0:09	0.01	0.01	0.02
4	0.06	0.14	0.05	0.09	0.08	0.03	0.01	0.03
3	0.17	0.08	0.01	0.02	0.16	0.02	0.02	0.02
2	0.16	0.06	0.01	0.03	0.18	0.02	0.05	0.03
1	0.09	0.03	0.01	0.02	0.09	0.02	0.02	0.02

STORY	6RCON8 BEAMS	6RCON8 COLUMN	6CPCON8 BEAMS	6CPCON8 COLUMN	6DCON8 BEAMS	6DCON8 COLUMN	6JCON8 BEAMS	6JCON8 COLUMN
6	0.15	0.07	0.15	0.09	0.01	0.02	0.01	0.02
5	0.10	0.08	0.12	0.04	0.13	0.02	0.02	0.03
4	0.13	0.18	0.11	0.15	0.24	0.03	0.03	0.03
3	0.36	0.11	0.03	0.02	0.31	0.02	0.05	0.02
2	0.34	0.08	0.03	0.04	0.35	0.03	0.11	0.03
1	0.20	0.03	0.03	0.03	0.25	0.04	0.03	0.03

STORY	6CCON4 BEAMS	6CCON4 COLUMN	6CCON8 BEAMS	6CCON8 COLUMN	6BCON4 BEAMS	6BCON4 COLUMN	6BCON8 BEAMS	6BCON8 COLUMN
6	0.18	0.04	0.18	0.07	0.07	0.09	0.15	0.09
5	0.12	0.05	0.12	0.08	0.05	0.13	0.10	0.13
4	0.15	0.14	0.15	0.23	0.06	0.32	0.13	0.32
3	0.42	0.08	0.42	0.11	0.17	0.15	0.36	0.15
2	0.39	0.06	0.39	0.08	0.16	0.13	0.34	0.13
1	0.24	0.03	0.24	0.03	0.09	0.05	0.20	0.05

Table B-9 Beam and Column Damage Indices for Nine Story Frames (Nahanni, PGA = 0.20 g)

STORY	9REAL BEAMS	9REAL COLUMN	9CPR BEAMS	9CPR COLUMN	9DPR BEAMS	9DPR COLUMN	9JSP BEAMS	9JSP COLUMN
9	0.15	0.06	0.07	0.07	0.01	0.02	0.01	0.02
8	0.04	0.03	0.05	0.09	0.02	0.02	0.01	0.02
7	0.07	0.03	0.08	0.24	0.02	0.03	0.02	0.04
6	0.04	0.03	0.03	0.20	0.04	0.03	0.03	0.03
5	0.16	0.06	0.04	0.36	0.13	0.03	0.04	0.04
4	0.39	0.12	0.16	0.22	0.31	0.04	0.27	0.05
3	0.37	0.06	0.22	0.28	0.51	0.02	0.23	0.03
2	0.36	0.04	0.26	0.21	0.48	0.03	0.26	0.04
1	0.27	0.05	0.22	0.09	0.44	0.05	0.19	0.04

STORY	9RCON4 BEAMS	9RCON4 COLUMN	9CPCON4 BEAMS	9CPCON4 COLUMN	9DCON4 BEAMS	9DCON4 COLUMN	9JCON4 BEAMS	9JCON4 COLUMN
9	0.06	0.03	0.06	0.03	0.01	0.01	0.01	0.01
8	0.02	0.01	0.02	0.04	0.01	0.01	0.01	0.01
7	0.03	0.01	0.08	0.10	0.01	0.01	0.01	0.02
6	0.01	0.01	0.01	0.02	0.02	0.01	0.01	0.01
5	0.06	0.03	0.01	0.44	0.05	0.02	0.01	0.02
4	0.16	0.06	0.09	0.06	0.13	0.02	0.11	0.02
3	0.15	0.04	0.13	0.10	0.21	0.01	0.21	0.01
2	0.24	0.02	0.14	0.06	0.19	0.02	0.15	0.02
1	0.11	0.03	0.10	0.03	0.18	0.03	0.14	0.02

STORY	9RCON8 BEAMS	9RCON8 COLUMN	9CPCON8 BEAMS	9CPCON8 COLUMN	9DCON8 BEAMS	9DCON8 COLUMN	9JCON8 BEAMS	9JCON8 COLUMN
9	0.13	0.05	0.13	0.05	0.01	0.02	0.01	0.02
8	0.03	0.02	0.04	0.06	0.01	0.01	0.01	0.02
7	0.06	0.02	0.17	0.16	0.02	0.02	0.02	0.03
6	0.03	0.02	0.03	0.04	0.04	0.02	0.03	0.02
5	0.14	0.05	0.03	0.61	0.01	0.03	0.03	0.03
4	0.34	0.09	0.20	0.07	0.27	0.03	0.24	0.03
3	0.32	0.05	0.26	0.16	0.44	0.02	0.46	0.02
2	0.52	0.03	0.30	0.13	0.42	0.02	0.32	0.03
1	0.23	0.03	0.25	0.04	0.39	0.03	0.29	0.03

STORY	9CCON4 BEAMS	9CCON4 COLUMN	9CCON8 BEAMS	9CCON8 COLUMN	9BCON4 BEAMS	9BCON4 COLUMN	9BCON8 BEAMS	9BCON8 COLUMN
9	0.15	0.03	0.15	0.05	0.06	0.06	0.13	0.06
8	0.04	0.01	0.04	0.02	0.02	0.03	0.03	0.03
7	0.07	0.01	0.07	0.02	0.03	0.03	0.06	0.03
6	0.04	0.01	0.04	0.02	0.01	0.03	0.03	0.03
5	0.16	0.03	0.16	0.05	0.06	0.06	0.14	0.06
4	0.39	0.06	0.39	0.09	0.16	0.12	0.34	0.12
3	0.37	0.04	0.37	0.05	0.15	0.06	0.32	0.06
2	0.60	0.02	0.60	0.03	0.24	0.04	0.52	0.04
1	0.27	0.03	0.27	0.03	0.11	0.05	0.23	0.05

Table B-10 Beam and Column Damage Indices for Three Story Frames (Taft, PGA = 0.20 g)

STORY	3REAL BEAMS	3REAL COLUMN	3CPR BEAMS	3CPR COLUMN	3DPR BEAMS	3DPR COLUMN	3JSP BEAMS	3JSP COLUMN
3	0.37	0.39	0.13	0.07	0.01	0.09	0.01	0.02
2	0.44	0.52	0.35	1.00	0.46	0.42	0.04	0.23
1	0.54	0.79	0.69	1.00	1.00	0.39	0.45	0.44

STORY	3RCON4 BEAMS	3RCON4 COLUMN	3CPCON4 BEAMS	3CPCON4 COLUMN	3DCON4 BEAMS	3DCON4 COLUMN	3JCON4 BEAMS	3JCON4 COLUMN
3	0.15	0.08	0.05	0.03	0.01	0.03	0.00	0.01
2	0.18	0.58	0.10	0.67	0.19	0.17	0.02	0.10
1	0.38	0.64	0.28	0.67	0.56	0.17	0.19	0.19

STORY	3RCON8 BEAMS	3RCON8 COLUMN	3CPCON8 BEAMS	3CPCON8 COLUMN	3DCON8 BEAMS	3DCON8 COLUMN	3JCON8 BEAMS	3JCON8 COLUMN
3	0.32	0.15	0.11	0.06	0.01	0.07	0.01	0.01
2	0.38	0.48	0.22	0.91	0.41	0.27	0.03	0.15
1	0.82	0.71	0.60	0.93	1.00	0.28	0.39	0.32

STORY	3CCON4 BEAMS	3CCON4 COLUMN	3CCON8 BEAMS	3CCON8 COLUMN	3BCON4 BEAMS	3BCON4 COLUMN	3BCON8 BEAMS	3BCON8 COLUMN
3	0.37	0.08	0.37	0.15	0.15	0.19	0.32	0.19
2	0.44	0.68	0.44	0.92	0.18	0.96	0.38	0.96
1	0.92	0.64	0.92	0.91	0.38	0.96	0.82	0.96

Table B-11 Beam and Column Damage Indices for Six Story Frames (Taft, PGA = 0.20 g)

STORY	6REAL BEAMS	6REAL COLUMN	6CPR BEAMS	6CPR COLUMN	6DPR BEAMS	6DPR COLUMN	6JSP BEAMS	6JSP COLUMN
6	0.05	0.21	0.06	0.31	0.08	0.11	0.02	0.07
5	0.10	0.57	0.10	0.87	0.22	0.37	0.11	0.28
4	0.62	1.00	0.68	1.00	0.96	0.46	0.36	0.22
3	0.90	0.70	0.21	0.83	0.78	0.14	0.47	0.08
2	0.55	0.58	0.26	0.83	0.99	0.10	0.32	0.07
1	0.38	0.34	0.18	0.22	0.71	0.18	0.29	0.14

STORY	6RCON4 BEAMS	6RCON4 COLUMN	6CPCON4 BEAMS	6CPCON4 COLUMN	6DCON4 BEAMS	6DCON4 COLUMN	6JCON4 BEAMS	6JCON4 COLUMN
6	0.02	0.00	0.02	0.00	0.01	0.03	0.01	0.05
5	0.04	0.26	0.04	0.49	0.40	0.13	0.05	0.16
4	0.27	0.53	0.27	0.90	0.45	0.16	0.15	0.33
3	0.36	0.37	0.09	0.40	0.41	0.02	0.50	0.03
2	0.22	0.36	0.10	0.50	0.45	0.04	0.30	0.05
1	0.16	0.07	0.07	0.10	0.30	0.09	0.18	0.07

STORY	6RCON8 BEAMS	6RCON8 COLUMN	6CPCON8 BEAMS	6CPCON8 COLUMN	6DCON8 BEAMS	6DCON8 COLUMN	6JCON8 BEAMS	6JCON8 COLUMN
6	0.05	0.01	0.05	0.01	0.02	0.04	0.02	0.08
5	0.09	0.44	0.08	0.81	0.81	0.22	0.10	0.24
4	0.58	0.62	0.59	1.00	0.89	0.17	0.31	0.33
3	0.68	0.52	0.18	0.58	0.72	0.03	0.93	0.04
2	0.46	0.50	0.22	0.70	0.92	0.04	0.62	0.05
1	0.33	0.10	0.16	0.14	0.61	0.12	0.39	0.09

STORY	6CCON4 BEAMS	6CCON4 COLUMN	6CCON8 BEAMS	6CCON8 COLUMN	6BCON4 BEAMS	6BCON4 COLUMN	6BCON8 BEAMS	6BCON8 COLUMN
6	0.05	0.00	0.05	0.01	0.02	0.01	0.05	0.01
5	0.10	0.26	0.10	0.44	0.04	0.59	0.09	0.59
4	0.62	0.93	0.62	1.00	0.27	1.00	0.58	1.00
3	0.90	0.37	0.73	0.52	0.36	0.79	0.68	0.79
2	0.55	0.36	0.53	0.50	0.22	0.73	0.46	0.73
1	0.38	0.07	0.38	0.10	0.16	0.14	0.33	0.14

Table B-12 Beam and Column Damage Indices for Nine Story Frames (Taft, PGA = 0.20 g)

STORY	9REAL BEAMS	9REAL COLUMN	9CPR BEAMS	9CPR COLUMN	9DPR BEAMS	9DPR COLUMN	9JSP BEAMS	9JSP COLUMN
9	0.08	0.33	0.10	0.21	0.02	0.15	0.02	0.05
8	0.11	0.69	0.09	0.55	0.65	0.17	0.07	0.13
7	0.46	0.66	0.41	0.72	0.62	0.07	0.14	0.08
6	0.57	0.69	0.03	0.77	0.64	0.05	0.35	0.06
5	0.87	0.72	0.05	0.85	0.61	0.04	0.51	0.05
4	0.77	0.83	0.13	0.88	0.77	0.05	0.51	0.07
3	0.95	0.71	0.27	0.93	0.87	0.03	0.71	0.03
2	0.74	0.76	0.37	0.94	0.70	0.03	0.68	0.05
1	0.69	0.83	0.49	0.85	0.56	0.06	0.37	0.07

STORY	9RCON4 BEAMS	9RCON4 COLUMN	9CPCON4 BEAMS	9CPCON4 COLUMN	9DCON4 BEAMS	9DCON4 COLUMN	9JCON4 BEAMS	9JCON4 COLUMN
9	0.03	0.01	0.04	0.01	0.01	0.07	0.01	0.02
8	0.04	0.30	0.03	0.15	0.26	0.08	0.03	0.06
7	0.19	0.28	0.16	0.18	0.25	0.03	0.06	0.04
6	0.23	0.35	0.01	0.01	0.27	0.02	0.14	0.03
5	0.54	0.66	0.02	0.09	0.25	0.02	0.21	0.03
4	0.31	0.71	0.06	0.41	0.32	0.03	0.21	0.03
3	0.42	0.77	0.11	0.74	0.36	0.01	0.29	0.02
2	0.31	0.69	0.16	0.93	0.30	0.02	0.29	0.02
1	0.28	0.47	0.31	0.83	0.23	0.04	0.15	0.04

STORY	9RCON8 BEAMS	9RCON8 COLUMN	9CPCON8 BEAMS	9CPCON8 COLUMN	9DCON8 BEAMS	9DCON8 COLUMN	9JCON8 BEAMS	9JCON8 COLUMN
9	0.07	0.02	0.08	0.01	0.01	0.11	0.02	0.02
8	0.09	0.50	0.07	0.22	0.56	0.14	0.06	0.09
7	0.40	0.47	0.33	0.25	0.54	0.05	0.12	0.06
6	0.49	0.48	0.03	0.02	0.56	0.03	0.31	0.04
5	0.84	0.70	0.04	0.10	0.53	0.03	0.45	0.04
4	0.67	0.70	0.12	0.44	0.67	0.04	0.44	0.04
3	0.88	0.73	0.20	0.86	0.76	0.02	0.62	0.03
2	0.64	0.72	0.33	0.96	0.61	0.03	0.59	0.03
1	0.60	0.68	0.44	0.83	0.49	0.05	0.32	0.05

STORY	9CCON4 BEAMS	9CCON4 COLUMN	9CCON8 BEAMS	9CCON8 COLUMN	9BCON4 BEAMS	9BCON4 COLUMN	9BCON8 BEAMS	9BCON8 COLUMN
9	0.08	0.01	0.08	0.02	0.03	0.03	0.07	0.03
8	0.11	0.30	0.11	0.48	0.04	0.69	0.09	0.69
7	0.46	0.28	0.46	0.48	0.19	0.66	0.40	0.66
6	0.57	0.35	0.57	0.48	0.23	0.69	0.49	0.69
5	0.87	0.66	0.87	0.70	0.54	0.72	0.84	0.72
4	0.77	0.71	0.77	0.70	0.31	0.83	0.67	0.83
3	0.95	0.77	0.95	0.73	0.42	0.71	0.88	0.71
2	0.74	0.69	0.74	0.72	0.31	0.76	0.64	0.76
1	0.69	0.47	0.69	0.68	0.28	0.83	0.60	0.83

APPENDIX C

MAXIMUM STORY DRIFTS AND STORY SHEARS

General Notes

1. Tables display the maximum story drifts along with maximum story shears as computed by the program IDARC. Values are tabulated for 3, 6 & 9 story buildings subjected to the same ground motion.

2. Story drift is expressed as a percentage of story height. Maximum story shear is expressed as a percentage of total building weight.

3. The values in the rows labelled "max." under the story drift heading represent the maximum top story displacement expressed as a percentage of total building height. This value should not be misconstrued to be the summation of story drifts, but should give an indication of the maximum overall building deflection.

4. The total maximum story shear is presented. Since the maximum building shear occurs generally at the base of the building, it was not necessary to have this shown again under a separate heading.

5. Since the level of confinement did not have any significant influence on the drift and shear values, the separate studies on the effect of confinement are not presented. Instead, only results from four specific detailing combinations for each building type are presented. As was discussed in Section 6, confinement is modelled in the program as having an effect on member ductility and not on strength or stiffness and its effect is primarily seen in the damage values.

6. Results are tabulated separately for the four ground motions listed below. For discussion of choice of these ground motions see Section 4.
   - -1940 El Centro (S 00 E): (PGA = 0.20 g)
   - -Artificially Generated Ground Motion: (PGA = 0.15 g)
   - -1985 Nahanni (N 00 W): (PGA = 0.20 g)
   - -1952 Taft (N 21 E) (PGA = 0.20 g)

7. Improved scale illustrations of the four reinforcing strategies are shown in Figures C-1. Figures shown are for interior beam-column joints. Exterior beam-column joints were modelled in the same manner (see Section 3).

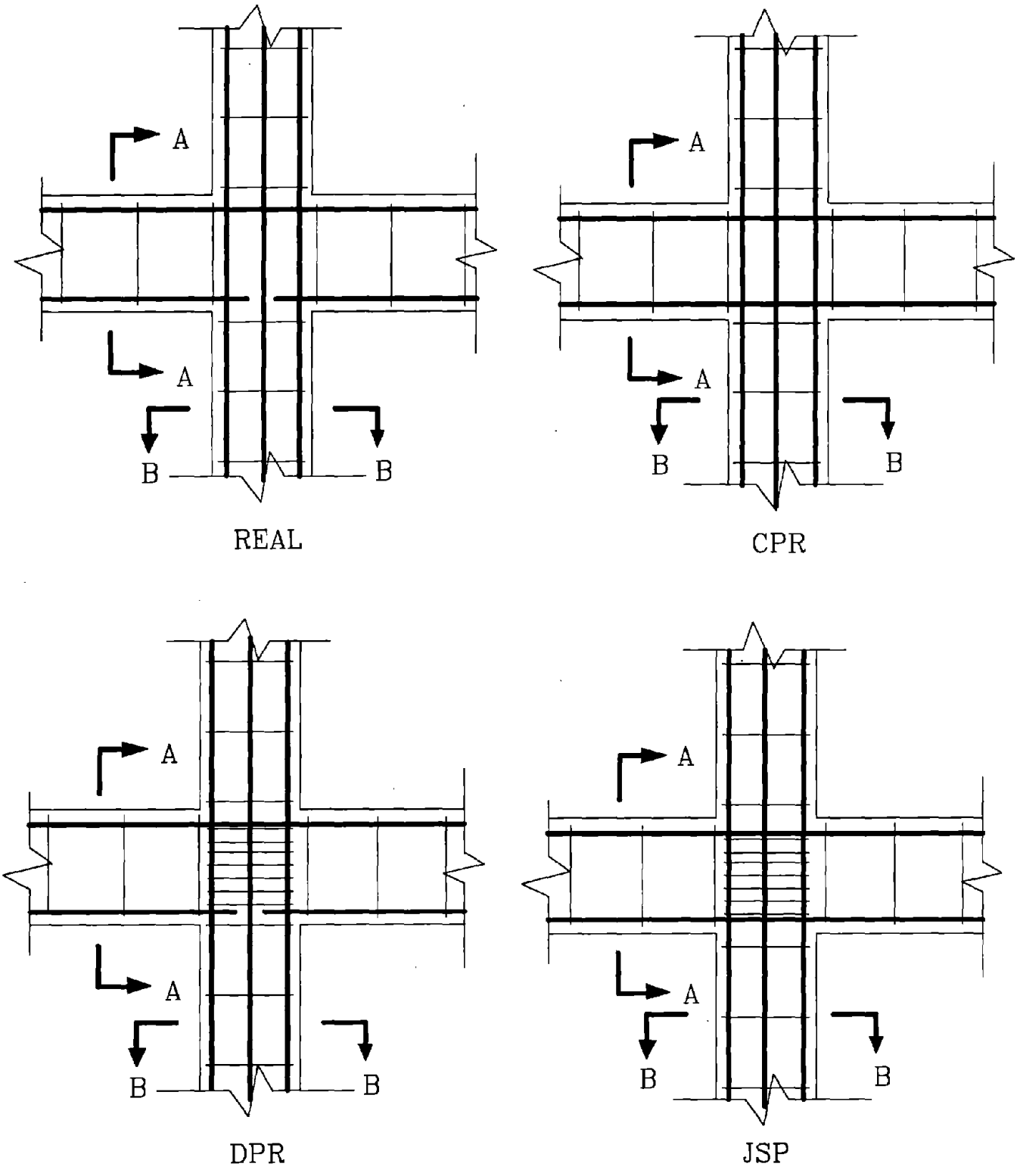

Fig. C-1 Beam-Column Joint Reinforcing Details

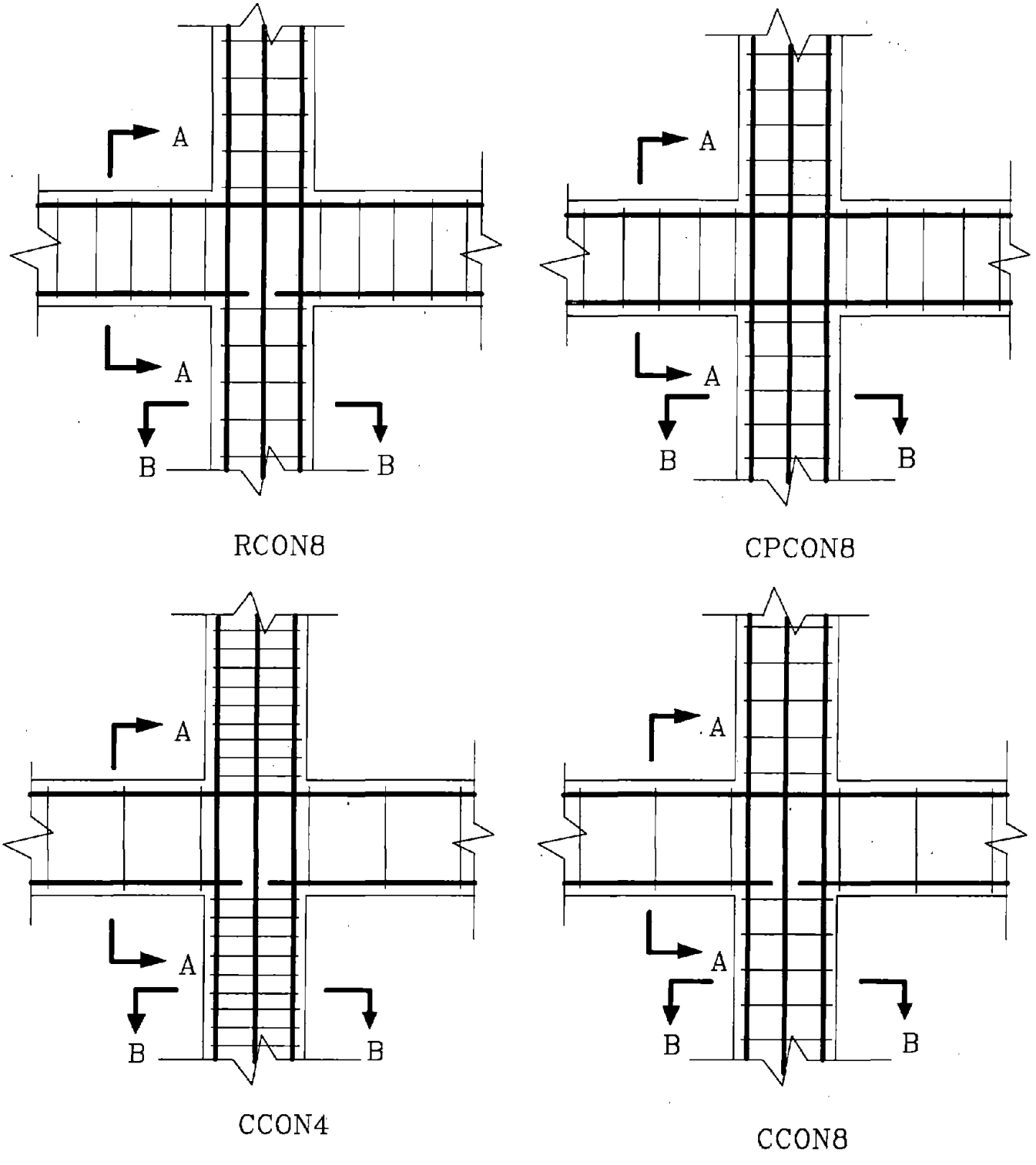

Fig. C-1 Beam-Column Joint Reinforcing Details (continued)

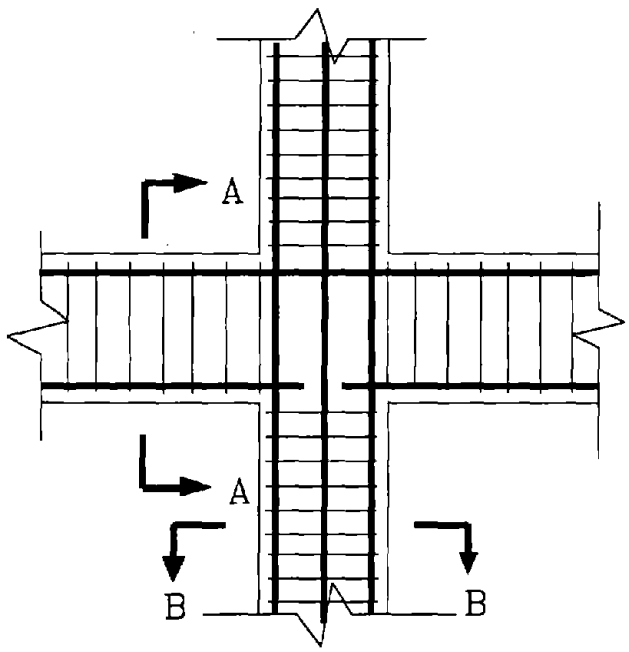

RCON4

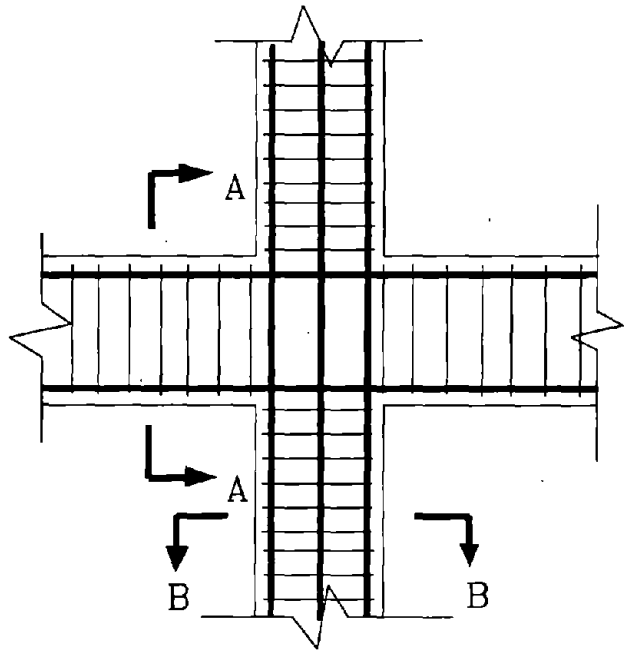

CPCON4

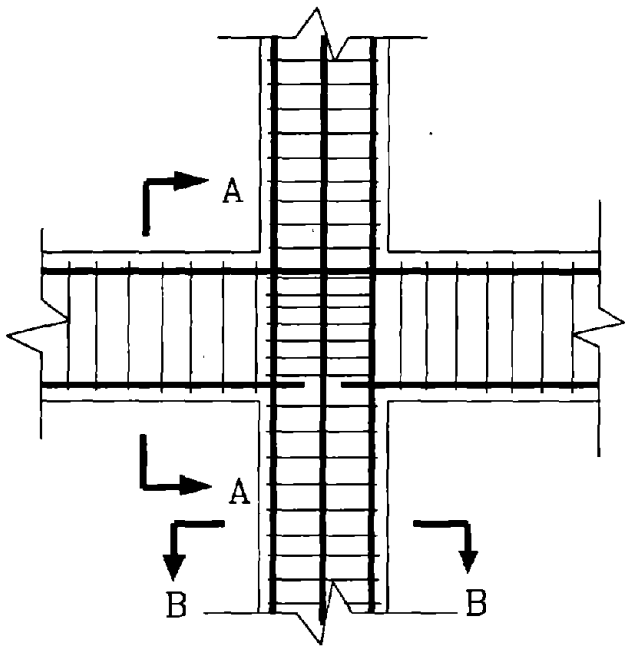

DCON4

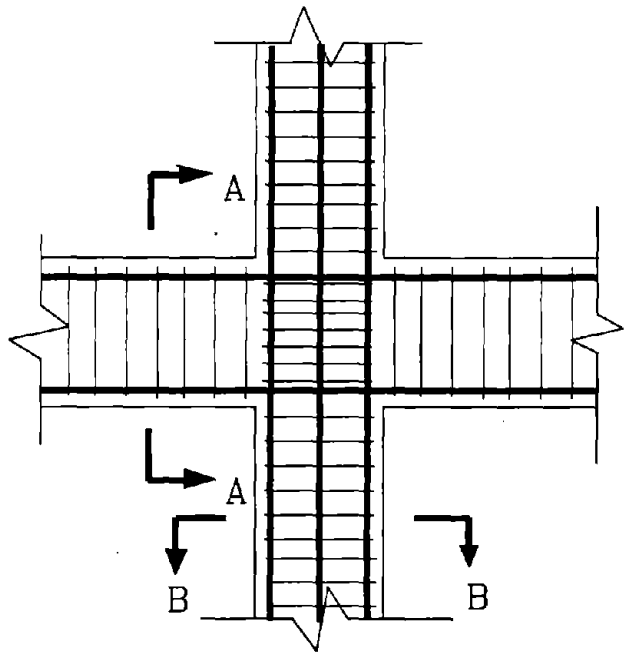

JCON4

Fig. C-1 Beam-Column Joint Reinforcing Details (continued)

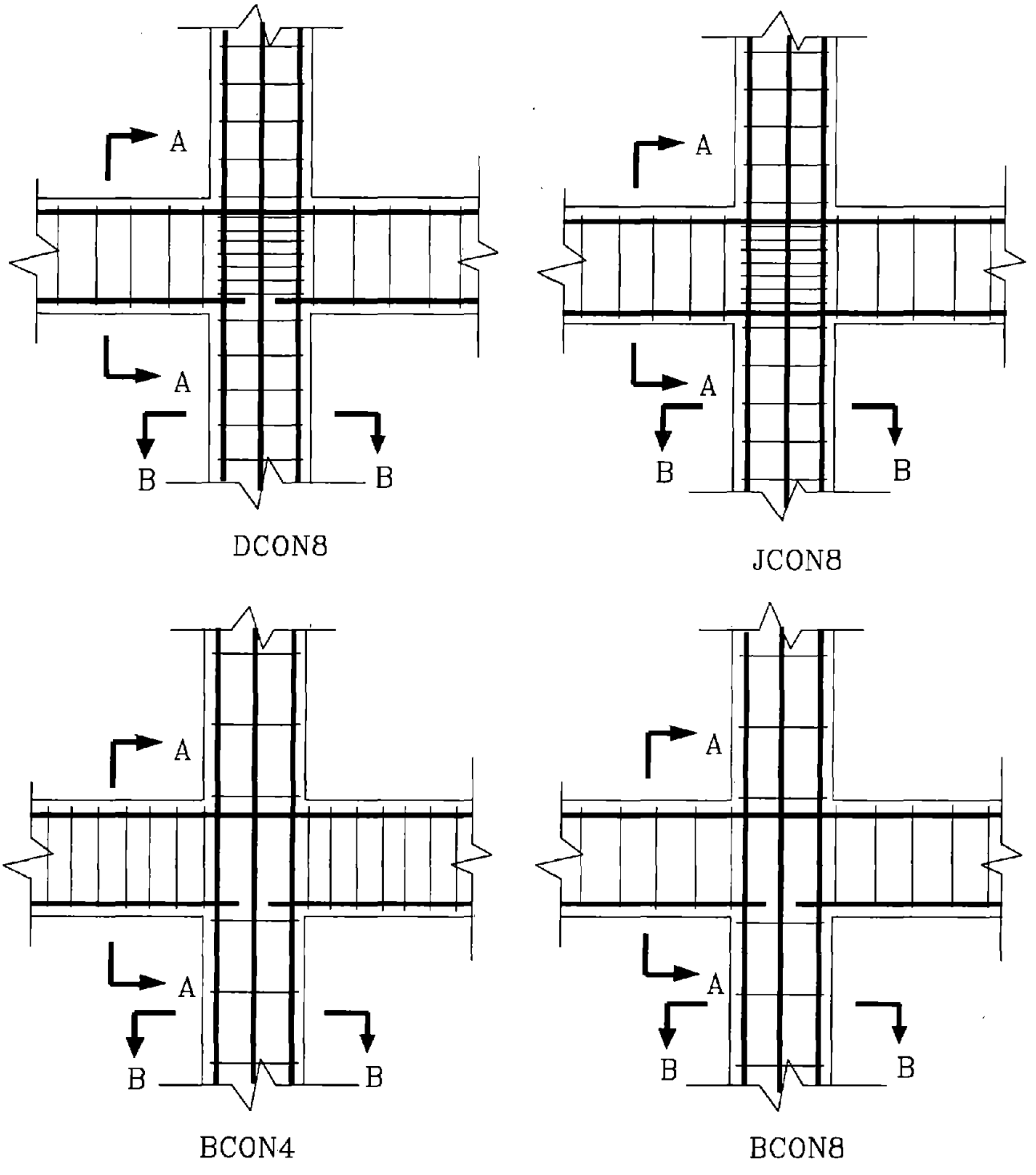

Fig. C-1 Beam-Column Joint Reinforcing Details (continued)

Table C-1 Maximum Story Drifts and Shears for 3, 6 & 9 Story Frames (El Centro, PGA = 0.2 g)

STORY	3REAL DRIFT (%)	3REAL SHEAR (%)	3CPR DRIFT (%)	3CPR SHEAR (%)	3DPR DRIFT (%)	3DPR SHEAR (%)	3JSP DRIFT (%)	3JSP SHEAR (%)
3	1.02	3.54	0.97	3.54	1.06	4.81	0.27	5.48
2	1.16	4.60	1.16	4.65	1.63	7.77	1.04	8.25
1	0.92	5.15	0.90	5.27	1.10	7.25	1.37	9.52
max*	0.99		0.95		1.18		0.85	
STORY	6REAL DRIFT (%)	6REAL SHEAR (%)	6CPR DRIFT (%)	6CPR SHEAR (%)	6DPR DRIFT (%)	6DPR SHEAR (%)	6JSP DRIFT (%)	6JSP SHEAR (%)
6	0.30	1.70	0.20	2.54	1.98	2.64	0.30	3.17
5	1.58	2.09	0.66	3.93	1.75	3.43	0.77	4.04
4	2.67	2.67	1.19	4.68	1.51	3.71	1.16	4.26
3	1.61	3.84	1.10	5.08	1.07	3.61	1.04	4.24
2	1.19	4.35	0.83	4.51	0.95	4.67	0.94	5.21
1	0.44	4.78	0.49	5.16	0.59	5.99	0.59	5.70
max*	0.76		0.70		1.12		0.72	
STORY	9REAL DRIFT (%)	9REAL SHEAR (%)	9CPR DRIFT (%)	9CPR SHEAR (%)	9DPR DRIFT (%)	9DPR SHEAR (%)	9JSP DRIFT (%)	9JSP SHEAR (%)
9	0.31	1.28	0.33	1.42	0.68	2.22	0.44	2.31
8	0.44	1.33	0.52	1.58	1.09	2.38	0.60	2.56
7	0.69	1.83	1.36	1.75	0.99	2.77	0.78	3.04
6	0.86	2.01	0.24	2.08	0.83	2.38	1.08	3.06
5	1.12	2.29	0.38	2.70	0.90	2.62	1.00	2.94
4	1.17	2.69	0.63	2.99	0.99	2.92	0.74	3.28
3	1.11	3.09	0.81	3.22	0.90	3.13	0.84	3.40
2	1.15	3.22	0.85	3.19	0.72	3.19	0.70	3.24
1	0.37	4.13	0.28	3.98	0.41	4.15	0.35	3.90
max*	0.56		0.40		0.61		0.55	

* See General Notes 3 & 4, Pg. C-2 for Explanation.

Table C-2 Maximum Story Drifts and Shears for 3, 6 & 9 Story Frames (Simulated Earthquake, PGA = 0.15 g)

STORY	3REAL DRIFT (%)	3REAL SHEAR (%)	3CPR DRIFT (%)	3CPR SHEAR (%)	3DPR DRIFT (%)	3DPR SHEAR (%)	3JSP DRIFT (%)	3JSP SHEAR (%)
3	0.30	3.13	0.34	3.56	0.31	4.77	0.23	5.08
2	0.53	4.42	0.38	4.25	0.63	5.81	0.38	7.46
1	0.38	5.88	0.40	5.65	0.45	6.25	0.36	8.13
max*	0.33		0.92		0.46		0.30	
STORY	6REAL DRIFT (%)	6REAL SHEAR (%)	6CPR DRIFT (%)	6CPR SHEAR (%)	6DPR DRIFT (%)	6DPR SHEAR (%)	6JSP DRIFT (%)	6JSP SHEAR (%)
6	0.41	1.86	0.37	1.83	0.15	2.03	0.18	2.45
5	0.67	2.35	1.25	2.43	0.36	2.46	0.28	2.83
4	0.95	2.64	0.76	2.71	0.63	2.81	0.47	3.55
3	0.60	3.36	0.26	3.52	0.67	3.33	0.60	4.07
2	0.52	4.01	0.29	4.44	0.51	4.07	0.66	4.54
1	0.26	4.19	0.21	4.76	0.30	4.46	0.40	4.92
max*	0.48		0.41		0.38		0.39	
STORY	9REAL DRIFT (%)	9REAL SHEAR (%)	9CPR DRIFT (%)	9CPR SHEAR (%)	9DPR DRIFT (%)	9DPR SHEAR (%)	9JSP DRIFT (%)	9JSP SHEAR (%)
9	0.17	1.07	0.19	1.07	0.15	1.31	0.17	1.38
8	0.32	1.41	0.62	1.42	0.21	1.53	0.30	2.00
7	0.32	1.74	1.03	1.78	0.27	1.75	0.34	2.22
6	0.40	2.17	0.28	2.54	0.42	2.39	0.34	2.85
5	0.58	2.51	0.29	2.58	0.55	2.28	0.47	2.89
4	0.63	2.28	0.36	2.53	0.52	2.24	0.56	2.50
3	0.53	2.35	0.54	2.81	0.60	2.19	0.58	2.81
2	0.56	2.94	0.56	3.30	0.62	2.78	0.53	3.30
1	0.33	3.21	0.32	3.86	0.39	3.17	0.31	4.00
max*	0.31		0.39		0.32		0.33	

* See General Notes 3 & 4, Pg. C-2 for Explanation.

Table C-3 Maximum Story Drifts and Shears for 3, 6 & 9 Story Frames (Nahanni, PGA = 0.2 g)

STORY	3REAL DRIFT (%)	3REAL SHEAR (%)	3CPR DRIFT (%)	3CPR SHEAR (%)	3DPR DRIFT (%)	3DPR SHEAR (%)	3JSP DRIFT (%)	3JSP SHEAR (%)
3	0.31	4.02	0.32	3.90	0.27	5.54	0.21	5.63
2	0.24	4.60	0.22	5.08	0.24	4.79	0.22	5.17
1	0.31	5.46	0.18	5.54	0.22	6.21	0.22	6.29
max*	0.18		0.19		0.17		0.17	

STORY	6REAL DRIFT (%)	6REAL SHEAR (%)	6CPR DRIFT (%)	6CPR SHEAR (%)	6DPR DRIFT (%)	6DPR SHEAR (%)	6JSP DRIFT (%)	6JSP SHEAR (%)
6	0.41	1.96	0.42	2.04	0.24	2.70	0.20	2.58
5	0.38	2.24	0.42	2.37	0.32	2.77	0.31	2.93
4	0.51	2.88	0.59	3.06	0.41	2.94	0.28	3.25
3	0.49	4.30	0.52	4.42	0.21	4.28	0.30	4.44
2	0.38	4.60	0.40	4.72	0.18	4.69	0.30	5.16
1	0.22	4.93	0.30	5.06	0.18	4.97	0.18	5.07
max*	0.32		0.23		0.36		0.21	

STORY	9REAL DRIFT (%)	9REAL SHEAR (%)	9CPR DRIFT (%)	9CPR SHEAR (%)	9DPR DRIFT (%)	9DPR SHEAR (%)	9JSP DRIFT (%)	9JSP SHEAR (%)
9	0.29	1.33	0.36	1.34	0.20	1.98	0.20	1.96
8	0.23	1.49	0.34	1.51	0.17	1.38	0.22	1.72
7	0.22	1.80	0.43	1.79	0.19	1.99	0.29	2.37
6	0.20	2.62	0.22	2.89	0.20	3.06	0.23	3.13
5	0.38	3.04	0.33	3.09	0.36	2.85	0.33	3.53
4	0.53	2.63	0.67	3.19	0.58	2.57	0.56	3.10
3	0.61	2.83	0.90	2.94	0.63	2.78	0.77	3.03
2	0.58	3.40	0.81	3.59	0.62	3.52	0.63	3.91
1	0.31	3.15	0.36	3.65	0.35	3.61	0.30	3.81
max*	0.27		0.40		0.27		0.33	

* See General Notes 3 & 4, Pg. C-2 for Explanation.

Table C-4 Maximum Story Drifts and Shears for 3, 6 & 9 Story Frames (Taft, PGA = 0.2 g)

STORY	3REAL DRIFT (%)	3REAL SHEAR (%)	3CPR DRIFT (%)	3CPR SHEAR (%)	3DPR DRIFT (%)	3DPR SHEAR (%)	3JSP DRIFT (%)	3JSP SHEAR (%)
3	1.01	2.90	0.48	2.90	0.51	4.33	0.22	4.85
2	3.06	4.35	2.33	4.31	1.92	6.46	1.01	7.67
1	2.03	6.52	2.14	5.94	2.13	8.71	1.36	9.60
max*	1.28		1.24		1.42		0.80	

STORY	6REAL DRIFT (%)	6REAL SHEAR (%)	6CPR DRIFT (%)	6CPR SHEAR (%)	6DPR DRIFT (%)	6DPR SHEAR (%)	6JSP DRIFT (%)	6JSP SHEAR (%)
6	0.28	1.63	0.40	1.61	0.64	2.36	0.42	3.15
5	0.90	2.09	2.07	2.09	1.24	3.48	1.04	3.83
4	2.37	2.88	2.65	2.90	1.60	3.83	1.38	4.27
3	1.67	3.93	1.96	4.06	1.72	4.57	1.37	5.55
2	1.11	4.44	1.16	4.63	1.58	4.56	1.20	5.31
1	0.50	5.10	0.81	5.38	0.89	5.55	0.65	5.99
max*	1.19		1.14		0.99		0.83	

STORY	9REAL DRIFT (%)	9REAL SHEAR (%)	9CPR DRIFT (%)	9CPR SHEAR (%)	9DPR DRIFT (%)	9DPR SHEAR (%)	9JSP DRIFT (%)	9JSP SHEAR (%)
9	0.22	1.01	0.40	1.19	0.89	1.71	0.31	2.33
8	0.75	1.33	0.66	1.33	0.97	2.39	0.62	2.82
7	1.17	1.71	1.25	1.78	0.97	2.24	0.67	2.69
6	1.33	1.99	1.53	2.08	1.03	2.07	0.72	2.89
5	1.48	2.24	1.55	2.49	1.19	2.58	0.83	3.04
4	1.29	2.62	1.44	2.50	1.33	3.03	1.06	3.33
3	1.20	3.08	1.34	3.13	1.33	3.19	1.17	3.76
2	1.11	3.58	1.21	3.69	1.13	3.58	1.04	3.92
1	0.48	3.76	0.42	4.19	0.54	3.95	0.54	4.37
max*	0.73		0.55		0.68		0.54	

* See General Notes 3 & 4, Pg. C-2 for Explanation.

NATIONAL CENTER FOR EARTHQUAKE ENGINEERING RESEARCH
LIST OF TECHNICAL REPORTS

The National Center for Earthquake Engineering Research (NCEER) publishes technical reports on a variety of subjects related to earthquake engineering written by authors funded through NCEER. These reports are available from both NCEER's Publications Department and the National Technical Information Service (NTIS). Requests for reports should be directed to the Publications Department, National Center for Earthquake Engineering Research, State University of New York at Buffalo, Red Jacket Quadrangle, Buffalo, New York 14261. Reports can also be requested through NTIS, 5285 Port Royal Road, Springfield, Virginia 22161. NTIS accession numbers are shown in parenthesis, if available.

NCEER-87-0001 "First-Year Program in Research, Education and Technology Transfer," 3/5/87, (PB88-134275).

NCEER-87-0002 "Experimental Evaluation of Instantaneous Optimal Algorithms for Structural Control," by R.C. Lin, T.T. Soong and A.M. Reinhorn, 4/20/87, (PB88-134341).

NCEER-87-0003 "Experimentation Using the Earthquake Simulation Facilities at University at Buffalo," by A.M. Reinhorn and R.L. Ketter, to be published.

NCEER-87-0004 "The System Characteristics and Performance of a Shaking Table," by J.S. Hwang, K.C. Chang and G.C. Lee, 6/1/87, (PB88-134259). This report is available only through NTIS (see address given above).

NCEER-87-0005 "A Finite Element Formulation for Nonlinear Viscoplastic Material Using a Q Model," by O. Gyebi and G. Dasgupta, 11/2/87, (PB88-213764).

NCEER-87-0006 "Symbolic Manipulation Program (SMP) - Algebraic Codes for Two and Three Dimensional Finite Element Formulations," by X. Lee and G. Dasgupta, 11/9/87, (PB88-218522).

NCEER-87-0007 "Instantaneous Optimal Control Laws for Tall Buildings Under Seismic Excitations," by J.N. Yang, A. Akbarpour and P. Ghaemmaghami, 6/10/87, (PB88-134333). This report is only available through NTIS (see address given above).

NCEER-87-0008 "IDARC: Inelastic Damage Analysis of Reinforced Concrete Frame - Shear-Wall Structures," by Y.J. Park, A.M. Reinhorn and S.K. Kunnath, 7/20/87, (PB88-134325).

NCEER-87-0009 "Liquefaction Potential for New York State: A Preliminary Report on Sites in Manhattan and Buffalo," by M. Budhu, V. Vijayakumar, R.F. Giese and L. Baumgras, 8/31/87, (PB88-163704). This report is available only through NTIS (see address given above).

NCEER-87-0010 "Vertical and Torsional Vibration of Foundations in Inhomogeneous Media," by A.S. Veletsos and K.W. Dotson, 6/1/87, (PB88-134291).

NCEER-87-0011 "Seismic Probabilistic Risk Assessment and Seismic Margins Studies for Nuclear Power Plants," by Howard H.M. Hwang, 6/15/87, (PB88-134267).

NCEER-87-0012 "Parametric Studies of Frequency Response of Secondary Systems Under Ground-Acceleration Excitations," by Y. Yong and Y.K. Lin, 6/10/87, (PB88-134309).

NCEER-87-0013 "Frequency Response of Secondary Systems Under Seismic Excitation," by J.A. HoLung, J. Cai and Y.K. Lin, 7/31/87, (PB88-134317).

NCEER-87-0014 "Modelling Earthquake Ground Motions in Seismically Active Regions Using Parametric Time Series Methods," by G.W. Ellis and A.S. Cakmak, 8/25/87, (PB88-134283).

NCEER-87-0015 "Detection and Assessment of Seismic Structural Damage," by E. DiPasquale and A.S. Cakmak, 8/25/87, (PB88-163712).

NCEER-87-0016 "Pipeline Experiment at Parkfield, California," by J. Isenberg and E. Richardson, 9/15/87, (PB88-163720). This report is available only through NTIS (see address given above).

NCEER-87-0017 "Digital Simulation of Seismic Ground Motion," by M. Shinozuka, G. Deodatis and T. Harada, 8/31/87, (PB88-155197). This report is available only through NTIS (see address given above).

NCEER-87-0018 "Practical Considerations for Structural Control: System Uncertainty, System Time Delay and Truncation of Small Control Forces," J.N. Yang and A. Akbarpour, 8/10/87, (PB88-163738).

NCEER-87-0019 "Modal Analysis of Nonclassically Damped Structural Systems Using Canonical Transformation," by J.N. Yang, S. Sarkani and F.X. Long, 9/27/87, (PB88-187851).

NCEER-87-0020 "A Nonstationary Solution in Random Vibration Theory," by J.R. Red-Horse and P.D. Spanos, 11/3/87, (PB88-163746).

NCEER-87-0021 "Horizontal Impedances for Radially Inhomogeneous Viscoelastic Soil Layers," by A.S. Veletsos and K.W. Dotson, 10/15/87, (PB88-150859).

NCEER-87-0022 "Seismic Damage Assessment of Reinforced Concrete Members," by Y.S. Chung, C. Meyer and M. Shinozuka, 10/9/87, (PB88-150867). This report is available only through NTIS (see address given above).

NCEER-87-0023 "Active Structural Control in Civil Engineering," by T.T. Soong, 11/11/87, (PB88-187778).

NCEER-87-0024 "Vertical and Torsional Impedances for Radially Inhomogeneous Viscoelastic Soil Layers," by K.W. Dotson and A.S. Veletsos, 12/87, (PB88-187786).

NCEER-87-0025 "Proceedings from the Symposium on Seismic Hazards, Ground Motions, Soil-Liquefaction and Engineering Practice in Eastern North America," October 20-22, 1987, edited by K.H. Jacob, 12/87, (PB88-188115).

NCEER-87-0026 "Report on the Whittier-Narrows, California, Earthquake of October 1, 1987," by J. Pantelic and A. Reinhorn, 11/87, (PB88-187752). This report is available only through NTIS (see address given above).

NCEER-87-0027 "Design of a Modular Program for Transient Nonlinear Analysis of Large 3-D Building Structures," by S. Srivastav and J.F. Abel, 12/30/87, (PB88-187950).

NCEER-87-0028 "Second-Year Program in Research, Education and Technology Transfer," 3/8/88, (PB88-219480).

NCEER-88-0001 "Workshop on Seismic Computer Analysis and Design of Buildings With Interactive Graphics," by W. McGuire, J.F. Abel and C.H. Conley, 1/18/88, (PB88-187760).

NCEER-88-0002 "Optimal Control of Nonlinear Flexible Structures," by J.N. Yang, F.X. Long and D. Wong, 1/22/88, (PB88-213772).

NCEER-88-0003 "Substructuring Techniques in the Time Domain for Primary-Secondary Structural Systems," by G.D. Manolis and G. Juhn, 2/10/88, (PB88-213780).

NCEER-88-0004 "Iterative Seismic Analysis of Primary-Secondary Systems," by A. Singhal, L.D. Lutes and P.D. Spanos, 2/23/88, (PB88-213798).

NCEER-88-0005 "Stochastic Finite Element Expansion for Random Media," by P.D. Spanos and R. Ghanem, 3/14/88, (PB88-213806).

NCEER-88-0006 "Combining Structural Optimization and Structural Control," by F.Y. Cheng and C.P. Pantelides, 1/10/88, (PB88-213814).

NCEER-88-0007 "Seismic Performance Assessment of Code-Designed Structures," by H.H-M. Hwang, J-W. Jaw and H-J. Shau, 3/20/88, (PB88-219423).

NCEER-88-0008 "Reliability Analysis of Code-Designed Structures Under Natural Hazards," by H.H-M. Hwang, H. Ushiba and M. Shinozuka, 2/29/88, (PB88-229471).

NCEER-88-0009 "Seismic Fragility Analysis of Shear Wall Structures," by J-W Jaw and H.H-M. Hwang, 4/30/88, (PB89-102867).

NCEER-88-0010 "Base Isolation of a Multi-Story Building Under a Harmonic Ground Motion - A Comparison of Performances of Various Systems," by F-G Fan, G. Ahmadi and I.G. Tadjbakhsh, 5/18/88, (PB89-122238).

NCEER-88-0011 "Seismic Floor Response Spectra for a Combined System by Green's Functions," by F.M. Lavelle, L.A. Bergman and P.D. Spanos, 5/1/88, (PB89-102875).

NCEER-88-0012 "A New Solution Technique for Randomly Excited Hysteretic Structures," by G.Q. Cai and Y.K. Lin, 5/16/88, (PB89-102883).

NCEER-88-0013 "A Study of Radiation Damping and Soil-Structure Interaction Effects in the Centrifuge," by K. Weissman, supervised by J.H. Prevost, 5/24/88, (PB89-144703).

NCEER-88-0014 "Parameter Identification and Implementation of a Kinematic Plasticity Model for Frictional Soils," by J.H. Prevost and D.V. Griffiths, to be published.

NCEER-88-0015 "Two- and Three- Dimensional Dynamic Finite Element Analyses of the Long Valley Dam," by D.V. Griffiths and J.H. Prevost, 6/17/88, (PB89-144711).

NCEER-88-0016 "Damage Assessment of Reinforced Concrete Structures in Eastern United States," by A.M. Reinhorn, M.J. Seidel, S.K. Kunnath and Y.J. Park, 6/15/88, (PB89-122220).

NCEER-88-0017 "Dynamic Compliance of Vertically Loaded Strip Foundations in Multilayered Viscoelastic Soils," by S. Ahmad and A.S.M. Israil, 6/17/88, (PB89-102891).

NCEER-88-0018 "An Experimental Study of Seismic Structural Response With Added Viscoelastic Dampers," by R.C. Lin, Z. Liang, T.T. Soong and R.H. Zhang, 6/30/88, (PB89-122212). This report is available only through NTIS (see address given above).

NCEER-88-0019 "Experimental Investigation of Primary - Secondary System Interaction," by G.D. Manolis, G. Juhn and A.M. Reinhorn, 5/27/88, (PB89-122204).

NCEER-88-0020 "A Response Spectrum Approach For Analysis of Nonclassically Damped Structures," by J.N. Yang, S. Sarkani and F.X. Long, 4/22/88, (PB89-102909).

NCEER-88-0021 "Seismic Interaction of Structures and Soils: Stochastic Approach," by A.S. Veletsos and A.M. Prasad, 7/21/88, (PB89-122196).

NCEER-88-0022 "Identification of the Serviceability Limit State and Detection of Seismic Structural Damage," by E. DiPasquale and A.S. Cakmak, 6/15/88, (PB89-122188). This report is available only through NTIS (see address given above).

NCEER-88-0023 "Multi-Hazard Risk Analysis: Case of a Simple Offshore Structure," by B.K. Bhartia and E.H. Vanmarcke, 7/21/88, (PB89-145213).

NCEER-88-0024 "Automated Seismic Design of Reinforced Concrete Buildings," by Y.S. Chung, C. Meyer and M. Shinozuka, 7/5/88, (PB89-122170). This report is available only through NTIS (see address given above).

NCEER-88-0025 "Experimental Study of Active Control of MDOF Structures Under Seismic Excitations," by L.L. Chung, R.C. Lin, T.T. Soong and A.M. Reinhorn, 7/10/88, (PB89-122600).

NCEER-88-0026 "Earthquake Simulation Tests of a Low-Rise Metal Structure," by J.S. Hwang, K.C. Chang, G.C. Lee and R.L. Ketter, 8/1/88, (PB89-102917).

NCEER-88-0027 "Systems Study of Urban Response and Reconstruction Due to Catastrophic Earthquakes," by F. Kozin and H.K. Zhou, 9/22/88, (PB90-162348).

NCEER-88-0028 "Seismic Fragility Analysis of Plane Frame Structures," by H.H-M. Hwang and Y.K. Low, 7/31/88, (PB89-131445).

NCEER-88-0029 "Response Analysis of Stochastic Structures," by A. Kardara, C. Bucher and M. Shinozuka, 9/22/88, (PB89-174429).

NCEER-88-0030 "Nonnormal Accelerations Due to Yielding in a Primary Structure," by D.C.K. Chen and L.D. Lutes, 9/19/88, (PB89-131437).

NCEER-88-0031 "Design Approaches for Soil-Structure Interaction," by A.S. Veletsos, A.M. Prasad and Y. Tang, 12/30/88, (PB89-174437). This report is available only through NTIS (see address given above).

NCEER-88-0032 "A Re-evaluation of Design Spectra for Seismic Damage Control," by C.J. Turkstra and A.G. Tallin, 11/7/88, (PB89-145221).

NCEER-88-0033 "The Behavior and Design of Noncontact Lap Splices Subjected to Repeated Inelastic Tensile Loading," by V.E. Sagan, P. Gergely and R.N. White, 12/8/88, (PB89-163737).

NCEER-88-0034 "Seismic Response of Pile Foundations," by S.M. Mamoon, P.K. Banerjee and S. Ahmad, 11/1/88, (PB89-145239).

NCEER-88-0035 "Modeling of R/C Building Structures With Flexible Floor Diaphragms (IDARC2)," by A.M. Reinhorn, S.K. Kunnath and N. Panahshahi, 9/7/88, (PB89-207153).

NCEER-88-0036 "Solution of the Dam-Reservoir Interaction Problem Using a Combination of FEM, BEM with Particular Integrals, Modal Analysis, and Substructuring," by C-S. Tsai, G.C. Lee and R.L. Ketter, 12/31/88, (PB89-207146).

NCEER-88-0037 "Optimal Placement of Actuators for Structural Control," by F.Y. Cheng and C.P. Pantelides, 8/15/88, (PB89-162846).

NCEER-88-0038 "Teflon Bearings in Aseismic Base Isolation: Experimental Studies and Mathematical Modeling," by A. Mokha, M.C. Constantinou and A.M. Reinhorn, 12/5/88, (PB89-218457). This report is available only through NTIS (see address given above).

NCEER-88-0039 "Seismic Behavior of Flat Slab High-Rise Buildings in the New York City Area," by P. Weidlinger and M. Ettouney, 10/15/88, (PB90-145681).

NCEER-88-0040 "Evaluation of the Earthquake Resistance of Existing Buildings in New York City," by P. Weidlinger and M. Ettouney, 10/15/88, to be published.

NCEER-88-0041 "Small-Scale Modeling Techniques for Reinforced Concrete Structures Subjected to Seismic Loads," by W. Kim, A. El-Attar and R.N. White, 11/22/88, (PB89-189625).

NCEER-88-0042 "Modeling Strong Ground Motion from Multiple Event Earthquakes," by G.W. Ellis and A.S. Cakmak, 10/15/88, (PB89-174445).

NCEER-88-0043 "Nonstationary Models of Seismic Ground Acceleration," by M. Grigoriu, S.E. Ruiz and E. Rosenblueth, 7/15/88, (PB89-189617).

NCEER-88-0044 "SARCF User's Guide: Seismic Analysis of Reinforced Concrete Frames," by Y.S. Chung, C. Meyer and M. Shinozuka, 11/9/88, (PB89-174452).

NCEER-88-0045 "First Expert Panel Meeting on Disaster Research and Planning," edited by J. Pantelic and J. Stoyle, 9/15/88, (PB89-174460).

NCEER-88-0046 "Preliminary Studies of the Effect of Degrading Infill Walls on the Nonlinear Seismic Response of Steel Frames," by C.Z. Chrysostomou, P. Gergely and J.F. Abel, 12/19/88, (PB89-208383).

NCEER-88-0047 "Reinforced Concrete Frame Component Testing Facility - Design, Construction, Instrumentation and Operation," by S.P. Pessiki, C. Conley, T. Bond, P. Gergely and R.N. White, 12/16/88, (PB89-174478).

NCEER-89-0001 "Effects of Protective Cushion and Soil Compliancy on the Response of Equipment Within a Seismically Excited Building," by J.A. HoLung, 2/16/89, (PB89-207179).

NCEER-89-0002 "Statistical Evaluation of Response Modification Factors for Reinforced Concrete Structures," by H.H-M. Hwang and J-W. Jaw, 2/17/89, (PB89-207187).

NCEER-89-0003 "Hysteretic Columns Under Random Excitation," by G-Q. Cai and Y.K. Lin, 1/9/89, (PB89-196513).

NCEER-89-0004 "Experimental Study of 'Elephant Foot Bulge' Instability of Thin-Walled Metal Tanks," by Z-H. Jia and R.L. Ketter, 2/22/89, (PB89-207195).

NCEER-89-0005 "Experiment on Performance of Buried Pipelines Across San Andreas Fault," by J. Isenberg, E. Richardson and T.D. O'Rourke, 3/10/89, (PB89-218440). This report is available only through NTIS (see address given above).

NCEER-89-0006 "A Knowledge-Based Approach to Structural Design of Earthquake-Resistant Buildings," by M. Subramani, P. Gergely, C.H. Conley, J.F. Abel and A.H. Zaghw, 1/15/89, (PB89-218465).

NCEER-89-0007 "Liquefaction Hazards and Their Effects on Buried Pipelines," by T.D. O'Rourke and P.A. Lane, 2/1/89, (PB89-218481).

NCEER-89-0008 "Fundamentals of System Identification in Structural Dynamics," by H. Imai, C-B. Yun, O. Maruyama and M. Shinozuka, 1/26/89, (PB89-207211).

NCEER-89-0009 "Effects of the 1985 Michoacan Earthquake on Water Systems and Other Buried Lifelines in Mexico," by A.G. Ayala and M.J. O'Rourke, 3/8/89, (PB89-207229).

NCEER-89-R010 "NCEER Bibliography of Earthquake Education Materials," by K.E.K. Ross, Second Revision, 9/1/89, (PB90-125352).

NCEER-89-0011 "Inelastic Three-Dimensional Response Analysis of Reinforced Concrete Building Structures (IDARC-3D), Part I - Modeling," by S.K. Kunnath and A.M. Reinhorn, 4/17/89, (PB90-114612).

NCEER-89-0012 "Recommended Modifications to ATC-14," by C.D. Poland and J.O. Malley, 4/12/89, (PB90-108648).

NCEER-89-0013 "Repair and Strengthening of Beam-to-Column Connections Subjected to Earthquake Loading," by M. Corazao and A.J. Durrani, 2/28/89, (PB90-109885).

NCEER-89-0014 "Program EXKAL2 for Identification of Structural Dynamic Systems," by O. Maruyama, C-B. Yun, M. Hoshiya and M. Shinozuka, 5/19/89, (PB90-109877).

NCEER-89-0015 "Response of Frames With Bolted Semi-Rigid Connections, Part I - Experimental Study and Analytical Predictions," by P.J. DiCorso, A.M. Reinhorn, J.R. Dickerson, J.B. Radziminski and W.L. Harper, 6/1/89, to be published.

NCEER-89-0016 "ARMA Monte Carlo Simulation in Probabilistic Structural Analysis," by P.D. Spanos and M.P. Mignolet, 7/10/89, (PB90-109893).

NCEER-89-P017 "Preliminary Proceedings from the Conference on Disaster Preparedness - The Place of Earthquake Education in Our Schools," Edited by K.E.K. Ross, 6/23/89, (PB90-108606).

NCEER-89-0017 "Proceedings from the Conference on Disaster Preparedness - The Place of Earthquake Education in Our Schools," Edited by K.E.K. Ross, 12/31/89, (PB90-207895). This report is available only through NTIS (see address given above).

NCEER-89-0018 "Multidimensional Models of Hysteretic Material Behavior for Vibration Analysis of Shape Memory Energy Absorbing Devices, by E.J. Graesser and F.A. Cozzarelli, 6/7/89, (PB90-164146).

NCEER-89-0019 "Nonlinear Dynamic Analysis of Three-Dimensional Base Isolated Structures (3D-BASIS)," by S. Nagarajaiah, A.M. Reinhorn and M.C. Constantinou, 8/3/89, (PB90-161936). This report is available only through NTIS (see address given above).

NCEER-89-0020 "Structural Control Considering Time-Rate of Control Forces and Control Rate Constraints," by F.Y. Cheng and C.P. Pantelides, 8/3/89, (PB90-120445).

NCEER-89-0021 "Subsurface Conditions of Memphis and Shelby County," by K.W. Ng, T-S. Chang and H-H.M. Hwang, 7/26/89, (PB90-120437).

NCEER-89-0022 "Seismic Wave Propagation Effects on Straight Jointed Buried Pipelines," by K. Elhmadi and M.J. O'Rourke, 8/24/89, (PB90-162322).

NCEER-89-0023 "Workshop on Serviceability Analysis of Water Delivery Systems," edited by M. Grigoriu, 3/6/89, (PB90-127424).

NCEER-89-0024 "Shaking Table Study of a 1/5 Scale Steel Frame Composed of Tapered Members," by K.C. Chang, J.S. Hwang and G.C. Lee, 9/18/89, (PB90-160169).

NCEER-89-0025 "DYNA1D: A Computer Program for Nonlinear Seismic Site Response Analysis - Technical Documentation," by Jean H. Prevost, 9/14/89, (PB90-161944). This report is available only through NTIS (see address given above).

NCEER-89-0026 "1:4 Scale Model Studies of Active Tendon Systems and Active Mass Dampers for Aseismic Protection," by A.M. Reinhorn, T.T. Soong, R.C. Lin, Y.P. Yang, Y. Fukao, H. Abe and M. Nakai, 9/15/89, (PB90-173246).

NCEER-89-0027 "Scattering of Waves by Inclusions in a Nonhomogeneous Elastic Half Space Solved by Boundary Element Methods," by P.K. Hadley, A. Askar and A.S. Cakmak, 6/15/89, (PB90-145699).

NCEER-89-0028 "Statistical Evaluation of Deflection Amplification Factors for Reinforced Concrete Structures," by H.H.M. Hwang, J-W. Jaw and A.L. Ch'ng, 8/31/89, (PB90-164633).

NCEER-89-0029 "Bedrock Accelerations in Memphis Area Due to Large New Madrid Earthquakes," by H.H.M. Hwang, C.H.S. Chen and G. Yu, 11/7/89, (PB90-162330).

NCEER-89-0030 "Seismic Behavior and Response Sensitivity of Secondary Structural Systems," by Y.Q. Chen and T.T. Soong, 10/23/89, (PB90-164658).

NCEER-89-0031 "Random Vibration and Reliability Analysis of Primary-Secondary Structural Systems," by Y. Ibrahim, M. Grigoriu and T.T. Soong, 11/10/89, (PB90-161951).

NCEER-89-0032 "Proceedings from the Second U.S. - Japan Workshop on Liquefaction, Large Ground Deformation and Their Effects on Lifelines, September 26-29, 1989," Edited by T.D. O'Rourke and M. Hamada, 12/1/89, (PB90-209388).

NCEER-89-0033 "Deterministic Model for Seismic Damage Evaluation of Reinforced Concrete Structures," by J.M. Bracci, A.M. Reinhorn, J.B. Mander and S.K. Kunnath, 9/27/89.

NCEER-89-0034 "On the Relation Between Local and Global Damage Indices," by E. DiPasquale and A.S. Cakmak, 8/15/89, (PB90-173865).

NCEER-89-0035 "Cyclic Undrained Behavior of Nonplastic and Low Plasticity Silts," by A.J. Walker and H.E. Stewart, 7/26/89, (PB90-183518).

NCEER-89-0036 "Liquefaction Potential of Surficial Deposits in the City of Buffalo, New York," by M. Budhu, R. Giese and L. Baumgrass, 1/17/89, (PB90-208455).

NCEER-89-0037 "A Deterministic Assessment of Effects of Ground Motion Incoherence," by A.S. Veletsos and Y. Tang, 7/15/89, (PB90-164294).

NCEER-89-0038 "Workshop on Ground Motion Parameters for Seismic Hazard Mapping," July 17-18, 1989, edited by R.V. Whitman, 12/1/89, (PB90-173923).

NCEER-89-0039 "Seismic Effects on Elevated Transit Lines of the New York City Transit Authority," by C.J. Costantino, C.A. Miller and E. Heymsfield, 12/26/89, (PB90-207887).

NCEER-89-0040 "Centrifugal Modeling of Dynamic Soil-Structure Interaction," by K. Weissman, Supervised by J.H. Prevost, 5/10/89, (PB90-207879).

NCEER-89-0041 "Linearized Identification of Buildings With Cores for Seismic Vulnerability Assessment," by I-K. Ho and A.E. Aktan, 11/1/89, (PB90-251943).

NCEER-90-0001 "Geotechnical and Lifeline Aspects of the October 17, 1989 Loma Prieta Earthquake in San Francisco," by T.D. O'Rourke, H.E. Stewart, F.T. Blackburn and T.S. Dickerman, 1/90, (PB90-208596).

NCEER-90-0002 "Nonnormal Secondary Response Due to Yielding in a Primary Structure," by D.C.K. Chen and L.D. Lutes, 2/28/90, (PB90-251976).

NCEER-90-0003 "Earthquake Education Materials for Grades K-12," by K.E.K. Ross, 4/16/90, (PB91-251984).

NCEER-90-0004 "Catalog of Strong Motion Stations in Eastern North America," by R.W. Busby, 4/3/90, (PB90-251984).

NCEER-90-0005 "NCEER Strong-Motion Data Base: A User Manual for the GeoBase Release (Version 1.0 for the Sun3)," by P. Friberg and K. Jacob, 3/31/90 (PB90-258062).

NCEER-90-0006 "Seismic Hazard Along a Crude Oil Pipeline in the Event of an 1811-1812 Type New Madrid Earthquake," by H.H.M. Hwang and C-H.S. Chen, 4/16/90(PB90-258054).

NCEER-90-0007 "Site-Specific Response Spectra for Memphis Sheahan Pumping Station," by H.H.M. Hwang and C.S. Lee, 5/15/90, (PB91-108811).

NCEER-90-0008 "Pilot Study on Seismic Vulnerability of Crude Oil Transmission Systems," by T. Ariman, R. Dobry, M. Grigoriu, F. Kozin, M. O'Rourke, T. O'Rourke and M. Shinozuka, 5/25/90, (PB91-108837).

NCEER-90-0009 "A Program to Generate Site Dependent Time Histories: EQGEN," by G.W. Ellis, M. Srinivasan and A.S. Cakmak, 1/30/90, (PB91-108829).

NCEER-90-0010 "Active Isolation for Seismic Protection of Operating Rooms," by M.E. Talbott, Supervised by M. Shinozuka, 6/8/9, (PB91-110205).

NCEER-90-0011 "Program LINEARID for Identification of Linear Structural Dynamic Systems," by C-B. Yun and M. Shinozuka, 6/25/90, (PB91-110312).

NCEER-90-0012 "Two-Dimensional Two-Phase Elasto-Plastic Seismic Response of Earth Dams," by A.N. Yiagos, Supervised by J.H. Prevost, 6/20/90, (PB91-110197).

NCEER-90-0013 "Secondary Systems in Base-Isolated Structures: Experimental Investigation, Stochastic Response and Stochastic Sensitivity," by G.D. Manolis, G. Juhn, M.C. Constantinou and A.M. Reinhorn, 7/1/90, (PB91-110320).

NCEER-90-0014 "Seismic Behavior of Lightly-Reinforced Concrete Column and Beam-Column Joint Details," by S.P. Pessiki, C.H. Conley, P. Gergely and R.N. White, 8/22/90, (PB91-108795).

NCEER-90-0015 "Two Hybrid Control Systems for Building Structures Under Strong Earthquakes," by J.N. Yang and A. Danielians, 6/29/90, (PB91-125393).

NCEER-90-0016 "Instantaneous Optimal Control with Acceleration and Velocity Feedback," by J.N. Yang and Z. Li, 6/29/90, (PB91-125401).

NCEER-90-0017 "Reconnaissance Report on the Northern Iran Earthquake of June 21, 1990," by M. Mehrain, 10/4/90, (PB91-125377).

NCEER-90-0018 "Evaluation of Liquefaction Potential in Memphis and Shelby County," by T.S. Chang, P.S. Tang, C.S. Lee and H. Hwang, 8/10/90, (PB91-125427).

NCEER-90-0019 "Experimental and Analytical Study of a Combined Sliding Disc Bearing and Helical Steel Spring Isolation System," by M.C. Constantinou, A.S. Mokha and A.M. Reinhorn, 10/4/90, (PB91-125385).

NCEER-90-0020 "Experimental Study and Analytical Prediction of Earthquake Response of a Sliding Isolation System with a Spherical Surface," by A.S. Mokha, M.C. Constantinou and A.M. Reinhorn, 10/11/90, (PB91-125419).

NCEER-90-0021 "Dynamic Interaction Factors for Floating Pile Groups," by G. Gazetas, K. Fan, A. Kaynia and E. Kausel, 9/10/90, (PB91-170381).

NCEER-90-0022 "Evaluation of Seismic Damage Indices for Reinforced Concrete Structures," by S. Rodriguez-Gomez and A.S. Cakmak, 9/30/90, PB91-171322).

NCEER-90-0023 "Study of Site Response at a Selected Memphis Site," by H. Desai, S. Ahmad, E.S. Gazetas and M.R. Oh, 10/11/90, (PB91-196857).

NCEER-90-0024 "A User's Guide to Strongmo: Version 1.0 of NCEER's Strong-Motion Data Access Tool for PCs and Terminals," by P.A. Friberg and C.A.T. Susch, 11/15/90, (PB91-171272).

NCEER-90-0025 "A Three-Dimensional Analytical Study of Spatial Variability of Seismic Ground Motions," by L-L. Hong and A.H.-S. Ang, 10/30/90, (PB91-170399).

NCEER-90-0026 "MUMOID User's Guide - A Program for the Identification of Modal Parameters," by S. Rodriguez-Gomez and E. DiPasquale, 9/30/90, (PB91-171298).

NCEER-90-0027 "SARCF-II User's Guide - Seismic Analysis of Reinforced Concrete Frames," by S. Rodriguez-Gomez, Y.S. Chung and C. Meyer, 9/30/90, (PB91-171280).

NCEER-90-0028 "Viscous Dampers: Testing, Modeling and Application in Vibration and Seismic Isolation," by N. Makris and M.C. Constantinou, 12/20/90 (PB91-190561).

NCEER-90-0029 "Soil Effects on Earthquake Ground Motions in the Memphis Area," by H. Hwang, C.S. Lee, K.W. Ng and T.S. Chang, 8/2/90, (PB91-190751).

NCEER-91-0001 "Proceedings from the Third Japan-U.S. Workshop on Earthquake Resistant Design of Lifeline Facilities and Countermeasures for Soil Liquefaction, December 17-19, 1990," edited by T.D. O'Rourke and M. Hamada, 2/1/91, (PB91-179259).

NCEER-91-0002 "Physical Space Solutions of Non-Proportionally Damped Systems," by M. Tong, Z. Liang and G.C. Lee, 1/15/91, (PB91-179242).

NCEER-91-0003 "Seismic Response of Single Piles and Pile Groups," by K. Fan and G. Gazetas, 1/10/91, (PB92-174994).

NCEER-91-0004 "Damping of Structures: Part 1 - Theory of Complex Damping," by Z. Liang and G. Lee, 10/10/91, (PB92-197235).

NCEER-91-0005 "3D-BASIS - Nonlinear Dynamic Analysis of Three Dimensional Base Isolated Structures: Part II," by S. Nagarajaiah, A.M. Reinhorn and M.C. Constantinou, 2/28/91, (PB91-190553).

NCEER-91-0006 "A Multidimensional Hysteretic Model for Plasticity Deforming Metals in Energy Absorbing Devices," by E.J. Graesser and F.A. Cozzarelli, 4/9/91, (PB92-108364).

NCEER-91-0007 "A Framework for Customizable Knowledge-Based Expert Systems with an Application to a KBES for Evaluating the Seismic Resistance of Existing Buildings," by E.G. Ibarra-Anaya and S.J. Fenves, 4/9/91, (PB91-210930).

NCEER-91-0008 "Nonlinear Analysis of Steel Frames with Semi-Rigid Connections Using the Capacity Spectrum Method," by G.G. Deierlein, S-H. Hsieh, Y-J. Shen and J.F. Abel, 7/2/91, (PB92-113828).

NCEER-91-0009 "Earthquake Education Materials for Grades K-12," by K.E.K. Ross, 4/30/91, (PB91-212142).

NCEER-91-0010 "Phase Wave Velocities and Displacement Phase Differences in a Harmonically Oscillating Pile," by N. Makris and G. Gazetas, 7/8/91, (PB92-108356).

NCEER-91-0011 "Dynamic Characteristics of a Full-Size Five-Story Steel Structure and a 2/5 Scale Model," by K.C. Chang, G.C. Yao, G.C. Lee, D.S. Hao and Y.C. Yeh," 7/2/91, (PB93-116648).

NCEER-91-0012 "Seismic Response of a 2/5 Scale Steel Structure with Added Viscoelastic Dampers," by K.C. Chang, T.T. Soong, S-T. Oh and M.L. Lai, 5/17/91, (PB92-110816).

NCEER-91-0013 "Earthquake Response of Retaining Walls; Full-Scale Testing and Computational Modeling," by S. Alampalli and A-W.M. Elgamal, 6/20/91, to be published.

NCEER-91-0014 "3D-BASIS-M: Nonlinear Dynamic Analysis of Multiple Building Base Isolated Structures," by P.C. Tsopelas, S. Nagarajaiah, M.C. Constantinou and A.M. Reinhorn, 5/28/91, (PB92-113885).

NCEER-91-0015 "Evaluation of SEAOC Design Requirements for Sliding Isolated Structures," by D. Theodossiou and M.C. Constantinou, 6/10/91, (PB92-114602).

NCEER-91-0016 "Closed-Loop Modal Testing of a 27-Story Reinforced Concrete Flat Plate-Core Building," by H.R. Somaprasad, T. Toksoy, H. Yoshiyuki and A.E. Aktan, 7/15/91, (PB92-129980).

NCEER-91-0017 "Shake Table Test of a 1/6 Scale Two-Story Lightly Reinforced Concrete Building," by A.G. El-Attar, R.N. White and P. Gergely, 2/28/91, (PB92-222447).

NCEER-91-0018 "Shake Table Test of a 1/8 Scale Three-Story Lightly Reinforced Concrete Building," by A.G. El-Attar, R.N. White and P. Gergely, 2/28/91, (PB93-116630).

NCEER-91-0019 "Transfer Functions for Rigid Rectangular Foundations," by A.S. Veletsos, A.M. Prasad and W.H. Wu, 7/31/91.

NCEER-91-0020 "Hybrid Control of Seismic-Excited Nonlinear and Inelastic Structural Systems," by J.N. Yang, Z. Li and A. Danielians, 8/1/91, (PB92-143171).

NCEER-91-0021 "The NCEER-91 Earthquake Catalog: Improved Intensity-Based Magnitudes and Recurrence Relations for U.S. Earthquakes East of New Madrid," by L. Seeber and J.G. Armbruster, 8/28/91, (PB92-176742).

NCEER-91-0022 "Proceedings from the Implementation of Earthquake Planning and Education in Schools: The Need for Change - The Roles of the Changemakers," by K.E.K. Ross and F. Winslow, 7/23/91, (PB92-129998).

NCEER-91-0023 "A Study of Reliability-Based Criteria for Seismic Design of Reinforced Concrete Frame Buildings," by H.H.M. Hwang and H-M. Hsu, 8/10/91, (PB92-140235).

NCEER-91-0024 "Experimental Verification of a Number of Structural System Identification Algorithms," by R.G. Ghanem, H. Gavin and M. Shinozuka, 9/18/91, (PB92-176577).

NCEER-91-0025 "Probabilistic Evaluation of Liquefaction Potential," by H.H.M. Hwang and C.S. Lee," 11/25/91, (PB92-143429).

NCEER-91-0026 "Instantaneous Optimal Control for Linear, Nonlinear and Hysteretic Structures - Stable Controllers," by J.N. Yang and Z. Li, 11/15/91, (PB92-163807).

NCEER-91-0027 "Experimental and Theoretical Study of a Sliding Isolation System for Bridges," by M.C. Constantinou, A. Kartoum, A.M. Reinhorn and P. Bradford, 11/15/91, (PB92-176973).

NCEER-92-0001 "Case Studies of Liquefaction and Lifeline Performance During Past Earthquakes, Volume 1: Japanese Case Studies," Edited by M. Hamada and T. O'Rourke, 2/17/92, (PB92-197243).

NCEER-92-0002 "Case Studies of Liquefaction and Lifeline Performance During Past Earthquakes, Volume 2: United States Case Studies," Edited by T. O'Rourke and M. Hamada, 2/17/92, (PB92-197250).

NCEER-92-0003 "Issues in Earthquake Education," Edited by K. Ross, 2/3/92, (PB92-222389).

NCEER-92-0004 "Proceedings from the First U.S. - Japan Workshop on Earthquake Protective Systems for Bridges," Edited by I.G. Buckle, 2/4/92.

NCEER-92-0005 "Seismic Ground Motion from a Haskell-Type Source in a Multiple-Layered Half-Space," A.P. Theoharis, G. Deodatis and M. Shinozuka, 1/2/92, to be published.

NCEER-92-0006 "Proceedings from the Site Effects Workshop," Edited by R. Whitman, 2/29/92, (PB92-197201).

NCEER-92-0007 "Engineering Evaluation of Permanent Ground Deformations Due to Seismically-Induced Liquefaction," by M.H. Baziar, R. Dobry and A-W.M. Elgamal, 3/24/92, (PB92-222421).

NCEER-92-0008 "A Procedure for the Seismic Evaluation of Buildings in the Central and Eastern United States," by C.D. Poland and J.O. Malley, 4/2/92, (PB92-222439).

NCEER-92-0009 "Experimental and Analytical Study of a Hybrid Isolation System Using Friction Controllable Sliding Bearings," by M.Q. Feng, S. Fujii and M. Shinozuka, 5/15/92, (PB93-150282).

NCEER-92-0010 "Seismic Resistance of Slab-Column Connections in Existing Non-Ductile Flat-Plate Buildings," by A.J. Durrani and Y. Du, 5/18/92.

NCEER-92-0011 "The Hysteretic and Dynamic Behavior of Brick Masonry Walls Upgraded by Ferrocement Coatings Under Cyclic Loading and Strong Simulated Ground Motion," by H. Lee and S.P. Prawel, 5/11/92, to be published.

NCEER-92-0012 "Study of Wire Rope Systems for Seismic Protection of Equipment in Buildings," by G.F. Demetriades, M.C. Constantinou and A.M. Reinhorn, 5/20/92.

NCEER-92-0013 "Shape Memory Structural Dampers: Material Properties, Design and Seismic Testing," by P.R. Witting and F.A. Cozzarelli, 5/26/92.

NCEER-92-0014 "Longitudinal Permanent Ground Deformation Effects on Buried Continuous Pipelines," by M.J. O'Rourke, and C. Nordberg, 6/15/92.

NCEER-92-0015 "A Simulation Method for Stationary Gaussian Random Functions Based on the Sampling Theorem," by M. Grigoriu and S. Balopoulou, 6/11/92, (PB93-127496).

NCEER-92-0016 "Gravity-Load-Designed Reinforced Concrete Buildings: Seismic Evaluation of Existing Construction and Detailing Strategies for Improved Seismic Resistance," by G.W. Hoffmann, S.K. Kunnath, A.M. Reinhorn and J.B. Mander, 7/15/92.